Exploring new avenues of surfactant mediated particle charging in apolar media

Benjamin Scott Ponto

A dissertation

submitted in partial fulfillment of the

requirements for the degree of

Doctor of Philosophy

University of Washington

2019

Reading Committee:

John Berg, Chair
Brian Hayes
Vincent Holmberg

Program Authorized to Offer Degree:

Chemical Engineering

University of Washington

Abstract

Exploring new avenues of surfactant mediated particle charging in apolar media

Benjamin Scott Ponto

Chair of the Supervisory Committee:
Rehnberg Professor John C. Berg
Chemical Engineering

The ability to control and understand particle charging in apolar media has led to advanced digital printers (e.g., HP Indigo®) and electrophoretic displays (e.g., the Amazon Kindle®). Previous work has investigated the surfactant mediated acid-base charging mechanisms of oxides and similar particles where it has been shown that the sign of particle charge can be determined by comparing the acid-base properties of a particle, i.e., point of zero charge (PZC), to an experimentally determined "effective pH" of a surfactant molecule. This work explores the surfactant mediated particle charging mechanisms in four new venues.

First, the present work shows that clay particles, which have multiple charging mechanisms in water, can charge only via an acid-base reverse micelle charging mechanism in apolar media. While the majority of clay particle charge is derived from isomorphous substitution in water, this

charging mechanism is not operable in apolar media. It is also demonstrated that the charge of clay particles can be predicted by comparing their surface acid-base properties to the acid-base properties of the surfactants used.

Second, the effect that reverse micelle size and structure has on particle charging in apolar media is investigated here. Results show that the size of the reverse micelle core dictates its particle charging ability. Third, binary surfactant systems in apolar media are investigated with the objective of tuning the surfactant acid-base properties for the target particles by mixing surfactants with different effective pH values. This would allow the practitioner another method to accurately control the sign and magnitude of nanoparticle charge in apolar media.

Finally, while particle charging has been studied in aqueous (ε=80) and apolar (ε=2) media, limited study has been conducted in solvents with intermediate dielectric constants, commonly referred to as leaky dielectrics, where many industrial applications of particle charging exist. The present work explores particle charging in leaky dielectrics where three charging mechanisms are identified arising from particle-solvent, particle-surfactant, and solvent-surfactant interactions. In leaky dielectrics, particles can acquire charge from the solvent as described by their donor numbers, from the adsorption of surfactant ions, and from the formation of reverse micelles which facilitate an acid-base charging mechanism.

TABLE OF CONTENTS

LIST OF FIGURES

LIST OF TABLES

ACKNOWLEDGEMENTS

John C. Berg for his inspiration, guidance, support and friendship.

The Center for Surfaces, Polymers, and Colloids at the University of Washington for supporting this work.

My advisory committee: Dr. Brian Hayes, Professor Elizabeth Nance, Professor Vincent Holmberg, and Professor Anthony Dichiara.

Berg Group members: Dr. Andy Kim, Dr. Kyle Caldwell, Dr. Ed Michor, Luke Khoury, Jake Fredrikson and Lane Bozman.

DEDICATION

To my family and friends, for their love and support on this journey.

Chapter 1. INTRODUCTION TO PARTICLE CHARGING IN APOLAR MEDIA

1.1 INTRODUCTION

The proposed research concerns the electrical charging of colloidal particles in nonaqueous media. In the mid-20th century, the danger of electrokinetic explosions in the petroleum industry spurred some of the early investigations into the existence of electrical charges in apolar media. Klinkenberg and van der Minne[1] found that trace compounds present in oil products were responsible for the buildup of large electrostatic fields when flowing insulating liquids through metal pipes. Under flow, they found that two charges would separate and preferential adsorption of a particular sign would set up an electric field so large that it could discharge by sparking. At larger concentration it was found that these same compounds could increase conductivity enough to prevent a buildup of charge, eliminating the risk of electrostatic explosions.[2] It was later discovered that these charge carrying species were in fact reverse micelles.[3,4]

Today, reverse micelles are used to charge colloidal particles in apolar media stabilizing them against aggregation.[5–12] The most common application of this is in electrophoretic displays, such as the Amazon Kindle®, which contain small oil capsules with oppositely charged black and white colloidal particles. By applying a small voltage to each capsule, the pixel on the screen can be changed from black to white. The benefit of this technology is that only a tiny amount of electricity is required allowing the consumer to read an entire book on a single battery charge.[13,14] This technology is also used to charge pigment particles in new high quality digital printers (e.g., HP Indigo®).[13,15]

For the past eight years, one area of focus in the Berg research group has been to understand colloidal particle charging in nonaqueous media. While much progress has been made, the goal of this author's research was to fill in some of the remaining gaps and to provide a more nearly complete story of this important area of research.

1.2 PREVIOUS WORK

The group's first study investigated the effect of surfactant and particle acid-base properties on the charging of colloidal particles in fully apolar media.[10] (Isopar-L is a commercial isoparafinic hydrocarbon consisting of C8-C15 saturated hydrocarbons and is the apolar solvent of choice). Two model spherical silica particles were used, one with acidic functionality and one with basic functionality with two different surfactants. OLOA 11000 was chosen as a basic surfactant and Span 80 was chosen as an acidic surfactant. What was found was that the acidic surfactant, Span 80, charged both particles positively, with the acidic silica particle being charged much less than the basic one (by comparing the maximum particle charge over the range of surfactant concentrations). Alternatively, OLOA charged both particles negatively, with the more basic silica particle being charged less. This study demonstrated that the acid-base property of the surfactant and the acid-base property of the particle were decisive in determining the sign and magnitude of particle. Additionally, the effect that surfactant concentration had on particle charging was observed. Below the critical micelle concentration (CMC) no charging occurred. At higher surfactant concentrations charge was screened out due to an increase in conductivity from reverse micelle disproportionation charging reactions.[10] Reverse micelles can acquire charge through a process of disproportionation where two neutrally charged reverse micelles exchange charge resulting in one positive and one negative reverse micelle.[2,13,16]

In the hope of creating a particle with no potential acid-base functionality, i.e., an "afunctional" silica particle, the second study investigated the effect that a surface treatment of hexadecyltrimethoxysilane would have on silica particle charge with three different surfactants (Aerosol-OT, OLOA 11000, and zirconyl 2-ethyl hexanoate).[11] What was found, however, was that all of the surfactants charged the untreated and treated silica particles negatively and that the surface treatment actually enhanced the magnitude of the negative charge. It was concluded that when the silane attached to the surface it brought with it two additional charging hydroxyl sites which could then participate in the acid-base reverse micelle charging mechanism. Again it was noted that particle charging was dependent on the surfactant concentration.[11]

The next two studies investigated the apparent correlation between a particle's acid-base properties and its apolar charging behavior.[17,18] A series of mineral oxides (SiO_2, TiO_2, Al_2O_3, ZnO, and MgO) with aqueous point of zero charges (PZC) or isoelectric points (IEP) ranging from 2 to 11 were charged with three surfactants (Span 80, Aerosol-OT, and OLOA 11000) in Isopar-L. In these studies care was taken to eliminate the applied field induced charging effects that were demonstrated by another group.[19] A linear relationship was discovered between the maximum zero-field electrophoretic mobility of the oxides and their aqueous PZCs. For each of the surfactants, an "effective pH" was determined from the linear fit intersection with the x-axis where the oxide charge reversal would take place. For Aerosol-OT this effective pH was 4-5 and for OLOA 11000 it was 8.5. Span 80 charged all of oxides positively and the effective pH was extrapolated to 0.[17,18]

To determine the effects of trace water on the charging of reverse micelles and the particles they charge, a study was conducted by measuring the conductivity, water content, and electrophoretic mobility of silica particles in Isopar-L with OLOA.[20] It was found that without

particles, the addition of water to the OLOA and Isopar-L solutions increased conductivity and reverse micelle charging because the swelling of the polar cores made it more energetically favorable for a disproportionation charging reaction to occur. Adding particles to this system at the same water content further increased the conductivity indicating the presence of a reverse micelle particle charging mechanism. Furthermore, it was found that at low OLOA concentrations above the CMC particle electrophoretic mobility was enhanced with the addition of water while at high OLOA concentrations above the CMC particle mobility decreased due to electrostatic screening from more charged reverse micelles in the bulk.[20]

Another study investigated cyan and magenta pigment particle charging with surfactants in apolar media. Supported by Xerox, who were interested in organic pigment particle charging for use in electrostatic lithography, the study investigated the effect of synergists on the particle charging of cyan and magenta pigment particles.[21] It was discovered that both of these pigment particles participated in an acid-base reverse micelle charging mechanism and that the synergist had an effect on particle charge.

The effect of surfactant hydrophile-lipophile balance (HLB) on mineral oxide particle charging in apolar media was studied next using three surfactants from the Span series (Span 20, Span 80, and Span 85) and the same mineral oxides from before (SiO_2, TiO_2, Al_2O_3, ZnO, and MgO).[22] It was found that as the HLB of the surfactant increased; the surfactant concentration needed to achieve maximum particle charge decreased while the value of the maximum particle charge increased. The increase in maximum particle charge with larger HLBs was attributed to the fact that surfactants with larger HLBs have larger cores and are more likely to house counter-charges from the particle surface.[22]

The culmination of the work from Dr. Berg's lab thus far was reported in a review article in 2015 where a relationship predicting the sign and magnitude of particle charge in apolar media was presented.[13]

$$\zeta_{\max} \propto HLB_{surfactant}\left(pH_{PZC} - pH_{surfactant}\right), \tag{1.1}$$

where $\zeta_{\max}$ is the maximum particle zeta potential as a function of surfactant concentration, $HLB_{surfactant}$ is the HLB of the surfactant, pH_{PZC} is the aqueous PZC of the particle, and $pH_{surfactant}$ is the "effective pH" of the surfactant as determined by the series of mineral oxides. This was an important result and was true for a number of carbon black, metal oxide, and pigment particles with the surfactants Span 20, Span 80, Span 85, Aerosol-OT, and OLOA 11000.[13] The graph of all of these data, with the relationship, Eq. (1.1), is shown in Figure 1.1 below. In Figure 1.1 it is clear that the relationship qualitatively describes the data; however, there is a deviation from the data in the negative region where more investigation is required.

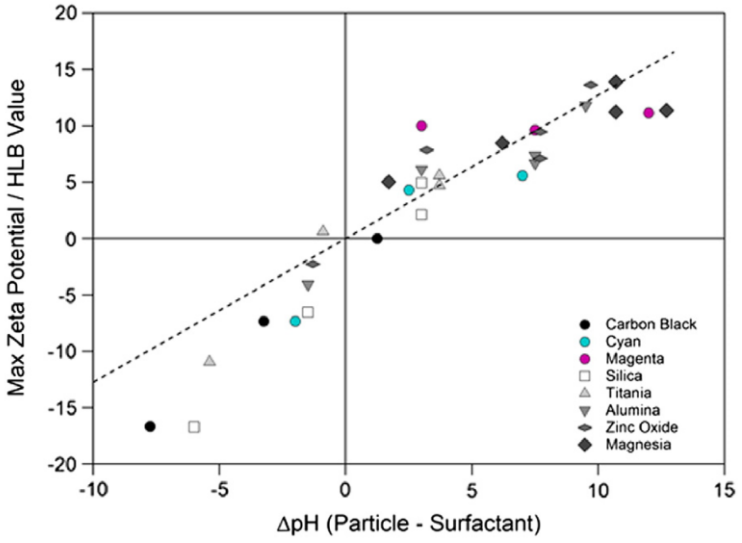

Figure 1.1. Combined charging data for all particles and surfactant systems studied thus far. Particles were dispersed in Isopar-L or Heptane.[13] (Reproduced from Gacek 2015).

Following the pivotal review paper, a study examined the effect that different solvents, characterized by their dielectric constant (ε), had on the micellization of Aerosol-OT (AOT).[23] It was found that in water (ε=80) AOT formed micelles, and in lower dielectric constant solvents (ε<48) AOT formed reverse micelles. What was interesting was that in solvents between these two dielectric constants (48< ε<80) no micellization occurred.[23]

Another study investigated particle charging with different analogs of AOT by exchanging the sodium ion in the head group with Ba^{2+}, Mg^{2+}, Ni^{2+}, Al^{3+}, and Zn^{2+}.[24] Each surfactant charged silica, alumina, and magnesia positively and for the most part, in order of their relative acidity. A general trend was also found showing that as the electronegativity of the head group cation increased the maximum electrophoretic mobility also increased.[24]

The next study from Dr. Berg's lab investigated the effect temperature has on the critical micelle concentration (CMC) and magnesia particle charging abilities of a series of Span surfactants in apolar media.[25] Span 20, 40, 60, 65, 80, and 85 were used in this study. It was discovered that as the temperature increased, for all but one of the Span surfactants, the CMC also increased. The explanation for the one surfactant exception, Span 65, was that at lower temperatures its three fully saturated hydrophobic tails would crystallize causing it to not form reverse micelles below 44°C. This study also measured the size of Span 20, 40, and 60 and tried to correlate the size of the reverse micelles to the maximum particle charge suggesting that as the reverse micelle size decreased the maximum particle charge increased due to less electrostatic screening in the bulk from disproportionation reactions.[25]

While it is clear that much progress has been made in trying to understand colloidal particle charging in nonaqueous media, several avenues of exploration remain. This dissertation presents four projects that address these remaining questions.

The first project, presented in Chapter 2, investigated clay particle charging in apolar media. Clay particles presented different electrostatic surface chemistry (isomorphic substitution) than the colloidal materials previously studied.[12]

The next two projects focused on the properties of the reverse micelles formed by oil-soluble surfactants. The first surfactant study, summarized in Chapter 3, investigated the effect that reverse micelle size and structure had on particle charging in apolar media.[26] Results from previous studies suggested that reverse micelle size was potentially one reason why water content, different Span surfactants, and HLB effected particle charging. Therefore, it was important to formally investigate the effects of reverse micelle structure on its ability to charge particles. This was conducted using a series of Span surfactants.

The second surfactant study explored the possibility of using surfactant mixtures to tune the acid-base properties, i.e., effective pH ($pH_{surfactant}$), of the core of the mixed reverse co-micelles. Previous studies had only investigated the acid-base charging of colloidal particles with single surfactant systems in apolar media. Investigating the use of mixed reverse micelles to charge colloidal particles in apolar media is presented in Chapter 4.

The final experiment, presented in Chapter 5, moved away from the ultra-low dielectric apolar solvents ($\varepsilon \leq 2$) and into solvents of *intermediate* dielectric constants ($5 < \varepsilon < 40$) where the particle charging mechanism becomes more complex. In this dielectric region of solvents which was called "leaky dielectrics", charging mechanisms similar to those found in both aqueous and apolar media can exist. Being able to control particle charging over this wide range of nonaqueous media benefits many applications as particle charge is vital to colloidal aggregation stability.

Chapter 6 proposes future projects regarding the continuation of the research presented in this dissertation. While the majority of future work is likely to be focused on specific applications

tied to industrial problems two projects are proposed. The first project proposed continues the investigation of reverse micelle charging in leaky dielectrics by exploring the size and structure of the reverse micelles and its effect on particle charging in different solvents. The second project proposed explores using AOT microemulsions (formed by adding excess water to an apolar-surfactant system) to charge particles in apolar media.

1.3 THEORY AND BACKGROUND

A brief review of the mechanism for charging mineral oxides and similar materials in apolar media is useful and follows. The differences in charge stabilization between aqueous and apolar media is best highlighted by the Bjerrum length. The Bjerrum length is defined as the separation distance at which two opposite charges possess a coulombic attractive energy that is equal to their thermal energy (k_BT). The Bjerrum length, λ_B, is shown below,

$$\lambda_B = \frac{e^2}{4\pi\varepsilon\varepsilon_o k_B T}, \tag{1.2}$$

where ε is the dielectric constant of the medium, ε_o is the permittivity of free space, e is the protonic charge, k_B is the Boltzmann constants and T is the temperature. In water, with a dielectric constant of 78, the Bjerrum length is ≈ 0.7 nm, a distance where the hydration sheath is all that is needed to separate an ion pair. In apolar media with a dielectric constant (ε) as low as 2, the Bjerrum length is ≈ 28 nm. Stabilizing charge in such media is significantly more difficult than in aqueous systems because the low dielectric allows coulombic attractive forces to be felt over much greater distances. To maintain such large distances of separation between opposite charges, reverse micelles are required in apolar media to stabilize charges against recombination. It is believed that these charges must be housed within the cores of the reverse micelles.[2,13,14,27]

Surfactants are molecules that are comprised of two distinct sections, a hydrophilic portion referred to as the "head group", and a hydrophobic portion, i.e., the "tail". As the surfactant concentration is increased above the critical micelle concentration (CMC), these amphiphiles spontaneously organize into structures satisfying the solubility characteristics of each of the two components. In water, surfactants organize into micelles where the polar head groups surround the hydrophobic tails inside the core. Even though surfactant molecules are becoming ordered (decreasing entropy), the water molecules structured around the tails of surfactant monomers due to the hydrophobic effect are released. The entropy increase from the water molecules around the tails is large enough to make the micellization process happen spontaneously. Therefore, the principle driving force for micellization in water is entropic. In nonpolar solvents, the formation of reverse micelles is enthalpically driven forming a polar core containing the head groups of the surfactant molecules and trace water surrounded by the hydrophobic tails extending into the solvent. Dipole-dipole interactions between the polar head groups promote surfactant aggregate formation and grow to form reverse micelles as the concentration of the oil-soluble surfactant is increased above its CMC.[27,28]

While other charging mechanisms have been proposed in apolar media, this research group believes that the acid-base reverse micelle charging mechanism is applicable to the majority of cases. The charging of oxides or similar particles may ensue via the formation and subsequent dissociation of acid-base adducts between the adsorbing surfactant molecules and functional groups on the particle surfaces, as shown schematically in Figure 1.2. The resulting charged surfactant ions are housed in the reverse micelles, and the charges on the particle surfaces are protected by other adsorbed surfactant monomers.

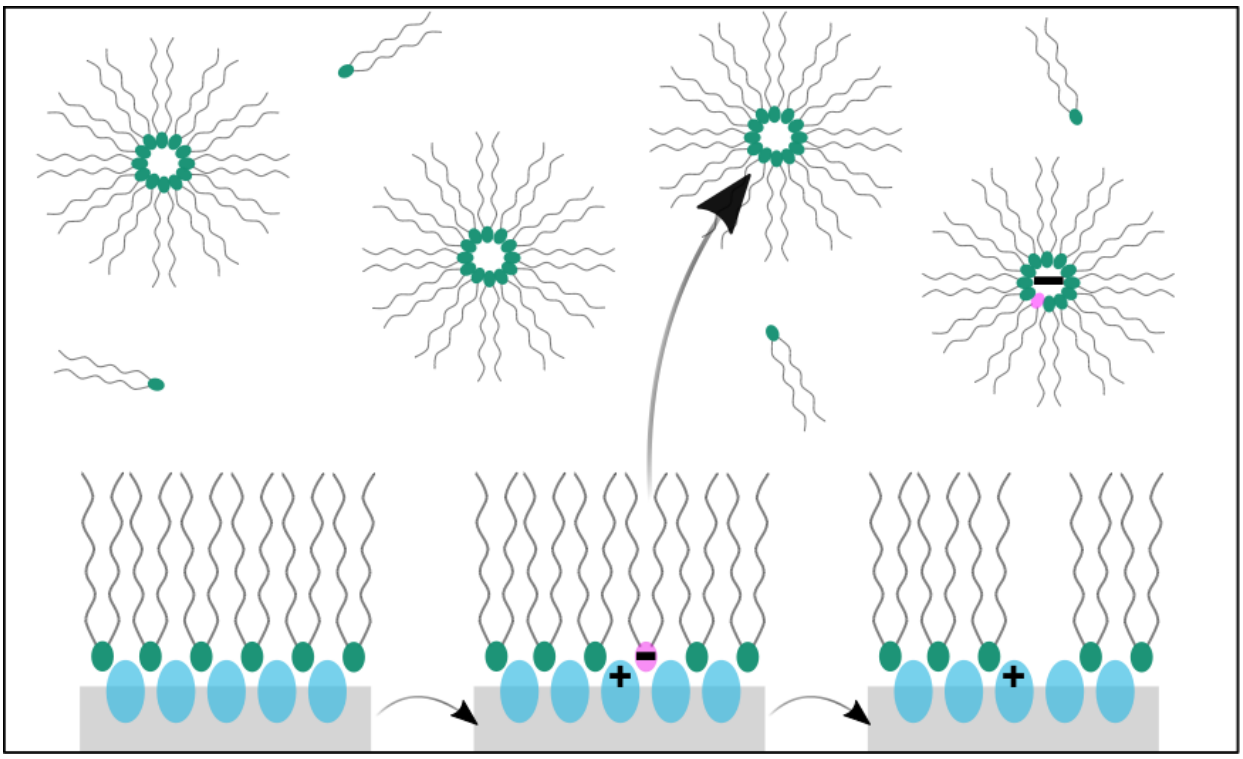

Figure 1.2. Schematic showing acid-base adduct formation, dissociation of surfactant at particle surface, and charge stabilization inside an inverse micelle in the bulk.[12] (Reproduced from reference 12).

In summary, the acid-base mechanism has three steps: first, the polar head group of a surfactant molecule will adsorb to the particle surface and form an acid-base adduct; second, charge is transferred between the surface and the surfactant molecule depending on the acid-base properties; and third, the charged surfactant molecule is stabilized by a reverse micelle which allows it to desorb leaving an opposite charge behind.[13,14,29,30] Therefore, in the absence of added surfactants to form inverse micelles, measurable particle charging in apolar media is not possible.

Surface charging can be quantified by measuring the particle electrophoretic mobility, u_E, i.e., its velocity divided by the applied electric field strength. Once measured, the effective electrical potential at the particle surface relative to solution interior, i.e., the zeta potential, ζ, may be calculated using appropriate theory. For apolar media, in which the electrical double layer thickness is large relative to the particle diameter, this is given by the Hückel Equation [27]:

$$\zeta = \frac{3\mu}{\varepsilon\varepsilon_o} u_E \ , \qquad (1.3)$$

where μ is the viscosity, ε is the dielectric constant and ε_o is the permittivity of free space. This equation is valid when κa<0.1 where a is the particle radius and κ is the Debye parameter. [27]

A typical particle charging trend for reverse micelle charging of oxides and similar particles in apolar media is shown schematically in Figure 1.3. It is common to measure the electrophoretic mobility (or the zeta potential) as a function of the surfactant concentration.[13,17,18,20,25] At low concentrations, below that needed for the formation of inverse micelles, the surfactant is present only as monomers, and no particle charging is observed.[2,13]

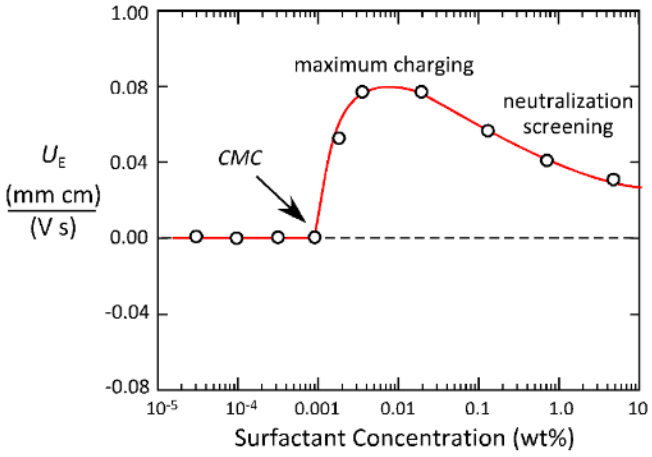

Figure 1.3. Particle charging as a function of surfactant concentration.[12] (Reproduced from reference 12).

After the critical micelle concentration (CMC) is exceeded, particle charging increases sharply, usually reaching a fairly well-defined maximum, beyond which it begins to decrease. The decrease is attributable to electrostatic screening caused by the increased concentration of charge-carrying reverse micelles.[13,16] The maximum charging value (or zeta potential) is taken as a descriptor which is a characteristic of the particle type and the surfactant used.[13]

Conductometric titrations can be used to measure the CMC of surfactants in apolar media. An example of a typical conductometric titration is shown below in Figure 1.4.

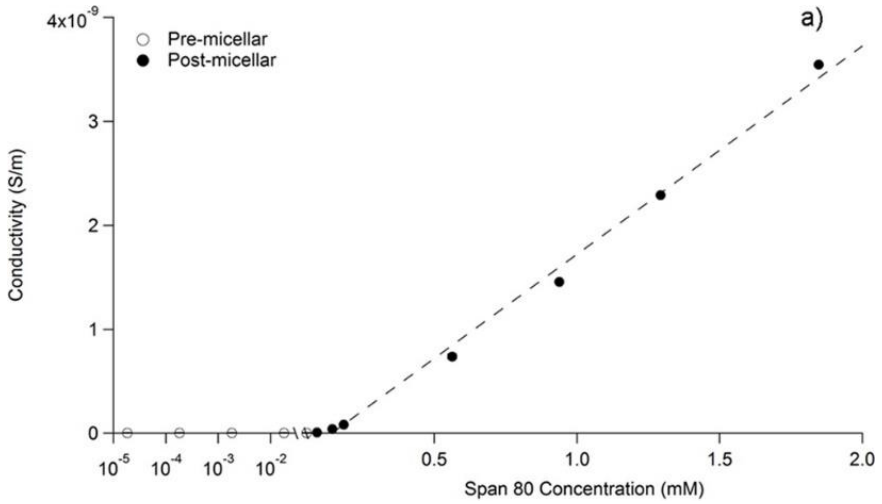

Figure 1.4. Example of conductometric titration results used to determine the critical micelle concentration of a surfactant in apolar media.[25] (Graph reproduced from reference 25).

The CMC is determined from the point of slope change in Figure 1.4 where at surfactant concentrations below the CMC the conductivity is too low to measure because there is no way to stabilize charge. Once surfactants are added in sufficient concentration to form reverse micelles in such systems, they exhibit measurable electrical conductivity. Above the CMC, conductivity increases as the number of reverse micelles increases. The CMC for Span 80, AOT, and OLOA in Isopar-L has been found to be approximately 0.003wt%, 0.001wt%, and 0.005wt%, respectively.[10,13,18]

To be able to make predictions about the acid-base reverse micelle charging mechanism the acid-base properties of the particles and the surfactants had to be determined. The aqueous point of zero charge (PZC) or isoelectric point (IEP) has been used to quantify the acid-base properties of the particles. To determine the acid-base property of a given reverse micelle-forming surfactant, the maximum particle charging is determined for an array of oxide particles covering a range of aqueous PZC or IEP values, as shown schematically in Figure 1.5. The PZC or IEP pH value at which the particle charging changes from negative to positive is identified as the "effective pH" or the acid-base number (ABN) for the surfactant. The ABN appears to be unique to the

surfactant provided that the moisture content of the system is kept low (< 100 ppm)[17,20] and the dielectric constant of the dispersion medium is ≈ 2.

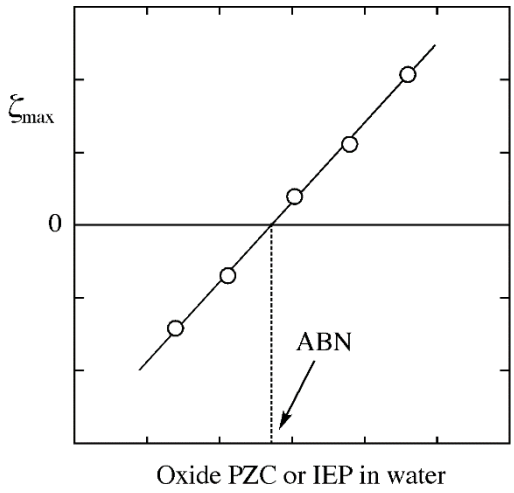

Figure 1.5. Determination of the effective acid-base number (ABN) for the charging of oxide particles in apolar media.[12] (Reproduced from reference 12).

Thus, by comparing a surfactant's ABN to a particle's measured aqueous PZC or IEP, an accurate prediction of the polarity can be made. For example, if a surfactant is more acidic than a particle (ABN<PZC), it will charge the particle positively. To date, mineral oxides, carbon black particles, pigment particle, and clays have been shown to charge in accord with the following relationship:

$$\zeta_{\max} \propto HLB_{surfactant}(pH_{PZC} - ABN)\,, \tag{1.4}$$

where $\zeta_{\max}$ is the maximum particle zeta potential as a function of surfactant concentration, $HLB_{surfactant}$ is the HLB of the surfactant, pH_{PZC} is the aqueous PZC of the particle, and ABN is the empirically determined effective pH or acid-base number of the surfactant.[13] The hydrophile-lipophile balance (HLB) is one way to classify the hydrophillicity of a surfactant and is defined as 20 times the mass of the hydrophilic portion divided by the total mass. Figure 1.6 below summarizes all of the particles tested to date including clay particles from Ch. 2 and shows a line graph of Eq. (1.4).

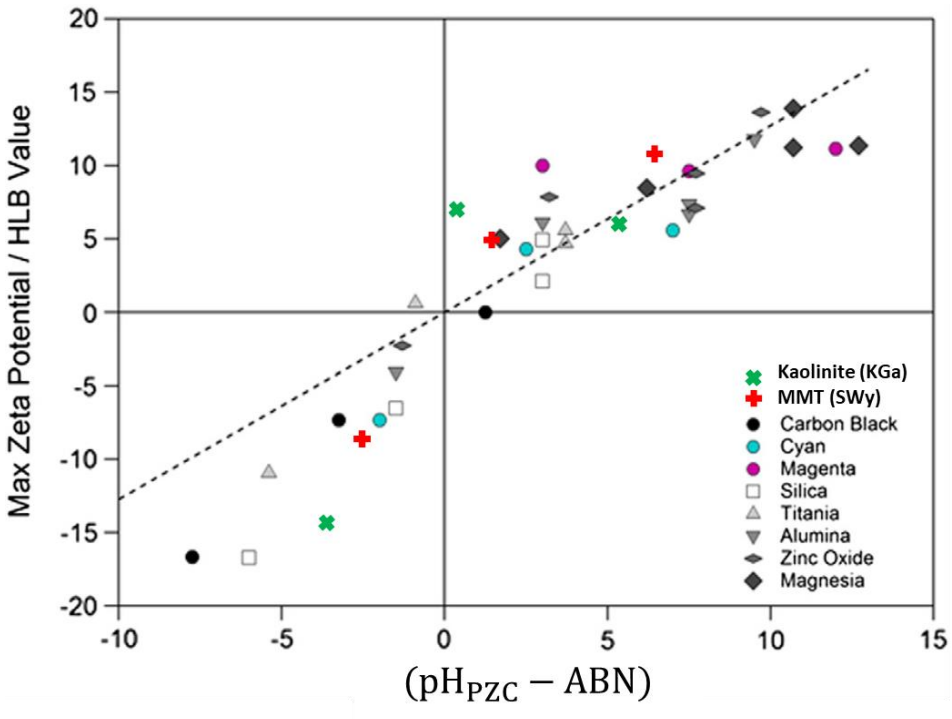

Figure 1.6. Graph reproduced from Gacek et al 2015 showing the acid-base relationship between particle and surfactant and its effect on maximum zeta potential.[13] Overlaid on the same graph are the results from the Kaolinite, and Montmorillonite clay particles.

The positively charged clay with Span 80 and AOT fits very well with the model and the previously tested particles. The negatively charged clay with OLOA deviated from the model, however, the other particles also deviated in the same direction.

1.4 Materials and Methods

It is useful to compile the materials and methods used throughout this dissertation as many of them are used repeatedly in different studies throughout. Figure 1.7 summarizes the relative acid-base properties of the materials used and depicts the structures of the three main surfactants used throughout this work.

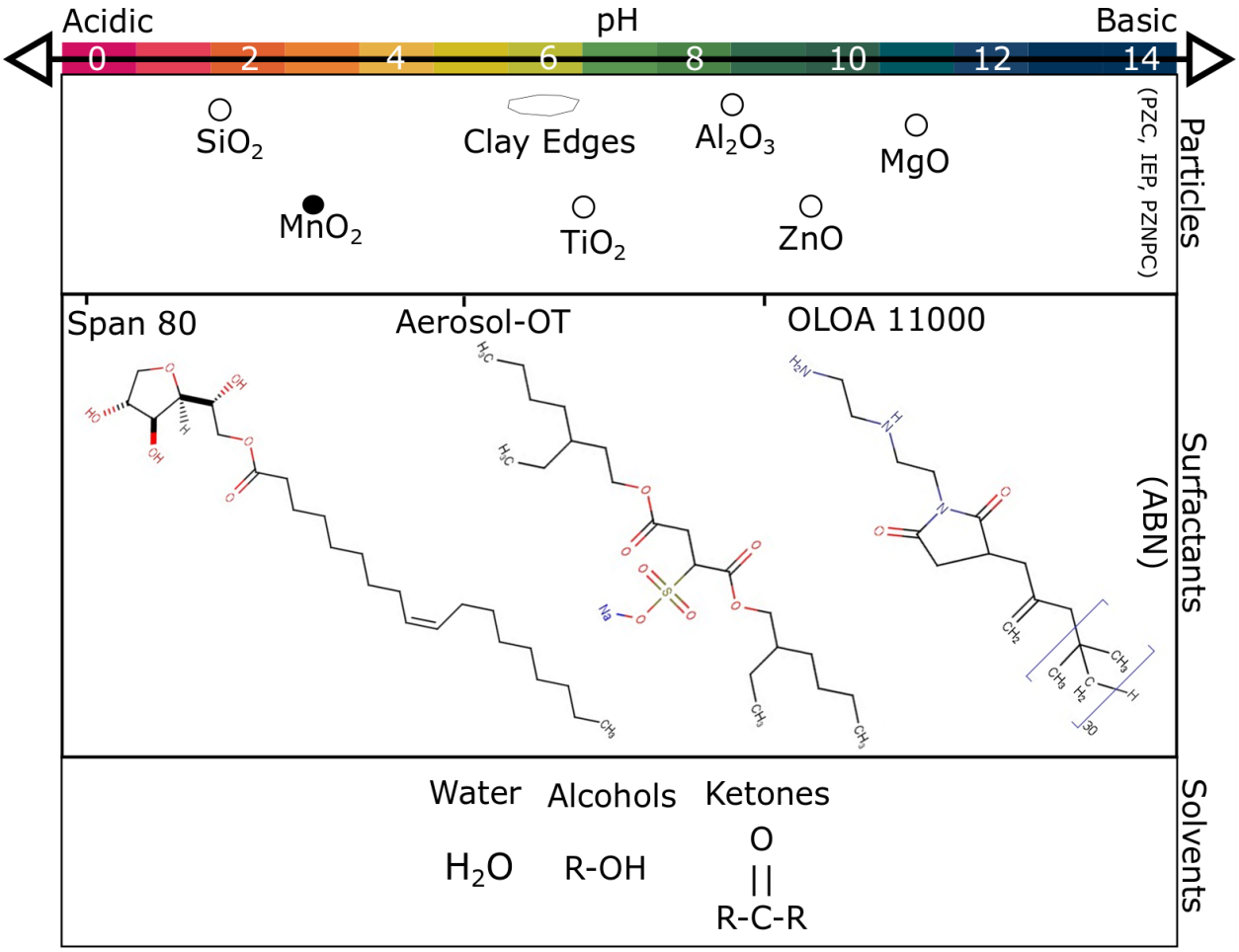

Figure 1.7. Summary of materials and their relative acid-base properties.

1.4.1 *Materials*

1.4.1.1 Particles

Several different mineral oxides and clay minerals were used throughout these studies. All of these solid minerals were in the size range of colloidal particles and contained surface hydroxyl functional groups which could participate in acid-base mechanisms. The relative acid-base properties determined from the particles' points of zero charge (PZC) or point of zero net proton charge (PZNPC) is shown at the top of Figure 1.7.

The different mineral oxides tested in these studies were silica, manganese dioxide, titania, and magnesia. Two silica particles with different crystal structures were used so that their refractive index could be altered without changing their surface functionality: a 250 nm diameter amorphous silica (SiO_2) from Fiber Optics Center, Inc. (New Bedford, MA) and a 1µm quartz silica from GetNanoMaterials (Las Cruces, NM). Both silica particles were required because some of the solvents had refractive indices that were too close to that of amorphous silica, making precise light scattering measurements difficult to obtain. Manganese dioxide (MnO_2) particles with a 50 nm diameter, 300 nm titania (TiO_2) particles, and 300 nm magnesia (MgO) particles all from US Research Nanomaterials, Inc. (Houston, TX) were also investigated in these studies. The aqueous point of zero charge (PZC) for SiO_2, MnO_2, TiO_2, and MgO is approximately 2.5, 4, 6.5, and 11, respectively.[13,27,31] This series of mineral oxide particles allowed for a broad range of particle PZCs to be changed exploring the acid-base reverse micelle charging mechanisms.

Two different kaolinite and montmorillonite clay minerals were studied in Chapter 2. The two kaolinite samples were Kaolin, which contains mostly kaolinite, from the J.T. Baker Chemical Company (Phillipsburg, NJ) and a kaolinite source clay, KGa-2 (Warren County, Georgia). The two montmorillonite samples studied were a montmorillonite from Southern Clay Products, Inc. (Gonzales, TX) and a montmorillonite source clay, SWy-3 (Crook County, Wyoming). The two source clays were received from the Clay Minerals Society (Chantilly, VA) and were used to compare the results from the other clays tested. KGa-2 and SWy-3 have previously been studied and shown to have a point of zero net proton charge (PZNPC) or edge PZC of approximately 5.4 and 6.5 respectively.[32,33]

1.4.1.2 Surfactants

Three different surfactants were used extensively throughout the research conducted in this dissertation: Aerosol-OT (AOT), OLOA 11000 (OLOA), and Span 80. They are all oil-soluble and form reverse micelles in apolar media.

Aerosol-OT or sodium dioctylsulfosuccinate is an anionic surfactant obtained from Fisher Scientific (Pittsburgh, PA). It was received as solid anhydrous AOT and has an acid-base number (ABN) of 5.[13,17] One benefit of AOT is its known ability to form spherical reverse micelles over the entire range of solvent dielectric constants explored in these studies.[23,34,35] The hydrophile-lipophile balance (HLB) is 10.2 and in apolar media it has a critical micelle concentration (CMC) around 0.001wt%.[10,13,18] The molecular weight is 445 g/mol and the molecule is shown in Figure 1.7. AOT has also been shown to be hygroscopic[18] and its reverse micelles can be swelled with the addition of water in nonaqueous systems.[36–38]

OLOA 11000 or polyisobutylene succinimide is a nonionic surfactant from Chevron Oronite (Bellaire, TX). OLOA 11000 has an HLB of 3.5 and an ABN of 9 making it the most basic surfactant used in these studies. OLOA's CMC in Isopar-L is 0.005wt%.[10,13,18] The repeat unit in its hydrophobic tail was assumed to be 30 resulting in a molar mass of ~1900 g/mol though it has been reported to be highly polydisperse and have a significantly lower molecular weight.[39]

Span 80 or sorbitan monooleate (Span 80) from SigmaAldrich Corp. (St. Louis, MO) is a nonionic surfactant with an ABN of 0.[13,17] It is the most acidic surfactant used in these studies and has a CMC in Isopar-L of approximately 0.003wt%.[10,13,18] Span 80's HLB is 4.3 and it has a molecular weight of 429 g/mol. A series of Span surfactants with the same head group and different tails was also examined in Chapter 3. The series allowed for the surfactant head group to remain constant, i.e., same acid-base properties, while different tails could be used to change

the HLB and the structures of the reverse micelles. The different tails of Span 20, 40, and 60 were linear saturated carbon chains with 11, 15, and 17 carbons respectively. Span 80's tail has 17 carbons with one double bond in the middle. Span 65 is a tri-tailed analog of Span 60 and Span 85 is the tri-tailed analog of Span 80.

1.4.1.3 Solvents

The apolar solvent of choice for the majority of past and present research in this lab is Isopar-L supplied by ExxonMobil Chemical (Houston, TX). It is a synthetic isoparaffin fluid with a dielectric constant of 2.0. Its structure contains C8 to C15 saturated hydrocarbons with less than 2% aromatics. Its cost-advantages make it a good lab grade apolar solvent for many applications.

Chapter 5 investigates surfactant mediated particle charging in other nonaqueous solvents. Eight different straight chain alcohols and three ketones were examined in this study: methanol HPLC grade ≥99.9% from Sigma-Aldrich (St. Luis, MO); ethanol 200 proof from Decon Laboratories, Inc. (King of Prussia, PA); 1-propanol and 1-butanol both HPLC grade from Fisher Scientific (Pittsburgh, PA); 1-pentanol 99% pure from Acros Organics (part of Thermo Fisher Scientific); and 1-hexanol 99%, 1-heptanol 99%, and 1-octanol 99% all from Alfa Aesar (Ward Hill, MA); acetone 99.8% HPLC grade from Fisher Scientific (Pittsburgh, PA); methyl ethyl ketone 99.9% from Fisher Scientific (Pittsburgh, PA); and 3-pentanone (diethyl ketone) reagent grade ≥ 99% from Honeywell (Charlotte, NC).

1.4.2 *Methods*

1.4.2.1 Sample Preparation

Similar sample preparations were used in the majority of the experiments in this dissertation. Samples were prepared by first making solutions of each surfactant in Isopar-L (or other nonaqueous solvents) at various weight percent ranging from 10^{-5} to 5 in 50 ml

polyproylene falcon tubes. Next, solutions were filtered with 20nm Whatman Anotop^{TM} 25 plus inorganic membrane filters to remove all dust and contaminates from the samples brought in with the solvents or surfactants. Each solution sample was then mixed or sonicated and allowed to equilibrate for 12 hrs. For samples containing particles, mineral oxide particles were dried in an oven for 2 hrs at 150^{o}C and then added to the solutions at a loading of 500 ppm (~0.001g/10mL). Each solution with particles was then sonicated for 3 min and allowed to equilibrate for 12 hrs before measuring its electrophoretic mobility. Surfactant and particle concentrations were assumed to be low enough to have a negligible effect on the viscosity or density of the samples. Therefore, the properties of the solutions were assumed to be equal to those of the specific solvent. The prepared samples were then measured using several different measurement techniques to determine water content, conductivity, particle size, electrophoretic mobility, and small-angle scattering of surfactant structures, all of which are discussed next.

1.4.2.2 Water content measurement and control

Measuring and maintaining low water content throughout these experiments was important since previous studies have shown that water content can impact the sign and magnitude of particle charge in apolar media.[17,19,20] To maintain a low water content in the samples, solvents were stored with 3 Å and 4 Å molecular sieves. The surfactant AOT was also kept with molecular sieves since it is known to be hygroscopic.[13,18] Additionally, all surfactant solutions and particles were stored in a desiccator.

Water content of the finished samples was measured by a C20 coulometric Karl Fischer titration from Mettler Toledo (Columbus, OH). The coulometric Karl Fischer analysis uses iodine which is generated electrochemically at the anode, Eq. (1.5) during the titration to monitor the consumption of water.

$$2\,I^- \rightarrow I_2 + 2\,e^- \quad (1.5)$$

$$ROH + SO_2 + 3\,RN + \ I_2 \ + \ H_2O \leftrightarrow (RNH)\cdot SO_4R + 2\,(RNH)I \quad (1.6)$$

Eq. (1.6) is the standard reaction equation for the KF reaction. The amount of water is determined by monitoring the electrical current, Coulombs (C), required to generate the iodine needed to consume all of the water present. The device's literature states that 1 mg of water consumes 10.712 C of electrical current. The C20 is capable of measuring water content from 1ppm to 5% water proving to be very useful throughout the experiments presented here.[40]

1.4.2.3 Conductivity measurements for determining critical micelle concentrations

Two different conductivity probes were used to perform conductometric titrations. In apolar media with a dielectric constant of 2.0, conductometric titrations were completed using a DT-700 Nonaqueous Conductivity Probe from Dispersion Technologies (Bedford Hills, NY). The conductivity of each sample was measured 20 times with a sinusoidal frequency of 1 Hz, and averaged. The DT-700 has been noted to have a lower limit of 10^{-11} S/m for accurately measuring conductivity. An example of a conductometric titration in apolar media measured by this device is shown in Figure 1.4 where conductivity is plotted against the surfactant concentration. The point of slope change indicates the presence of micelles as the system now has the ability to stabilize charge and undergo disproportionation reactions which increase conductivity.

In leaky dielectric solvents, which have intermediate dielectric constants ($5<\varepsilon<40$), the conductivity is significantly greater and requires a different conductivity probe. Conductivity measurements in these solvents were measured using a Mettler-Toledo (Columbus, OH) SevenCompact conductivity meter with the InLab 741 probe which has a range of 10^{-3} – 500 µS/cm. Each sample was measured at least five times at room temperature and then averaged. Conductivity measurements were collected over a broad range of surfactant concentrations (0 to

12mM) to determine the surfactant's CMC in these solvents. The results from these conductivity measurements differ from those in apolar media due to the measurable conductivity below the CMC. Similar in shape to the titration results found in water, two linear regions were established as shown in Figure 5.2. The intersection of two linear trend lines determines the critical micelle concentration (CMC) of the surfactant in a given solvent which is a technique for determining CMC that has been previously described.[23,27]

1.4.2.4 Phase Analysis Light Scattering (PALS) for determining particle charge

Particle charge is quantified by the zeta potential which is defined as the electrokinetic potential in the double layer at the slip plane. Zeta potential is determined by first measuring the movement of colloidal particles in an electric field. The larger the magnitude of particle charge, the greater their velocity is in an electric field. The electrophoretic mobility is the velocity of a particle divided by the applied electric field strength. Phase analysis light scattering (PALS) was used to measure the electrophoretic mobility of each sample using the ZetaPals instrument from the Brookhaven Instruments Corporation (Holtsville, NY).[27]

Once the electrophoretic mobility was measured, the zeta potential could be calculated using the appropriate relationships. In apolar media, where it was determined that the electric double layer is very large ($\kappa a < 0.1$), the zeta potential can be calculated with the Hückel Equation shown in Eq. (1.3).[27] If κa is too large, then other relationships must be employed to calculate zeta potential. If $\kappa a > 200$ like it is in water, the Helmholtz-Smoluchowski equation must be used. Alternatively, if $0.1 < \kappa a < 200$ as it is in leaky dielectrics, then the determination of zeta potential requires the use of O'Brien and White computations.[27]

Electric field induced charging has been shown to impact the magnitude of charge on particles in apolar media.[17,19,20] To avoid this, ZetaPals measurements were made at a range of

applied voltages. By using four different voltages from 40 V to 200 V, induced charging effects can be accounted for by extrapolating the electrophoretic mobility to zero, determining the zero field electrophoretic mobility.[17,19,20] If no induced charging was observed, then all of the measurements can be averaged. Electrophoretic mobility measurements were made on the ZetaPals at 25°C with an electrode spacing of 0.5 cm and a sinusoidal frequency of 2 Hz. Due to the increase in conductivity for leaky dielectric solvents the voltage setting had to be set significantly lower and was often optimized by the machine.

1.4.2.5 Small-Angle Scattering

Small-angle neutron and x-ray scattering experiments were conducted to investigate the size and structure of reverse micelles. Neutrons interact and scatter through nuclear interactions while x-rays scatter through electromagnetic interactions with the atom's electron clouds.[41] The ability for an object to scatter per volume is characterized by its scattering length density (SLD). A simple scattering experiment diagram is shown in Figure 1.8 below.

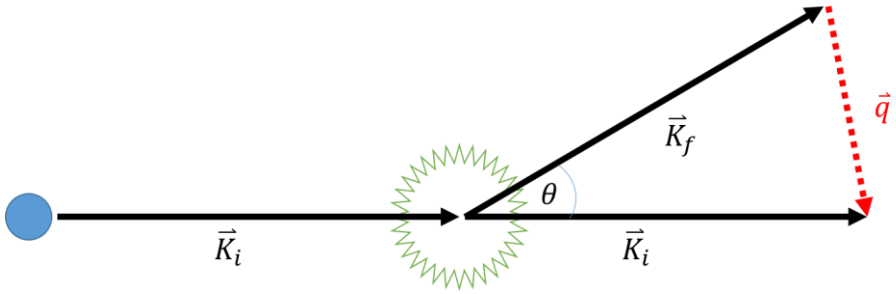

Figure 1.8. Simple scattering experiment. X-ray or neutron source (blue). Scattering object (green). Scattering vector (q) (red).

The source emits x-rays or neutrons targeted toward the scattering object with an incident wavevector, $\vec{K}_i$. The neutron (or x-ray) scatters off the object according to its SLD emerging by some final wavevector, $\vec{K_f}$. q is the scattering vector and is defined in Eq. (1.7) below:[42]

$$q = \frac{4\pi}{\lambda}\sin(\frac{\theta}{2}), \quad (1.7)$$

where λ is the wavelength of the neutron or x-ray and θ is the scattering angle. The main advantage of neutron scattering over other scattering methods is because of the technique called contrast variation. By replacing hydrogen with deuterium, one can drastically alter the SLD of components and examine systems in ways which might otherwise be impossible. Hydrogen has a scattering length of -3.74x10^{-5} Å while deuterium has a drastically different scattering length of 6.67x10^{-5} Å. When examining reverse micelles, x-rays can measure only the core of the reverse micelles because the hydrocarbon surfactant tails have the same x-ray scattering length density (SLD) as the hydrocarbon solvent. Neutrons, however, can be used to probe the size and structure of the hydrocarbon tails of reverse micelles by deuterating the background solvent to achieve the necessary contrast.

The scattering intensity I or $\frac{d\Sigma}{d\Omega}(\mathrm{q})$ is the neutron flux per area per time and is shown in Equation (1.8) below:

$$\frac{d\Sigma}{d\Omega}(\mathrm{q}) = \frac{N}{V}(\rho_1 - \rho_2)^2 V_p^2 P(q) S(q), \quad (1.8)$$

where ρ_1 and ρ_2 are scattering length densities, $\frac{N}{V}$ is the volume fraction of the scatterers, V_p is the volume of the individual scatterers, $P(q)$ is the form factor that represents the interference of neutrons scattered from different parts within the same object, and $S(q)$ is the structure factor which represents the interference between different objects.[41–43] Scattering data must be fit with previously determined models to analyze. A core shell sphere model is often chosen for analyzing reverse micelle data as it gives dimensions of both the polar core and the hydrophobic tails. All of the reduced intensity (I) versus scattering vector (q) data is these studies were modeled using SasView 4.2.1 (sasview.org).

The Guinier analysis is a useful method for determining the size of the scattering object. In the low-q limit, a Guinier analysis can be conducted to extract the radius of gyration from the slope of a plot of $\ln\big(I(q)\big)$ vs q^2. Equation (1.9) below shows the resulting equations from the Guinier approximation:[27,42]

$$\ln\big(I(q)\big) = \ln\big(I(0)\big) - \frac{R_g^2}{3} q^2, \tag{1.9}$$

where R_g is the radius of gyration. The radius of a sphere can be determined from the radius of gyration as shown in Eq. (1.10) below:[27]

$$R_g^2 = \frac{3}{5} R^2, \tag{1.10}$$

where R is the radius of a sphere. This method proved to be useful when analyzing results from both small-angle neutron (SANS) and small-angle x-ray (SAXS) scattering experiments.

1.5 REFERENCES

(1) Klinkenberg, A.; van der Minne, J. L. *Electrostatics in the Petroleum Industry: The Prevention of Explosion Hazards*; Elsevier, 1958.

(2) Morrison, I. D. Electrical Charges in Nonaqueous Media. *Colloids Surf. Physicochem. Eng. Asp.* **1993**, *71* (1), 1–37.

(3) Nelson, S.; Pink, R. Solutions of Metal Soaps in Organic Solvents .3. the Aggregation of Metal Soaps in Toluene, Isobutyl Alcohol, and Pyridine. *J. Chem. Soc.* **1952**, No. MAY, 1744–1750. https://doi.org/10.1039/jr9520001744.

(4) Nelson, S.; Pink, R. Solutions of Metal Soaps in Organic Solvents .14. Direct-Current Conductivity in Solutions of Some Metal Oleates in Toluene. *J. Chem. Soc.* **1954**, No. DEC, 4412–4417. https://doi.org/10.1039/jr9540004412.

(5) Gacek, M. M.; Berg, J. C. Investigation of Surfactant Mediated Acid–Base Charging of Mineral Oxide Particles Dispersed in Apolar Systems. *Langmuir* **2012**, *28* (51), 17841–17845. https://doi.org/10.1021/la303943k.

(6) Espinosa, C. E.; Guo, Q.; Singh, V.; Behrens, S. H. Particle Charging and Charge Screening in Nonpolar Dispersions with Nonionic Surfactants. *Langmuir* **2010**, *26* (22), 16941–16948. https://doi.org/10.1021/la1033965.

(7) Guo, Q.; Lee, J.; Singh, V.; Behrens, S. H. Surfactant Mediated Charging of Polymer Particles in a Nonpolar Liquid. *J. Colloid Interface Sci.* **2013**, *392*, 83–89. https://doi.org/10.1016/j.jcis.2012.09.070.

(8) Guo, Q.; Singh, V.; Behrens, S. H. Electric Charging in Nonpolar Liquids Because of Nonionizable Surfactants. *Langmuir* **2009**, *26* (5), 3203–3207. https://doi.org/10.1021/la903182e.

(9) Michor, E. L.; Berg, J. C. The Temperature Effects on Micelle Formation and Particle Charging with Span Surfactants in Apolar Media. *Langmuir* **2015**, *31* (35), 9602–9607.
(10) Poovarodom, S.; Berg, J. C. Effect of Particle and Surfactant Acid–Base Properties on Charging of Colloids in Apolar Media. *J. Colloid Interface Sci.* **2010**, *346* (2), 370–377. https://doi.org/10.1016/j.jcis.2010.03.012.
(11) Poovarodom, S.; Poovarodom, S.; Berg, J. C. Effect of Alkyl Functionalization on Charging of Colloidal Silica in Apolar Media. *J. Colloid Interface Sci.* **2010**, *351* (2), 415–420.
(12) Ponto, B. S.; Berg, J. C. Clay Particle Charging in Apolar Media. *Appl. Clay Sci.* **2018**, *161*, 76–81. https://doi.org/10.1016/j.clay.2018.04.016.
(13) Gacek, M. M.; Berg, J. C. The Role of Acid–Base Effects on Particle Charging in Apolar Media. *Adv. Colloid Interface Sci.* **2015**, *220*, 108–123. https://doi.org/10.1016/j.cis.2015.03.004.
(14) Smith, G. N.; Eastoe, J. Controlling Colloid Charge in Nonpolar Liquids with Surfactants. *Phys Chem Chem Phys* **2013**, *15* (2), 424–439. https://doi.org/10.1039/C2CP42625K.
(15) HP ElectroInk FAQ Document. Hewlett-Packard Development Co. 2012.
(16) Hsu, M. F.; Dufresne, E. R.; Weitz, D. A. Charge Stabilization in Nonpolar Solvents. *Langmuir* **2005**, *21* (11), 4881–4887.
(17) Gacek, M. M.; Berg, J. C. Investigation of Surfactant Mediated Acid–Base Charging of Mineral Oxide Particles Dispersed in Apolar Systems. *Langmuir* **2012**, *28* (51), 17841–17845.
(18) Gacek, M.; Brooks, G.; Berg, J. C. Characterization of Mineral Oxide Charging in Apolar Media. *Langmuir* **2012**, *28* (5), 3032–3036.
(19) Espinosa, C. E.; Guo, Q.; Singh, V.; Behrens, S. H. Particle Charging and Charge Screening in Nonpolar Dispersions with Nonionic Surfactants. *Langmuir* **2010**, *26* (22), 16941–16948.
(20) Gacek, M.; Bergsman, D.; Michor, E.; Berg, J. C. Effects of Trace Water on Charging of Silica Particles Dispersed in a Nonpolar Medium. *Langmuir* **2012**, *28* (31), 11633–11638.
(21) Gacek, M. M.; Berg, J. C. Effect of Synergists on Organic Pigment Particle Charging in Apolar Media. *Electrophoresis* **2014**, *35* (12–13), 1766–1772.
(22) Gacek, M. M.; Berg, J. C. Effect of Surfactant Hydrophile-Lipophile Balance (HLB) Value on Mineral Oxide Charging in Apolar Media. *J. Colloid Interface Sci.* **2015**, *449*, 192–197.
(23) Michor, E. L.; Berg, J. C. Micellization Behavior of Aerosol OT in Alcohol/Water Systems. *Langmuir* **2014**, *30* (42), 12520–12524.
(24) Michor, E. L.; Berg, J. C. The Particle Charging Behavior of Ion-Exchanged Surfactants in Apolar Media. *Colloids Surf. Physicochem. Eng. Asp.* **2017**, *512*, 1–6.
(25) Michor, E. L.; Berg, J. C. Temperature Effects on Micelle Formation and Particle Charging with Span Surfactants in Apolar Media. *Langmuir* **2015**, *31* (35), 9602–9607.
(26) Michor, E. L.; Ponto, B. S.; Berg, J. C. Effects of Reverse Micellar Structure on the Particle Charging Capabilities of the Span Surfactant Series. *Langmuir* **2016**, *32* (40), 10328–10333.
(27) Berg, J. C. *An Introduction to Interfaces & Colloids: The Bridge to Nanoscience*; World Scientific, 2010.
(28) Israelachvili, J. N. *Intermolecular and Surface Forces: Revised Third Edition*; Academic press, 2011.

(29) Pugh, R. J.; Matsunaga, T.; Fowkes, F. M. The Dispersibility and Stability of Carbon Black in Media of Low Dielectric Constant. 1. Electrostatic and Steric Contributions to Colloidal Stability. *Colloids Surf.* **1983**, *7* (3), 183–207.
(30) Pugh, R. J.; Fowkes, F. M. The Dispersibility and Stability of Coal Particles in Hydrocarbon Media with a Polyisobutene Succinamide Dispersing Agent. *Colloids Surf.* **1984**, *11* (3–4), 423–427.
(31) Kosmulski, M. *Chemical Properties of Material Surfaces*; CRC press, 2001.
(32) Tombácz, E.; Szekeres, M. Colloidal Behavior of Aqueous Montmorillonite Suspensions: The Specific Role of PH in the Presence of Indifferent Electrolytes. *Appl. Clay Sci.* **2004**, *27* (1–2), 75–94. https://doi.org/10.1016/j.clay.2004.01.001.
(33) Schroth, B. K.; Sposito, G. Surface Charge Properties of Kaolinite. In *MRS Proceedings*; Cambridge Univ Press, 1996; Vol. 432, p 87.
(34) Hollamby, M. J.; Tabor, R.; Mutch, K. J.; Trickett, K.; Eastoe, J.; Heenan, R. K.; Grillo, I. Effect of Solvent Quality on Aggregate Structures of Common Surfactants. *Langmuir* **2008**, *24* (21), 12235–12240.
(35) Kotlarchyk, M.; Huang, J. S.; Chen, S. H. Structure of AOT Reversed Micelles Determined by Small-Angle Neutron Scattering. *J. Phys. Chem.* **1985**, *89* (20), 4382–4386.
(36) Eskici, G.; Axelsen, P. H. The Size of AOT Reverse Micelles. *J. Phys. Chem. B* **2016**, *120* (44), 11337–11347.
(37) Eicke, H.-F.; Rehak, J. On the Formation of Water/Oil-Microemulsions. *Helv. Chim. Acta* **1976**, *59* (8), 2883–2891.
(38) Mathews, M. B.; Hirschhorn, E. Solubilization and Micelle Formation in a Hydrocarbon Medium. *J. Colloid Sci.* **1953**, *8* (1), 86–96.
(39) Parent, M. E.; Yang, J.; Jeon, Y.; Toney, M. F.; Zhou, Z.-L.; Henze, D. Influence of Surfactant Structure on Reverse Micelle Size and Charge for Nonpolar Electrophoretic Inks. *Langmuir* **2011**, *27* (19), 11845–11851.
(40) Muhr, H. J.; Rohner, R. Good Titration Practice TM in Karl Fischer Titration. *Mettler Toledo* **2011**, *98*.
(41) Hammouda, B. Probing Nanoscale Structures-the sans Toolbox. *Natl. Inst. Stand. Technol.* **2008**, 1–717.
(42) Jackson, A. J. Introduction to Small-Angle Neutron Scattering and Neutron Reflectometry. *NIST Cent. Neutron Res.* **2008**, 1–24.
(43) Sivia, D. S. *Elementary Scattering Theory: For X-Ray and Neutron Users*; Oxford University Press, 2011.

Chapter 2. CLAY PARTICLE CHARGING IN APOLAR MEDIA

B. S. Ponto and J. C. Berg, "Clay particle charging in apolar media," Appl. Clay Sci., vol. 161, pp. 76–81, Sep. 2018.

2.1 ABSTRACT

Advancements in electrophoretic displays (e.g., the Amazon Kindle®) and new high-quality printing technologies (e.g., HP Indigo®) have been made possible by the ability to control and understand particle charging in apolar media. While previous work has investigated the acid-base charging mechanisms of oxides and similar particles which have only one charging mechanism in water, the purpose of this study was to determine if and how clay particles, which have two known aqueous charging mechanisms, charge in apolar media. Characterization of kaolinite and montmorillonite surface charging properties and mechanisms were conducted in apolar media utilizing different surfactants. It was found that clay particle charging behavior as a function of surfactant concentration mimicked the expected trend of previously studied oxides, which can charge only via an acid-base mechanism. Furthermore, by comparing the point of zero charge of the edge groups (edge PZC) or the point of zero net proton charge (PZNPC) of the clay particle to the acid-base number (ABN) of the surfactant, the polarity of the particle charge can be predicted. In addition to particle charging, it was shown that the surfactants also improve the stability against aggregation and settling of the particles.

2.2 INTRODUCTION

Clays are unique materials that find application in building materials, ceramics, paints, moisture barriers, and many other products.[1–4] Most are naturally-occurring, platelet-shaped layered phyllosilicates with particle diameters < 2 μm and thicknesses < 100 nm.[1,5,6] While easily

exfoliated and dispersible in water, they may also be modified with long chain alkylammonium cations to make "organoclays," which are swellable and dispersible in organic media where they find application as structure-forming and thickening agents in oil-based paints, greases, adhesives, cosmetics, etc.[3,7,8] Clay particles also appear to play an important role in the production of tar sand oil and bitumen recovery.[2,9] Most applications involving clays depend on the practitioner's ability to control their stability with respect to aggregation. In aqueous media they are generally stabilized against aggregation by electrostatic forces, whereas in nonaqueous "apolar media," i.e., media of ultra-low dielectric constant ($\varepsilon \approx 2$), it is presumed that they are stabilized or at least lubricated by their adsorbed layers of long-chain cations. It is possible, however, that electrostatic forces also play an important role in stabilizing organoclays in apolar media. While clay particle charging is well understood for aqueous systems, there is only limited knowledge of the process in non-aqueous environments. The present research thus seeks to understand how clay particles charge in apolar media and strategies for controlling the sign and magnitude of such charging.

As a result of their layered structures consisting commonly of tetrahedral sheets of SiO_4 linkages and octahedral sheets forming $Mg_6O_{12}^{12-}$ or $Al_4O_{12}^{12-}$ linkages, clays acquire charge in water by two distinct mechanisms. First, substitution of Si^{4+} atoms with lower-valence Al^{3+} atoms in the tetrahedral layers or occasionally lower-valance substitution of octahedral cations (Al^{3+} or Mg^{2+}), i.e., "isomorphic substitution," causes a permanent negative charge on the clay surfaces. In kaolinite, which is a 1:1 or tetrahedral-octahedral (TO) type clay with a tetrahedral SiO_4 layer on only one side, for example, yields a cation exchange capacity (CEC) of 1-10 meq per 100 g.[1,6,10] Montmorillonite is a 2:1 or TOT type clay with tetrahedral layers on both the top and bottom surfaces resulting in a higher CEC than kaolinite, with values of 70-100 meq/100 g.[1,6,11] The excess negative charges are balanced by a layer of adsorbed exchangeable cations such as Ca^{2+},

Mg^{2+}, Na^{+}, or K^{+} which in water can dissociate and leave behind a permanent negative surface charge.[2,12] The second charging mechanism derives from the edges and, in the case of kaolinite, the bottom alumina octahedral sheets as well, which have -OH functional groups that are known to charge with pH dependence in water in the same way as mineral oxides. These charge by an acid-base mechanism.[1,2,5,6,11] At low pH values, -OH groups are protonated and thus acquire a positive charge, whereas at high pH values they are de-protonated and acquire a negative charge. At a particular pH, viz., the "point of zero charge" (PZC), dependent on the mineral's identity, the net charge is zero. For mineral oxides, the PZC is easily determined by a potentiometric titration, or an electrokinetic titration, leading to the "isoelectric point" (IEP), defined as the pH at which the particle electrophoretic mobility is zero. (In the absence of specific ion adsorption, the PZC and IEP are the same.)

Obtaining the acid-base properties of clay particles in water is challenging, however, due to the multiple charging mechanisms, lack of a common intersection point during raw titrations, ion exchange, and aggregation.[11,13] The latter occurs at low-to-moderate pH values, when the edge charge is positive and the plate charge is negative, producing edge-to-plate aggregation. To determine only the acid-base properties of the -OH groups on the clay particles, the "edge PZC," or the point of zero net proton charge (PZNPC), must be determined.[11] It is defined as the PZC of the amphoteric clay hydroxyl groups or the pH where the net proton surface charge density equals zero.[11,14] In kaolinite, with one basal surface as well as the edge with hydroxyl groups, the PZNPC was found in one study to be 6-6.5 [5], and montmorillonite samples were found to have a value of 6.5.[11]

While the charging of mineral oxides and other materials in apolar media, which finds application in electrophoretic displays (e.g., the Amazon Kindle®) and digital printing (e.g., HP

Indigo®), appears to be well-understood [15], the literature on the charging of clay particles in non-aqueous media is scant. One study investigated the surface charging of kaolinite particles in air using force microscopy techniques [2], and found that kaolinite nanoparticles had a heterogeneous surface potential distribution which was layer dependent. Another study investigated the charging of organoclays in media of intermediate dielectric constant and found the charging (as evidenced by measured electrophoretic mobility leading to zeta potentials) to be dependent on the identity of the suspending medium. The charging was likely the result of acid-base interaction between the clay surfaces and the suspending medium, dependent on the relative donicity of the materials, as has been studied extensively for oxides and other minerals in moderate dielectrics.[16] The charging of clay particles in liquid media of ultra-low dielectric constant, i.e., "apolar media," appears not to have been investigated, and the present work is focused on this type of system. Such knowledge could lead to new or improved products consisting of clay dispersions in such media, and new methods for removing residual clay particles from oil.[2]

2.2.1 *Background*

It is useful to review briefly the mechanism of charging mineral oxides and similar materials in apolar media. Stabilizing charge in such media is more difficult than in aqueous systems because the low dielectric allows coulombic attractive forces to be felt over much greater distances. The Bjerrum length λ_B, shown below, is the separation distance at which two opposite charges possess coulombic attractive energy equal to the thermal energy (k_BT).

$$\lambda_B = \frac{e^2}{4\pi\varepsilon\varepsilon_o k_B T}, \tag{2.1}$$

where ε is the dielectric constant of the medium, ε_o is the permittivity of free space, and e is the elementary charge. In water, with a dielectric constant of 78, the Bjerrum length is ≈ 0.7 nm, a

distance easily accommodated by the hydration shell of the ions, while in a medium of dielectric constant as low as 2, it is ≈ 28 nm. To maintain such large distances of separation required to stabilize the charges against recombination, it is believed that they must be housed within protective supramolecular structures such as inverse micelles. Once surfactants are added in sufficient concentration to form inverse micelles in such systems, they exhibit measurable electrical conductivity.[10,15,17,18]

There is abundant evidence in the literature suggesting that the charging of oxides or similar particles may ensue via the formation and subsequent dissociation of acid-base adducts between the adsorbing surfactant molecules and functional groups on the particle surfaces, as shown schematically in Figure 2.1. The resulting charged surfactant ions are housed in the inverse micelles, and the charges on the particle surfaces are protected by adsorbed surfactant. Thus the acid-base mechanism has three steps: first, the polar head group of a surfactant molecule will adsorb to the particle surface and form an acid-base adduct; second, charge is transferred between the surface and the surfactant molecule depending on the acid-base properties; and third, the charged surfactant molecule is stabilized by an inverse micelle which allows it to desorb leaving an opposite charge behind.[15,17,19,20] Thus in the absence of added surfactants to form inverse micelles, measurable particle charging in apolar media is not possible.

In addition to the acid-base mechanism it should be noted that other particle charging mechanisms in low permittivity solvents have been proposed for different systems. One example involves preferential adsorption of either an ionized surfactant or its counter ion onto the surface of a solid particle which has been shown to impart charge.[18,21] An additional mechanism has been hypothesized that involves asymmetrical adsorption of charged inverse micelles in the bulk onto polymer particles. It was empirically found that larger inverse micelles were entropically favored

to adsorb and thus in a system where negative inverse micelles are larger than their counterparts, a negative particle charge would be observed.[22,23]

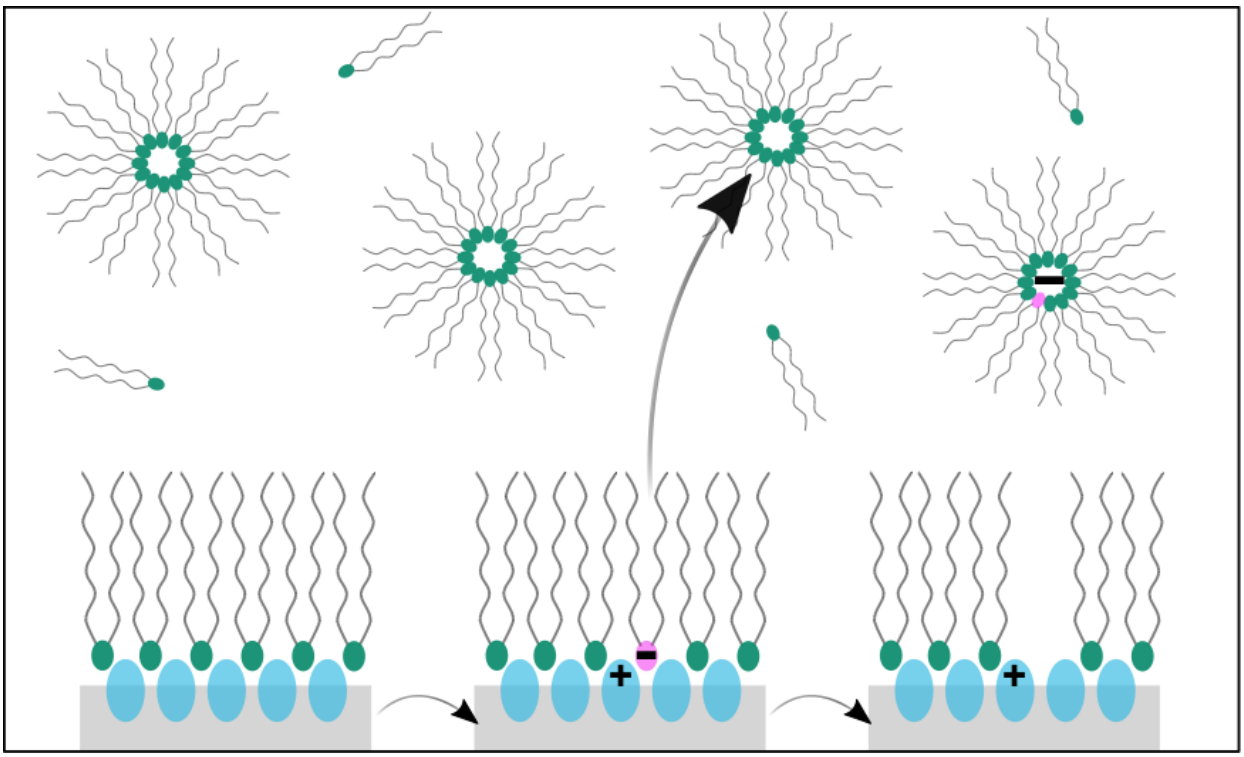

Figure 2.1. Schematic showing acid-base adduct formation, dissociation of surfactant at particle surface, and charge stabilization inside an inverse micelle in the bulk.

Surface charging can be quantified by measuring the particle electrophoretic mobility, u_E, i.e., its velocity divided by the applied electric field strength. Once measured, the effective electrical potential at the particle surface relative to solution interior, i.e., the zeta potential, ζ, may be calculated using appropriate theory. In apolar media, when the electrical double layer thickness is large relative to the particle diameter, this is given by the Hückel Equation:[10]

$$\zeta = \frac{3\mu}{2\varepsilon\varepsilon_o} u_E, \tag{2.2}$$

where μ is the viscosity, ε is the dielectric constant and ε_o is the permittivity of free space.

For oxides in apolar media it is common to monitor the electrophoretic mobility (or the zeta potential) as a function of the concentration of added surfactant, typically yielding results as shown schematically in Figure 2.2.[15,24–27] At low concentrations, below that needed for the formation of inverse micelles, the surfactant is present only as monomers, and no particle charging is observed.[15,18]

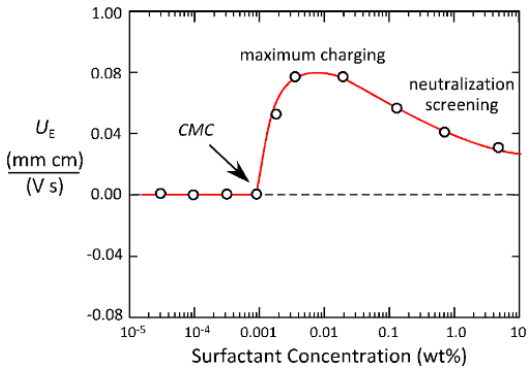

Figure 2.2. Particle charging as a function of surfactant concentration.

After the critical micelle concentration (CMC) is exceeded, particle charging increases sharply, usually reaching a fairly well-defined maximum, beyond which it begins to decrease. The decrease is attributable to electrostatic screening by the increasing concentration of charge-carrying inverse micelles.[15,28] The polarity and magnitude of the maximum charging (or zeta potential) achieved are characteristic primarily of the particle/surfactant system.[15]

The polarity of a particle surface charge is predictable in apolar media when the acid-base properties of both the surfactant and the particles are known. The aqueous point of zero charge (PZC) or isoelectric point (IEP) has been used to quantify the acid-base properties of the particles. Then for a given inverse micelle-forming surfactant, the maximum particle charging is determined for an array of oxide particles covering a range of aqueous PZC or IEP values, as shown schematically in Figure 2.3. The PZC or IEP pH value at which the particle charging changes from negative to positive is identified as the acid-base number (ABN) for the surfactant which is

determined experimentally. The ABN of a given surfactant corresponds to the PZC of an oxide below which particles in apolar media are charged negatively and above which particles are charged positively. It is a useful descriptor of surfactants in apolar media with respect of their ability to charge particles positively or negatively. The ABN appears to be unique to the surfactant provided that the moisture content of the system is kept low (< 100 ppm) [24,26] and the dielectric constant of the dispersion medium is ≈ 2.

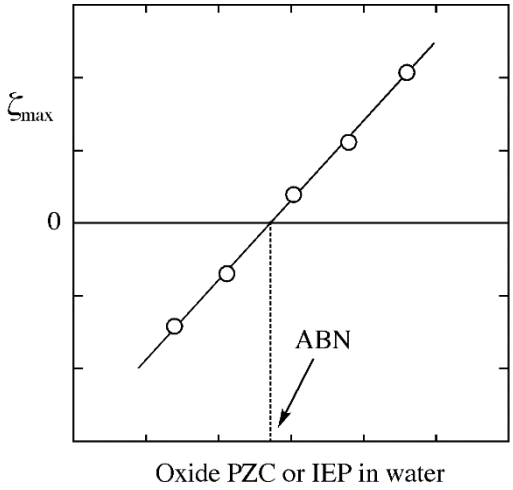

Figure 2.3. Determination of the effective acid-base number (ABN) for the charging of oxide particles in apolar media.

Thus an accurate polarity determination can be made by comparing a surfactant's ABN to a particle's measured PZC or IEP. For example, if a surfactant is more acidic than a particle it will charge the particle positively. Mineral oxides, carbon black particles, and particles for which an effective aqueous PZC or IEP can be determined, have been shown to charge in accord with the following relationship.[15]

$$\zeta_{max} \propto (pH_{PZC\ or\ IEP} - ABN), \tag{2.3}$$

where $\zeta_{max}$is the maximum particle zeta potential, $pH_{PZC\ or\ IEP}$ is the particle's point of zero charge or isoelectric point, and ABN is the acid-base number or "effective pH" of the surfactant.[15] Particles examined thus far have only one means of charging in water, i.e., the pH-dependent acid-

base mechanism, so that their charging in apolar media is described by Eq. (2.3)(2.3). It may be anticipated that the edges of clay particles may charge by the same mechanism in apolar media, but the role, if any, of isomorphic substitution, is unknown.

The objective of the present study is to determine if and how clay particles, which have two known aqueous charging mechanisms, charge in apolar media. It may be hypothesized that the exchangeable cations will not be able to desorb from the clay surface because in the low dielectric, the electrostatic attraction will be too strong and there will be no way to stabilize these charges, but the possibility that these ions may interact with the surfactant to leave a charge on these surfaces remains open. Therefore, it may only be possible to charge the clay particles with inverse micelle interactions with the hydroxyl surface groups and therefore only an acid-base charging mechanism will be observed. If only an acid-base mechanism occurs, then comparing the edge PZC of the clay to the previously-determined ABN for the surfactant should allow one to predict the polarity of the clay particle charge. Two nonionic surfactants, Span 80 (acidic, with ABN ≈ 0) and OLOA 11000 (basic, with ABN ≈ 9) and one ionic surfactant, AOT (with ABN ≈ 5), were used in this study.[15]

2.3 MATERIALS AND METHODS

Four different clay samples were tested in this study: kaolin from the J.T. Baker Chemical Company (Phillipsburg, NJ), montmorillonite from Southern Clay Products, Inc. (Gonzales, TX), a kaolinite source clay KGa-2 (Warren County, Georgia), and a montmorillonite source clay SWy-3 (Crook County, Wyoming). These samples will be referred to as kaolinite, montmorillonite, KGa-2, and SWy-3 respectively. Kaolin contains mostly kaolinite clay. The two source clays were received from the Clay Minerals Society (Chantilly, VA) and were used to compare the results

from the other clays tested. KGa-2 and SWy-3 have previously been studied and shown to have a PZNPC or edge PZC of approximately 5.4 and 6.5 respectively.[11,14]

The apolar solvent selected for this experiment was Isopar-L supplied by ExxonMobil Chemical (Houston, TX). It is a synthetic isoparaffin fluid containing C8 to C15 saturated hydrocarbons with less than 2 % aromatics. The dielectric constant is 2.0 for Isopar-L.

The three surfactants used in this experiment were sorbitan monooleate (Span 80) from SigmaAldrich Corp. (St. Louis, MO), sodium dioctylsulfosuccinate (Aerosol-OT or AOT) from Fisher Scientific (Pittsburgh, PA), and polyisobutylene succinimide (OLOA 11000) from Chevron Oronite (Bellaire, TX). SPAN 80 and OLOA 11000 are both nonionic surfactants with an ABN of 0, and 9, respectively, and AOT is an ionic surfactant with an ABN of 5.[15,24]

Samples were prepared by first making solutions of each surfactant in Isopar-L at various weight percent ranging from 10^{-5} to 1. Next, oven dried clay particles (2 hr at 120˚C) were added to the surfactant solutions at a small loading of ~0.5 mg per 25 ml of solution. Each solution sample was then sonicated for one minute and set to rest for 24 hours after which it was sonicated again for one minute before measuring electrophoretic mobility to disperse the particles that may have settled. Surfactant and particle concentrations were low enough that the viscosity and density of samples were found to be equal to those of Isopar-L.

Previous studies have shown that both water content and electric field induced charging can impact the magnitude of charge on particles in apolar media.[24,26,29] Precautions were taken to eliminate these effects. To maintain a low water content in the samples Isopar-L was stored with size 4A molecular sieves. Additionally, since AOT is known to be hygroscopic, all surfactant solutions and samples were kept in a desiccator.[25] Water content of the finished samples was also

monitored by a C20 coulometric Karl Fischer titration from Mettler Toledo (Columbus, OH) and water content was found to be below ~100 ppm.

Phase analysis light scattering (PALS) was used to measure the electrophoretic mobility of each sample using ZetaPals from the Brookhaven Instruments Corporation (Holtsville, NY). To avoid electric field induced charging effects measurements were made at a range of applied voltages. After concluding that induced charging effects were not significant for the kaolinite, and montmorillonite samples, each measurement was conducted with an applied sinusoidal voltage of 75 V across electrodes spaced 0.5 cm and a frequency of 2 Hz. A more in-depth approach was taken for the two source clay measurements. At each concentration electrophoretic mobility measurements were made at an applied sinusoidal voltage of 40 V, 75 V, 110 V, and 150 V across electrodes spaced 0.5 cm and a frequency of 2 Hz. If induced charging occurred, then the mobility was extrapolated back to zero field strength mobility, as shown in other studies.[24] If no induced charging was observed, then all of the measurements were averaged. While it was determined that $\kappa a < 1$ for the systems investigated in this study, it was assumed that the Hückel regime ($\kappa a < 0.1$) provided a reasonable approximation, so that the zeta potential could be calculated and presented from the electrophoretic mobility measurements.

The HORIBA LA-900 Laser Scattering Particle Size Distribution Analyzer (Kyoto, Japan) was used to measure clay particle size distributions as a function of time. Samples for size measurements had a particle loading of 0.4 mg of clay per 20 ml of 20 nm filtered Isopar-L. For the case with added OLOA the surfactant concentration was set to 0.012 wt%, which is above the critical micelle concentration (CMC).[24] Samples were initially sonicated once for 2 minutes and then immediately measured in the LA-900. Dynamic light scattering (DLS) was used to verify size

distribution measurements using the same ZetaPals from the Brookhaven Instruments Corporation (Holtsville, NY).

2.4 RESULTS AND DISCUSSION

2.4.1 *Electrophoretic Mobility*

There were 12 different clay and surfactant combinations tested in this experiment. Particle size measurements were consistent with literature values for clay particles and were between 0.1 and 2 μm. Systems with no surfactant concentration showed no clay particle charging. Figure 2.4 shows the zeta potential results for each combination as a function of surfactant weight percent.

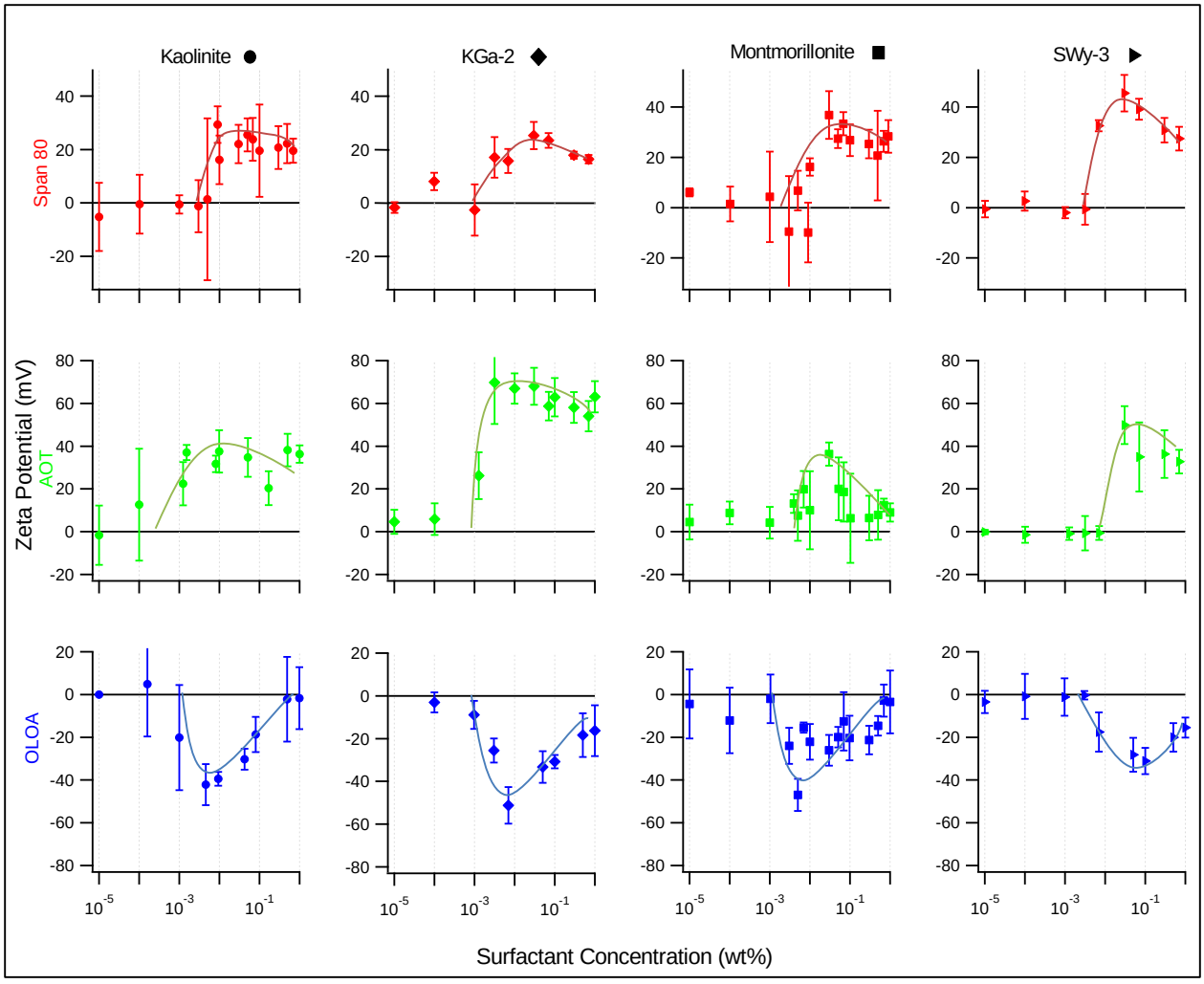

Figure 2.4. Zeta potential of Kaolinite (●), Source Clay KGa-2 (◆), Montmorillonite (■), and Source Clay SWy-3 (▶) with surfactants Span 80, AOT, and OLOA 11000. Zeta potential is graphed as a function of surfactant wt%. Red indicates Span 80, green indicates AOT, and blue indicates OLOA 11000. Error bars are 90% confidence intervals. Traces on each graph guide the eye to the expected acid-base charging trend as shown in Figure 2.2.

The zeta potential response as a function of surfactant concentration was similar to the expected acid-base inverse micelle charging mechanism shown in Figure 2.2. A trace has been added to each plot to guide the eye to the expected trend. In each case, particle charging was not significant until the surfactant concentration exceeded the CMC. The CMC for Span 80, AOT, and OLOA in Isopar-L has been found to be approximately 0.003wt%, 0.001wt%, and 0.01wt%,

respectively.[15,25,30] Above the CMC charge increased to a maximum before decreasing with increasing surfactant concentration. This decrease is caused by screening or neutralization as there are more charged micelles in the bulk from micelle-micelle charging interactions. Two neutral inverse micelles exchange charge producing two oppositely charged inverse micelles in the bulk.[15,28] The maximum charge of each clay surfactant combination was taken from Figure 2.4 and compared in Figure 2.5. Span 80 and AOT charged the clay particles positively while OLOA charged all clay samples negatively.

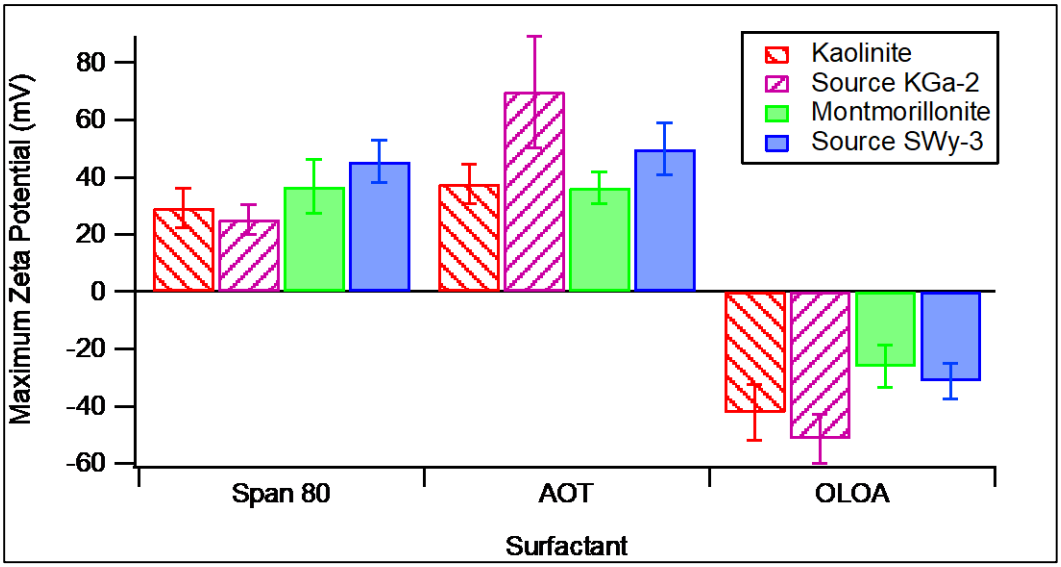

Figure 2.5. Bar graph comparing the maximum particle charge for each clay and surfactant combination. This demonstrates the acid-base relationship between particle and surfactant and its effect on Zeta Potential. Error bars are 90% confidence intervals.

The results in Figure 2.5 can be predicted using Eq. (2.3) if the edge PZC or the point of zero net proton charge (PZNPC) is the correct acid-base characteristic of clay particles in apolar media. For the clay particles used in this study which have PZNPC values ranging from 5.4-6.5 it would be predicted by Eq. (2.3) that OLOA, with a higher ABN of 9, would charge clay particles negatively. Alternatively, Span 80 and AOT, which have lower ABNs of 0 and 5 respectively, would be predicted to charge these clay particles positively. This implies that isomorphic

substitution does not play a role in charging clays in apolar media and that only the -OH groups on the clay particle's surface can participate in the acid-base charging mechanism. This might be anticipated since these permanent negative charges are balanced by exchangeable cations adsorbed to the surface which when in contact with water ($\varepsilon=80$), readily desorb and leave behind a permanently negative charged surface.[2,12] In apolar media ($\varepsilon=2$), however, these ions can no longer desorb and be stabilized by the solvent and thus remain on the surface neutralizing the permanent negative charge from isomorphic substitution.

An additional finding was that even though kaolinite and montmorillonite have different structures and properties there was no statistical difference or pattern seen in charging of the different clay samples. Kaolinite particles are thicker than montmorillonite with less isomorphic substitution.[6] Both basal surfaces in kaolinite have 40 % of the surface area while the edges have 20 % and therefore 60 % of the surface area has OH functional groups.[6] Montmorillonite, however, has only 5-10 % of its surface area as -OH functional edges.[13] With more OH functionality on the kaolinite particles it might have been expected to charge at a higher magnitude than montmorillonite. One explanation for this not occurring is that to achieve the zeta potential magnitudes measured here a particle would only need approximately 15 surface charges. The number of surface charges, 15, was determined by estimating the surface charge density needed for the clay particles in these systems to achieve the measured electrophoretic mobilities. To calculate this, it was assumed that particles were spherical, $\kappa a \ll 0.1$, and zeta potential was equal to the surface potential. Estimating the total particle surface -OH groups suggest that a 0.5 μm kaolinite particle would have 600,000 surface -OH groups and a montmorillonite particle of equal size would have 20,000 surface -OH groups. With plenty of hydroxyl groups available to charge on both types of clay particles it is unlikely a difference would be observed.

2.4.2 *Clay Stability Improvements with Surfactants*

Finally, the stability of kaolinite KGa-2 was investigated in Isopar-L with and without OLOA 11000. Particle size distributions were measured as a function of time and the addition of surfactant improved the stability of the clay particles. Figure 2.6 shows the size distributions of KGa-2 clay at different time intervals. Each graph also shows the size distribution in deionized (DI) water as a comparison.

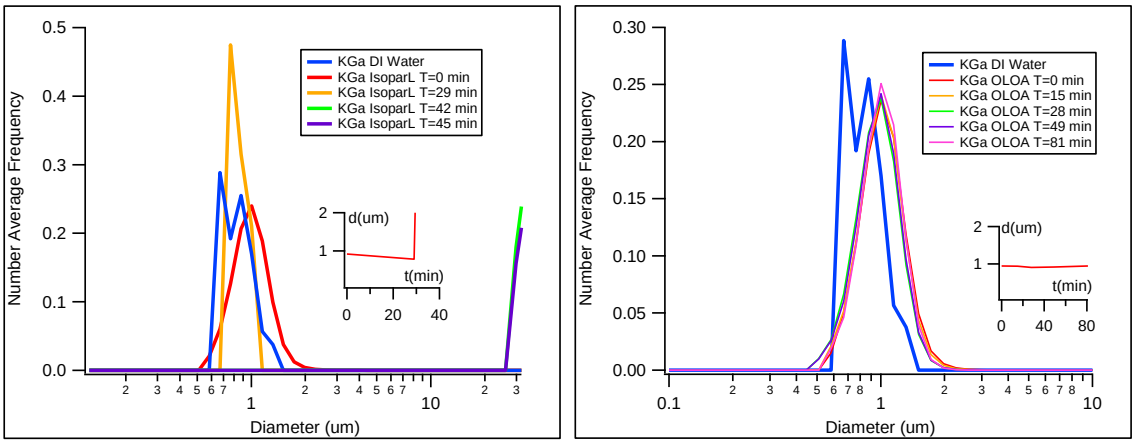

Figure 2.6. Particle stability comparison of KGa-2 in Isopar-L as a function of time. Left shows number averaged size distribution without surfactant. Right shows number average distribution with OLOA 11000. The insets show the average diameter as a function of time.

For the case with no surfactant present the particle size distribution increased in each measurement and after 30 min only large >30 μm particles were detected. This indicated the instability against particle aggregation and settling without the OLOA surfactant. In the case with OLOA added at a concentration above the CMC the particle size distributions were unchanged for the entire 81-minute duration of the experiment. The addition of the OLOA surfactant likely improved stability in two ways. First, it adsorbs to the particle surface lubricating it among other particles through steric stabilization and second, by imparting a charge to the particles, stabilized them against aggregation by electrostatic repulsive forces.

2.5 CONCLUSIONS

This study discovered the mechanism for clay particle charging in apolar media. Kaolinite and montmorillonite particles have two distinct charging mechanisms in water. First, permanent excess negative charges are found in the clay structure due to "isomorphous substitution" where lattice cations (Si^{4+} and Al^{3+}) are exchanged for cations with lower valence (Al^{3+} and Mg^{2+}, respectively). These permanent negative charges are balanced by exchangeable cations adsorbed to the surface which when in contact with water desorb and leave behind a permanent negative charged surface. The second charging mechanism arises from -OH functionalized surfaces on the clay particles which are free to charge, depending on the pH, by an acid-base mechanism.[1,2,5,6,10–12] The presence of a permanent negatively charged surface on clay particles in water leads to low isoelectric point (IEP) or point of zero charge (PZC) measured values (< 3) while the edge PZC or point of zero net proton charge (PZNPC) of kaolinite and montmorillonite has previously been determined to be between 6-6.5.[11,14]

In apolar media ($\varepsilon \approx 2$), there have been many examples of particles which only charge via an acid-base mechanism in water also charge via an acid-base mechanism in apolar media ($\varepsilon \approx 2$) with the addition of surfactants which can form inverse micelles to stabilize charges. Previous studies have found that by comparing the acid-base number (ABN) of the surfactant to the characteristic acid-base property of the particle (PZC or IEP) that the polarity of the particle charge could be predicted.[15] In this study, kaolinite and montmorillonite particles were charged in apolar media with three different surfactants, Span 80, AOT, and OLOA 11000.

It has been shown that in apolar media with a low dielectric constant, the inverse micelle charging of clay particles with surfactant behaves only as an acid-base interaction with the surface -OH groups. Without the ability to stabilize adsorbed cations in the bulk media the permanent

negative charge (from isomorphic substitution) on the surface of the clay particle will remain balanced due to the inability of the positive counter ions to dissociate from the surface. Therefore, the only charging mechanism that the clay particle has in apolar media is from the surface -OH groups on the clay. Furthermore, the edge PZC or PZNPC of 6-6.5 rather than the overall clay IEP of <3 from potentiometric titrations is the characteristic acid-base property that will predict the charge polarity by using Eq. (2.3) and the surfactant's ABN. This further suggests that only acid-base interaction occurs leading to particle charging.

In apolar media it was found that OLOA with an ABN of 9 charged the clay particles negatively while the AOT and Span 80 which have lower ABNs than the PZNPC both charged the clay particles positively. The benefit of adding surfactants to improve the stability of clay dispersions in apolar media was also shown and complemented the charging results. Future work could investigate removal of residual clay in oil using these charging techniques or investigating the charging of organoclays in apolar media.

2.6 REFERENCES

(1) Van Olphen, H. H. *An Introduction to Clay Colloid Chemistry: For Clay Technologists, Geologists, and Soil Scientists*; 1977.

(2) Liu, J.; Gaikwad, R.; Hande, A.; Das, S.; Thundat, T. Mapping and Quantifying Surface Charges on Clay Nanoparticles. *Langmuir* **2015**, *31* (38), 10469–10476.

(3) Jones, T. R. The Properties and Uses of Clays Which Swell in Organic Solvents. *Clay Miner.* **1983**, *18* (4), 399–401.

(4) Murray, H. H. Current Industrial Applications of Clays. *Clay Sci.* **2006**, *12* (Supplement2), 106–112.

(5) Tombácz, E.; Szekeres, M. Surface Charge Heterogeneity of Kaolinite in Aqueous Suspension in Comparison with Montmorillonite. *Appl. Clay Sci.* **2006**, *34* (1–4), 105–124. https://doi.org/10.1016/j.clay.2006.05.009.

(6) Yariv, S.; Cross, H. *Organo-Clay Complexes and Interactions*; CRC Press, 2001.

(7) Esfandiari, A.; Nazokdast, H.; Rashidi, A.-S.; Yazdanshenas, M.-E. Review of Polymer-Organoclay Nanocomposites. *J. Appl. Sci.* **2008**, *8* (3), 545–561.

(8) Moraru, V. N. Structure Formation of Alkylammonium Montmorillonites in Organic Media. *Appl. Clay Sci.* **2001**, *19* (1–6), 11–26. https://doi.org/10.1016/S0169-1317(01)00053-9.

(9) Masliyah, J.; Czarnecki, J.; Xu, Z. Handbook on Theory and Practice of Bitumen Recovery from Athabasca Oil Sands. *Theor. Basis* **2011**, *1*.
(10) Berg, J. C. *An Introduction to Interfaces & Colloids: The Bridge to Nanoscience*; World Scientific, 2010.
(11) Tombácz, E.; Szekeres, M. Colloidal Behavior of Aqueous Montmorillonite Suspensions: The Specific Role of PH in the Presence of Indifferent Electrolytes. *Appl. Clay Sci.* **2004**, *27* (1–2), 75–94. https://doi.org/10.1016/j.clay.2004.01.001.
(12) Schoonheydt, R. A.; Johnston, C. T. The Surface Properties of Clay Minerals. *Layer. Struct. Their Appl. Adv. Technol.* **2011**, *11*, 337–373.
(13) Duc, M.; Gaboriaud, F.; Thomas, F. Sensitivity of the Acid–Base Properties of Clays to the Methods of Preparation and Measurement: 1. Literature Review. *J. Colloid Interface Sci.* **2005**, *289* (1), 139–147.
(14) Schroth, B. K.; Sposito, G. Surface Charge Properties of Kaolinite. In *MRS Proceedings*; Cambridge Univ Press, 1996; Vol. 432, p 87.
(15) Gacek, M. M.; Berg, J. C. The Role of Acid–Base Effects on Particle Charging in Apolar Media. *Adv. Colloid Interface Sci.* **2015**, *220*, 108–123. https://doi.org/10.1016/j.cis.2015.03.004.
(16) Labib, M. E.; Williams, R. The Use of Zeta-Potential Measurements in Organic Solvents to Determine the Donor—Acceptor Properties of Solid Surfaces. *J. Colloid Interface Sci.* **1984**, *97* (2), 356–366.
(17) Smith, G. N.; Eastoe, J. Controlling Colloid Charge in Nonpolar Liquids with Surfactants. *Phys Chem Chem Phys* **2013**, *15* (2), 424–439. https://doi.org/10.1039/C2CP42625K.
(18) Morrison, I. D. Electrical Charges in Nonaqueous Media. *Colloids Surf. Physicochem. Eng. Asp.* **1993**, *71* (1), 1–37.
(19) Pugh, R. J.; Matsunaga, T.; Fowkes, F. M. The Dispersibility and Stability of Carbon Black in Media of Low Dielectric Constant. 1. Electrostatic and Steric Contributions to Colloidal Stability. *Colloids Surf.* **1983**, *7* (3), 183–207.
(20) Pugh, R. J.; Fowkes, F. M. The Dispersibility and Stability of Coal Particles in Hydrocarbon Media with a Polyisobutene Succinamide Dispersing Agent. *Colloids Surf.* **1984**, *11* (3–4), 423–427.
(21) Smith, P. G.; Patel, M. N.; Kim, J.; Milner, T. E.; Johnston, K. P. Effect of Surface Hydrophilicity on Charging Mechanism of Colloids in Low-Permittivity Solvents. *J. Phys. Chem. C* **2007**, *111* (2), 840–848.
(22) Lee, J.; Zhou, Z.-L.; Behrens, S. H. Charging Mechanism for Polymer Particles in Nonpolar Surfactant Solutions: Influence of Polymer Type and Surface Functionality. *Langmuir* **2016**, *32* (19), 4827–4836.
(23) Lee, J.; Zhou, Z.-L.; Alas, G.; Behrens, S. H. Mechanisms of Particle Charging by Surfactants in Nonpolar Dispersions. *Langmuir* **2015**, *31* (44), 11989–11999.
(24) Gacek, M. M.; Berg, J. C. Investigation of Surfactant Mediated Acid–Base Charging of Mineral Oxide Particles Dispersed in Apolar Systems. *Langmuir* **2012**, *28* (51), 17841–17845.
(25) Gacek, M.; Brooks, G.; Berg, J. C. Characterization of Mineral Oxide Charging in Apolar Media. *Langmuir* **2012**, *28* (5), 3032–3036.
(26) Gacek, M.; Bergsman, D.; Michor, E.; Berg, J. C. Effects of Trace Water on Charging of Silica Particles Dispersed in a Nonpolar Medium. *Langmuir* **2012**, *28* (31), 11633–11638.

(27) Michor, E. L.; Berg, J. C. Temperature Effects on Micelle Formation and Particle Charging with Span Surfactants in Apolar Media. *Langmuir* **2015**, *31* (35), 9602–9607.
(28) Hsu, M. F.; Dufresne, E. R.; Weitz, D. A. Charge Stabilization in Nonpolar Solvents. *Langmuir* **2005**, *21* (11), 4881–4887.
(29) Espinosa, C. E.; Guo, Q.; Singh, V.; Behrens, S. H. Particle Charging and Charge Screening in Nonpolar Dispersions with Nonionic Surfactants. *Langmuir* **2010**, *26* (22), 16941–16948.
(30) Gacek, M. M.; Berg, J. C. Effect of Surfactant Hydrophile-Lipophile Balance (HLB) Value on Mineral Oxide Charging in Apolar Media. *J. Colloid Interface Sci.* **2015**, *449*, 192–197.

Chapter 3. THE EFFECTS OF REVERSE MICELLAR STRUCTURE ON THE PARTICLE CHARGING CAPABILITIES OF THE SPAN SURFACTANT SERIES

E. L. Michor, B. S. Ponto, and J. C. Berg, "Effects of Reverse Micellar Structure on the Particle Charging Capabilities of the Span Surfactant Series," Langmuir, vol. 32, no. 40, pp. 10328–10333, 2016.

3.1 INTRODUCTION

In addition to examining how different particles can be charged in apolar media, as shown in Ch. 2, this chapter examines how the behavior of surfactants impacts particle charge. More specifically this chapter summarizes a study which investigated the effect that reverse micelle structure has on particle charging in apolar media.

A previous study from Dr. Berg's lab investigated the effect temperature has on the critical micelle concentration (CMC) and particle charging abilities of a series of Span surfactants in apolar media.[1] The structures of the Span surfactant series is shown in Figure 3.1 below.

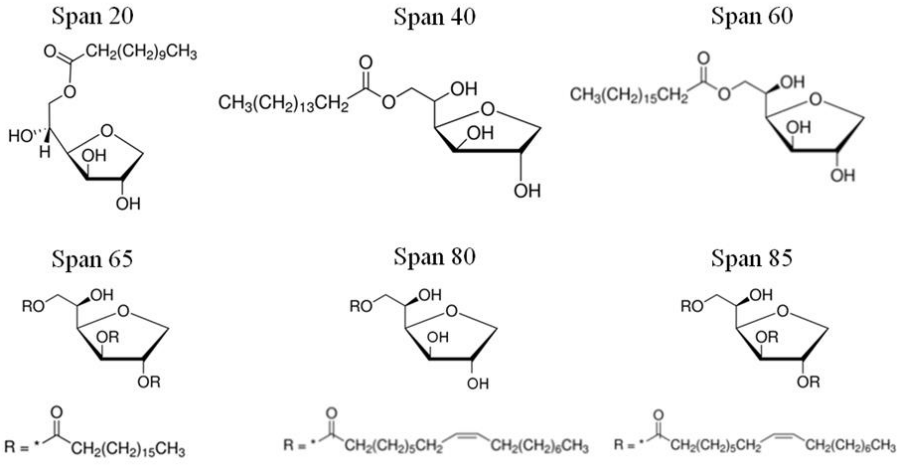

Figure 3.1. Structures of the Span surfactant series.[2] (Reproduced from reference 2)

It was discovered that as the temperature increased, for all but one of the Span surfactants the CMC also increased. The explanation for the one surfactant exception, Span 65, was that at lower temperatures its three fully saturated tails would crystallize causing it to not form reverse micelles below 44^{o}C. This study also measured the size of Span 20, 40, and 60 and tried to correlate the size of the reverse micelles to the maximum particle charge. While the evidence suggested that as the reverse micelle size decreased the maximum particle charge increased due to less electrostatic screening in the bulk from disproportionation reactions, it was concluded that a more detailed study was needed.

The objective of the present study was to use small-angle neutron scattering (SANS) to measure the core and shell sizes of Span reverse micelles and to correlate these parameters with particle charging trends from the previous study. The experiments were conducted with Dr. Michor at the National Institute for Standards and Technology (NIST) Center for Neutron Research (Gaithersburg, MD).

3.2 EXPERIMENTAL

3.2.1 *Chemicals*

The apolar solvent used in this study was deuterated n-decane (97% chemical purity), *d*-decane, and was purchased from Cambridge Isotope Laboratories (Andover, MA). Decane was a suitable substitute for the apolar solvent, Isopar-L, which was not available in its deuterated form. Deuterated chemicals are often used with neutron scattering techniques because they enhance contrast among different components in the system allowing for accurate dimensions of reverse micelles to be measured. This enhancement is achieved from the drastic differences in an object's scattering length density (SLD) that can be created through deuteration. Without a deuterated

background, the surfactant's hydrocarbon tails would be indistinguishable from the hydrocarbon solvent.

The six Span surfactants used in this study are shown in Figure 3.1 and were Span 20, 40, 60, 80, 65, and 85. All of the Span surfactants were obtained from Sigma-Aldrich (St. Louis, MO) except Span 65 which was obtained from Uniqema (New Castle, DE). All of the surfactants have the same head group and therefore, the same acid-base properties. The tails, however, all vary altering the hydrophile-lipophile balances (HLB) of the surfactants, as shown in Table 3.1. Span 20, 40, and 60 surfactants have a single saturated tail which increases in length from 11, 15, to 17 carbons, respectively. Span 80 has a similar tail to Span 60 with one double bond. Span 85 and Span 65 are both three tailed versions of Span 80 and Span 60, respectively.

3.2.2 *Small-Angle Neutron Scattering*

Small-angle neutron scattering experiments were performed at the NIST Center for Neutron Research (Gaithersburg, MD). Surfactant solutions were prepared at concentrations of approximately 1 wt% which was well above the critical micelle concentrations (CMC) for all of these surfactants. This ensured that a strong scattering signal from the reverse micelles could be collected. Three different sets of samples were prepared in this study each being allowed to equilibrate with moisture for 2 hrs. The first set was equilibrated with water vapor, the second was equilibrated with deuterated water (D_2O) vapor, and the third was swollen with D_2O by injecting 1 μL of deuterated water into each sample before sonicating. The deuterated water was also supplied from Cambridge Isotope Laboratories (Andover, MA).

Samples were placed into demountable titanium and quartz cells with a 1 mm path length and measured on the NG7 beam line. Neutron wavelengths were selected at 6 Å and the detectors

were placed at 1 m and 4 m positions. This experimental setup allowed for data collection over the scattering vector (q) range of 0.008 to 0.6 $Å^{-1}$.

3.3 Results and Discussion

The scattering profiles of each surfactant's reverse micelle is shown below in Figure 3.2 and was plotted as scattering intensity (I) vs. scattering vector (q). The results from the three different sample sets were very similar and only the D_2O equilibrated reverse micelle scattering results are shown here.

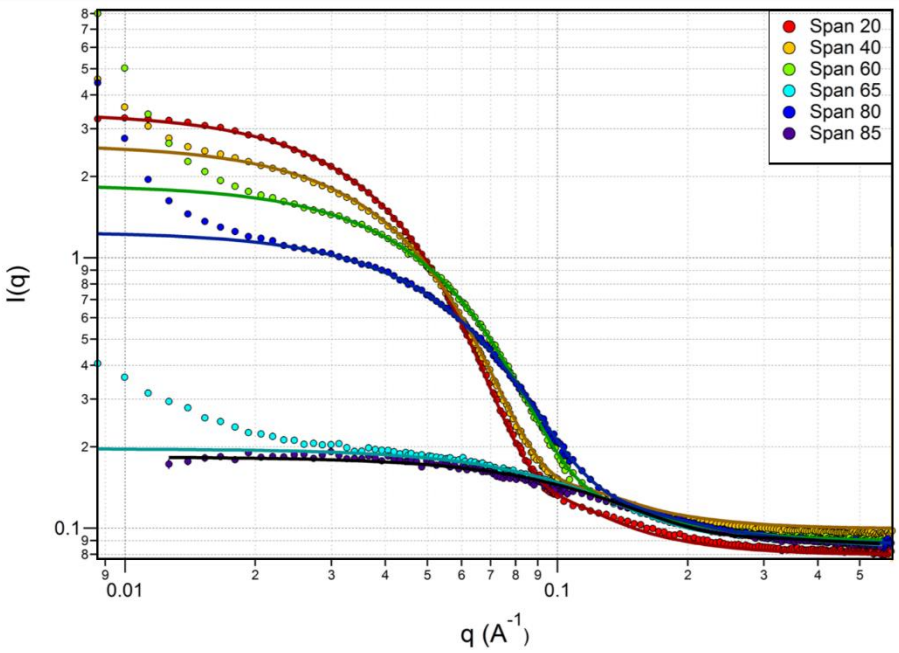

Figure 3.2. Scattering intensity (I) vs. scattering vector (q) of six Span surfactant reverse micelles in decane equilibrated with D_2O. The core shell sphere model fits are shown by the solid lines and match the data point colors.[2] (Reproduced from reference 2)

The spherical core shell models were fit using SasView software (www.sasview.org). It is clear that this model fits the reverse micelle scattering data well and all of these fits resulted in $\frac{\chi^2}{N}$

values below 10. The reverse micelle size and structure results for the samples equilibrated with D_2O from the model fitting in Figure 3.2 are tabulated in Table 3.1 below.

Table 3.1. Reverse micelle size results for the Span surfactant series equilibrated with D_2O. Tabulated are the surfactants' hydrophile-lipophile balance (HLB), polar core radius, and hydrocarbon shell thickness.[2]

Surfactant	HLB	Core Radius(Å)	Shell Thickness (Å)
Span 20	8.3	24.6	8.2
Span 40	6.7	22.5	8.4
Span 60	4.7	16.2	7.4
Span 80	4.3	10.2	6.9
Span 65	2.1	3.9	5.7
Span 85	1.8	3.7	5.1

The core size of the reverse micelles was found to decrease as the surfactant's tail gets longer, becomes unsaturated, or the surfactant has multiple tails. Having unsaturated or multiple tails increases the rigidity of the surfactant monomers and perhaps structurally prevents the rearrangement or swelling of the reverse micelles. The results from the three different sets of moisture equilibrations, H_2O, D_2O, and swollen D_2O, were similar and some of the reverse micelles showed an increase in size with the injection of D_2O. It was found that the results for the shell thickness was fairly consistent between the three sets of trials resulting in a thickness between 5-9 Å. This result was approximately half the length predicted by measuring the length of the molecular structures and could be explained by the intercalation of the solvent among the tails resulting in an SLD gradient.

The two key results from this experiment are shown in Figure 3.3 below. The first result was the positive correlation between the reverse micelle core size and the surfactant's hydrophile-lipophile balance (HLB). The left graph of Figure 3.3 shows that as the HLB of the surfactant increases, the size of the polar core increases as well.

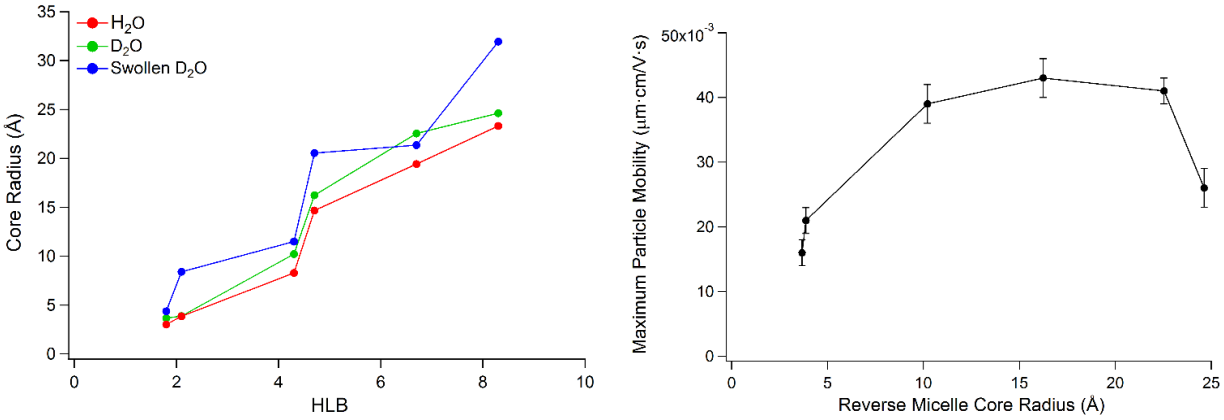

Figure 3.3. Core size of reverse micelles as a function of the surfactant HLB value (Left). The maximum particle electrophoretic mobilities of magnesia particles in Isopar-L as a function of the core radius of the reverse micelles performing the charging (Right).[2] (Reproduced from reference 2)

Previous work by Gacek and Berg[3] found a linear relationship between the maximum particle electrophoretic mobilities normalized to the HLB and the relative difference in the particle and surfactant acid-base properties (Eq. (1.1) and Figure 1.1). While they demonstrated the importance of the HLB, the results in Figure 3.3 confirm that the HLB is an important factor in determining the charging behavior of a specific surfactant. This is because it is correlated to the size of the reverse micelle cores. Furthermore, since each of the Span surfactants have the same polar head group, the differences in their abilities to charge particles must solely arise from variations in their reverse micelle structures caused by the different hydrophobic tails.

The second result was that when plotting particle mobility against reverse micelle core radius a point of maximum particle charging was found, as show on the right graph of Figure 3.3. It was concluded that the reverse micelles with the smallest core sizes (Span 65 and 85) imparted the lowest mobilities on the magnesia particles because the smaller the core the harder it is for a charging event to occur. Reverse micelles with a core that is too big increases the likelihood of charging via a disproportionation reaction which electrostatically screens charge reducing the

particle mobility. Reverse micelles with intermediate core sizes offer a large enough polar environment to favorably charge particles, yet not enough to promote excessive disproportionation reactions which electrostatically screen charge.

3.4 CONCLUSIONS

The results from this study showed the important impact that the reverse micelle size and structure has on charging particles in apolar media. For the series of Span surfactants there appears an optimal reverse micelle size to maximize charging.

The neutron research facility used in this work was provided by the National Institute of Standards and Technology (NIST) Center for Neutron Research (Gaithersburg, MD).

3.5 REFERENCES

(1) Michor, E. L.; Berg, J. C. The Temperature Effects on Micelle Formation and Particle Charging with Span Surfactants in Apolar Media. *Langmuir* **2015**, *31* (35), 9602–9607.
(2) Michor, E. L.; Ponto, B. S.; Berg, J. C. Effects of Reverse Micellar Structure on the Particle Charging Capabilities of the Span Surfactant Series. *Langmuir* **2016**, *32* (40), 10328–10333.
(3) Gacek, M. M.; Berg, J. C. Effect of Surfactant Hydrophile-Lipophile Balance (HLB) Value on Mineral Oxide Charging in Apolar Media. *J. Colloids Interface Sci.* **2015**.

Chapter 4. NANOPARTICLE CHARGING WITH MIXED REVERSE MICELLES IN APOLAR MEDIA

4.1 ABSTRACT

The charging of colloidal particles using mixed surfactants in apolar media is investigated. Previous work has shown that one can predict the sign and magnitude of particle charge by comparing the acid-base properties of an oil-soluble surfactant to the acid-base properties of a specific particle. The present work sought to tune the acid-base properties by using mixed surfactants. Unexpected mineral oxide particle charging results were obtained however, from mixing an acidic surfactant (SPAN 80) with a basic surfactant (OLOA 11000), requiring further investigation into the mixed reverse co-micelle particle charging mechanism. Conductometric titrations and small-angle neutron and x-ray scattering measurements showed that the surfactant mixtures formed spherical reverse co-micelles. Quartz crystal microbalance adsorption measurements demonstrated that both surfactants can adsorb to the particle surface. Lastly, electrophoretic mobility measurements showed that the surfactant mixture could enhance the negative particle charge beyond that imparted from either pure surfactant. It was discovered that in the mixed surfactant system studied the basic surfactant would charge the hydroxyl groups on both the oxide surface, and the adsorbed acidic surfactant head groups. The results showed that particle charging behavior in apolar media using mixed micelles requires knowledge beyond that for the individual surfactants and their proportions in the mixture.

4.2 INTRODUCTION

The charging of nanoparticles in liquid media of ultra-low dielectric constant, i.e., “apolar media”, with oil-soluble surfactants has been investigated for decades. Two current applications

of this research are found in electrophoretic displays (e.g., the Amazon Kindle®) and digital printers (e.g., HP Indigo®).[1] To stabilize charges in apolar media requires the presence of surfactants which can form reverse micelles, and it is believed that they then house charge within their polar cores.[1–3] While other charging mechanisms have been proposed for various systems, we believe that the reverse micelle acid-base charging mechanism is applicable in the majority of cases. Surfactant mediated charging of mineral oxides and similar particles, i.e., carbon black particles, pigments, and clays, begins via the formation and dissociation of acid-base adducts between adsorbed surfactant monomers and functional groups on the particle surface. The charged surfactant monomer is then desorbed and housed within reverse micelles in the bulk, leaving behind a charge on the particle surface which can then be protected by other surfactant monomers.

The acid-base charging mechanism for a single surfactant species has three steps: first, the polar head group of a surfactant molecule will adsorb to the particle surface and form an acid-base adduct; second, charge is transferred between the surface and the surfactant molecule depending on the acid-base properties; and third, the charged surfactant molecule is stabilized by a reverse micelle which allows it to desorb, leaving an opposite charge behind on the particle's surface.[1,3–5] An example of this is shown in Figure 4.1, where a metal oxide particle is charged positively in an apolar solvent by a surfactant which stabilizes the negative counterions in reverse micelles.

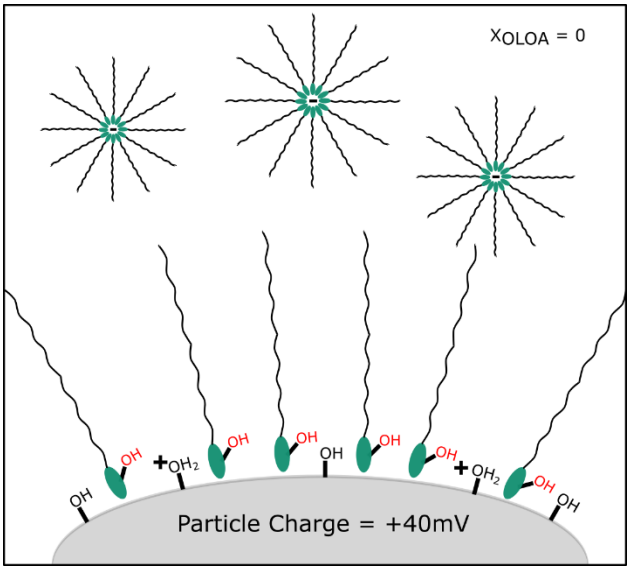

Figure 4.1. Single surfactant acid-base charging of a metal oxide particle in apolar media.

Particle charge can be determined by measuring the electrophoretic mobility, u_E, i.e. its velocity divided by the applied electric field strength. In apolar media, u_E can be related to the surface potential at the slip plane, i.e. its zeta potential, by applying the Hückel equation.[6] It is common to measure the electrophoretic mobility as a function of surfactant concentration and to take the maximum charging value as the characteristic charging value of a given surfactant and particle combination.[1,5,7–11] These common charging trends show no particle charging below a surfactant's critical micelle concentration (CMC), since it is not possible to stabilize counterions in the bulk. Conductometric titration is thus one technique which can be used to determine a surfactant's CMC.[1,8,10,12]

Previous work has shown that the sign and magnitude of particle charge in apolar media can be determined by comparing the acid-base properties of a particle, i.e., point of zero charge (PZC) or isoelectric point (IEP), to an experimentally determined "effective pH" (pH_{EFF}) or acid-base number (ABN) of a surfactant molecule.[1] The ABN for a surfactant molecule can be determined by plotting the maximum electrophoretic mobility of a series of mineral oxide particles

against the particle's PZCs for the given surfactant. The two surfactants studied in this experiment were sorbitan monooleate (SPAN 80) and polyisobutylene succinimide (OLOA 11000). The ABN is defined as the x-intercept of the linear fit of the electrophoretic mobility vs. the aqueous particle PZC for a series of oxide particles, and is shown in Figure 4.3 for SPAN 80 (ABN ≈ 0) and OLOA 11000 (ABN ≈ 9). A useful relationship has been found relating the maximum particle charge to the difference in acid-base properties between the particle and the surfactant:[1]

$$\zeta_{\max} \propto (pH_{PZC} - ABN), \tag{4.4}$$

where $\zeta_{\max}$ is the maximum particle zeta potential, pH_{PZC} is the particle's aqueous point of zero charge or isoelectric point, and ABN is the acid-base number of the surfactant.[1,5]

Previous studies have investigated only the acid-base charging mechanism of single surfactants in apolar media; however, it was thought to be advantageous to be able to tune the surfactant acid-base properties by mixing surfactants with different ABN values. This would allow the practitioner another variable to manipulate, improving their ability to accurately control the sign and magnitude of nanoparticle charge in apolar media. While previous studies have investigated the size and conductivity of mixed reverse micelles in apolar media, using them to charge particles has not been thoroughly explored.[13–15] The only prior example of investigating particle charging with mixed surfactants was found in a presentation by Morrison in 2003.[2] In Figure 4.2, Morrison mixed two surfactants, CCA 1 and 2 (proprietary compounds of the Cabot Corp.), to charge carbon black particles and found that the surfactant mixtures charged the particles with a combined effect between the pure components. Explanation of the specific surfactants or the mechanism behind the mixture's particle charge was not given.

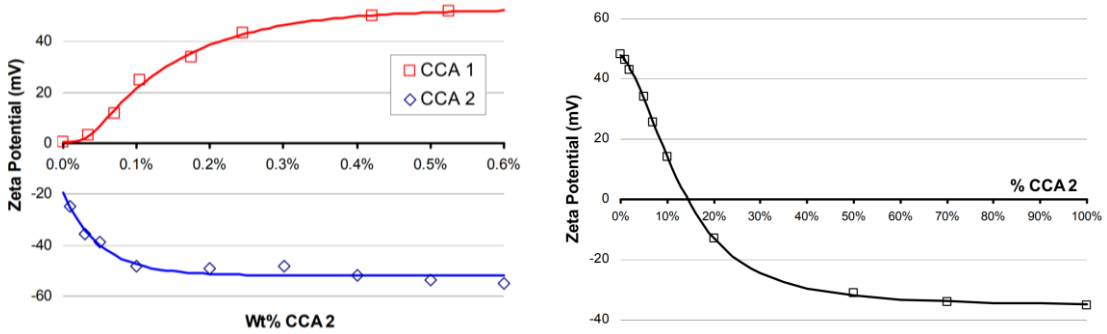

Figure 4.2. The zeta potential of basic carbon black particles with pure CCA1 and CCA2 surfactants. CCA1 is a polyhydroxystearic acid tail attached to a quaternary ammonium - methyl sulfate head group. CCA2 is C13 hydrocarbon chain tail attached to a sodium sulfosuccinate head group. The figure on the left is the charging in each of the pure surfactants and the figure on the right is the charging of the surfactant mixture.[2] (Reproduced from reference 2)

The present study seeks to investigate the charging of oxides with surfactant mixtures in an attempt to be able to tune the surfactant system to any desired ABN. In preliminary work, two nonionic surfactants were chosen, SPAN 80 (acidic, with an ABN ≈ 0) and OLOA 11000 (basic, with an ABN ≈ 9), to investigate because their ABN's were different enough that it would allow various mixing ratios to have significantly different ABNs.[1] It was hypothesized that the surfactant mixtures would form co-micelles and would perform like a surfactant with an effective ABN equal to the averaged pure ABN weighted to the mixing ratio. These preliminary charging results obtained for the surfactant mixtures were unexpected. Figure 4.3 shows results for several different oxides with the pure surfactants SPAN 80, OLOA, and three different mixtures of the two. The oxides in order of increasing PZC values from 2.5 to 11 are SiO_2, MnO_2, TiO_2, Al_2O_3, ZnO, and MgO.

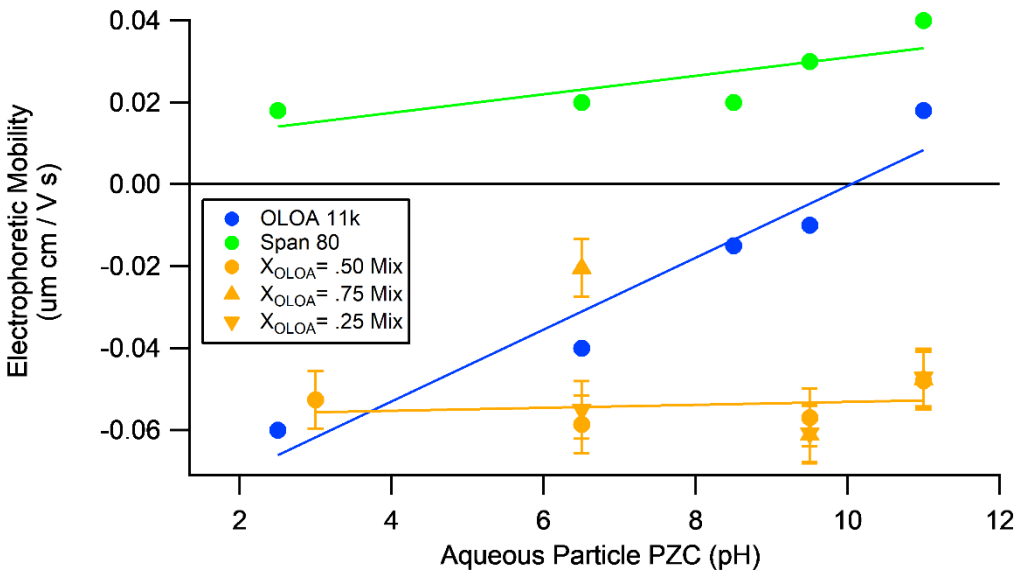

Figure 4.3. Charging of oxide nanoparticles with SPAN 80 (green), OLOA 11000 (blue), and 50:50, 25:75, and 75:25 mixtures (orange). SPAN and OLOA data were reprinted here for SiO_2, TiO_2, Al_2O_3, ZnO, and MgO particles with PZCs of 2.5, 6.5, 8.5, 9.5, and 11 respectively.[1] Surfactant concentration was approximately 0.5wt% as each of these values was the zero voltage maximum electrophoretic mobility obtained from a concentration sweep. The x-axis is the oxide particle's aqueous PZC.

SPAN 80, which is an acidic surfactant with a low ABN, charged all of the oxides positively, as expected. OLOA, which is a basic surfactant with a high ABN, charged particles where ABN>PZC negatively and particles where ABN<PZC positively, also as expected. However, the 50:50 and two other mixtures charged every oxide particle negatively. This is an unexpected result because it was hypothesized that the 50:50 mixture would form co-micelles with an ABN of about 4.5, which is the average of the two pure surfactants. This was clearly not the case, and further investigation was required.

The objective of this study was to understand the puzzling charging results by investigating the charging mechanism of the mixed surfactant system. To accomplish this, each part of the acid-base reverse micelle charging mechanism was examined. First, the existence of mixed reverse micelles was determined, and the dimensions of their structure was measured. Second, the

surfactant adsorption on the particle surfaces was measured. Finally, a closer examination of particle charging over the entire range of surfactant mixing ratios was completed. All of these experiments helped explain the unexpected charging results of the SPAN 80 and OLOA 11000 surfactant mixtures.

4.3 EXPERIMENTAL

4.3.1 *Chemicals*

Five different metal oxide particles were tested in this study: amorphous silica (SiO_2) from Fiber Optics Center Inc. (New Bedford, MA), quartz silica from GetNanoMaterials (Las Cruces, NM), titania (TiO_2) from Rutile US Research Nanomaterials, Inc. (Houston, TX), Manganese dioxide (MnO_2) from US Research Nanomaterials, Inc. (Houston, TX), and magnesia (MgO) from US Research Nanomaterials Inc. (Houston, TX). The average particle diameter of the amorphous SiO_2 particles was 250 nm, the quartz silica was 1µm, the MnO_2 was 50 nm, and the TiO_2 and MgO particles were both 300 nm. The aqueous point of zero charge (PZC) for SiO_2, MnO_2, TiO_2, ZnO, and MgO was approximately 2.5, 3, 6.5, 9.5, and 11, respectively.[16]

Isopar-L was the apolar solvent selected for the majority of this experiment and was supplied by ExxonMobil Chemical (Houston, TX). It is a synthetic isoparaffin fluid containing C8 to C15 saturated hydrocarbons with less than 2% aromatics. Isopar-L is a relatively inexpensive apolar solvent with a dielectric constant of 2.0. For the scattering studies, Isopar-L was replaced with decane and deuterated decane, *d*-decane, so that the scattering length density of the solvent could be known. Furthermore, deuterated Isopar-L could not be obtained, so decane was used as a substitute as has been done in past research.[11] Decane (99.6 mol% pure) from Fisher

Scientific (Pittsburgh, PA), and deuterated n-decane (97% chemical purity), *d*-decane, was purchased from Cambridge Isotope Laboratories (Andover, MA).

The two surfactants used in this experiment were sorbitan monooleate (SPAN 80) from SigmaAldrich Corp. (St. Louis, MO) and polyisobutylene succinimide (OLOA 11000) from Chevron Oronite (Bellaire, TX). SPAN 80 and OLOA 11000 are both nonionic surfactants with an effective pH (pH_{EFF}) or ABN of 0, and 9, respectively.[1,7]

4.3.2 *Conductometric Titrations*

Conductometric titrations were completed using a DT-700 Nonaqueous Conductivity Probe from Dispersion Technologies (Bedford Hills, NY). The conductivity of each sample was measured 20 times with a sinusoidal frequency of 1 Hz and averaged. A 0.1 wt% stock surfactant solution was made and allowed to equilibrate for 12 hr before being loaded into a dosemat. Using the dosemat and the conductivity probe, the conductivity for various surfactant mixtures was measured over a range of surfactant concentrations from 0 to 0.1 wt%.

4.3.3 *Electrophoretic Mobility Measurements*

Particle charge was determined with phase analysis light scattering (PALS), and particle size was determined with dynamic light scattering (DLS) using a ZetaPals zeta potential analyzer from the Brookhaven Instruments Corporation (Holtsville, NY). Surfactant solutions were made where the percent ratio of the mixture was the molar ratio between the surfactants, and the surfactant mixture wt% was its loading by mass. Samples were filtered with a 20 nm Anotop^{TM} filter and allowed to rest for 12 hr overnight to equilibrate. Particles were dried in an oven at 120 °C for 2 hr, and dispersions were then made in filtered Isopar-L (1mg/mL) and sonicated for 15 min. Immediately after sonication, 0.5 mL of the particle dispersion was added to each of the 10

mL surfactant solutions (~50 ppm particle loading). The individual samples were again sonicated for 2 min before being allowed to equilibrate again for 12 hr. Electrophoretic mobility measurements were then made on the ZetaPals at 25°C with an electrode spacing of 0.5 cm and a sinusoidal frequency of 2 Hz. To account for induced charging effects which has been shown to impact particle charge, measurements were taken with applied voltages of 50 V, 100 V, 150 V, and 200 V and extrapolated to zero to determine the zero field electrophoretic mobility.[7,9,17] Between each test the probe was cleaned with acetone and dried. Water content was also monitored with a C20 Coulometric Karl Fischer titration from Mettler Toledo (Columbus, OH) and 3 Å molecular sieves were used to keep the solvents dry.

4.3.4 *Small-Angle Scattering*

Neutron and x-ray scattering measurements were used to investigate the mixed reverse micelles in this experiment. Small-angle neutron scattering (SANS) was conducted using the Extended Q-Range Small-Angle Neutron Scattering Diffractometer (EQ-SANS) on beam line six at the Spallation Neutron Source at Oak Ridge National Lab (Oak Ridge, TN). Filtered surfactant solutions were prepared with a decane and *d*-decane mixed solvent, ($X_{d\text{-decane}} = 0.75$), and loaded into 0.3 mL Banjo cells with a 1 mm path length. A 2.5 Å neutron wavelength with the detector at the 4 m position was used to obtain scattering data at a q range of .01 – 1 $Å^{-1}$. Each sample was measured for approximately 1 hr. The initial intent of the neutron scattering study was to use contrast matching to determine the surfactant make-up of the micelles in the system at different mixing ratios. However, due to the inaccessibility of deuterated surfactant SPAN 80 and a signal-to-noise ratio that was too low from the contrast matched samples, a combination of neutron and x-ray scattering was used to help determine the size and composition of the mixed reverse micelles. X-rays can measure only the core of the reverse micelles because the hydrocarbon surfactant tails

have the same scattering length density (SLD) as the hydrocarbon solvent. Neutrons, however, can be used to probe the size and structure of the hydrocarbon tails of reverse micelles by altering the background solvent SLD through deuteration. This was achieved by using *d*-decane. Solutions of SPAN 80 and OLOA 11000 at different molar mixtures, ($0 \leq X_{OLOA} \leq 1$), were made in decane at a surfactant loading of 0.5 wt%. All samples were filtered with 20 nm Anotop^{TM} filters to remove any dust and contaminants. Once made, samples were allowed 12 hr to equilibrate before measuring.

Small-angle x-ray scattering (SAXS) was performed using an Anton Paar SAXess instrument (Graz, Austria) with a line-collimation system using a Cu Kα source with a wavelength of 1.5 Å. Samples were loaded into Quarzkapillaren capillary tubes with 1 mm O.D. from Charles Supper Company (Natick, MA). Each sample was measured for 1 hr. X-rays were detected on a Dectris Mythen DCS1 detector (Baden, Switzerland) and SAXSquant 3.70 software from Anton-Paar was used to reduce the two dimensional scattering data to intensity (*I*) versus scattering vector (*q*) plots.

All of the reduced intensity (*I*) versus scattering vector (*q*) data from SAXS and SANS was modeled using SasView 4.2.1 (sasview.org). The SAXS data were fit using a sphere model where literature SLD values for the core and the solvent could be set to fit the scale, radius, and polydispersity index (PDI) of the mixed reverse micelles. Using the radius and radius PDI from the SAXS results along with the known SLDs, the SANS data were fit using the core shell sphere model to determine the scale, background, thickness radius, and the PDI of the thickness. PDIs were kept below 0.5 and the reduced chi-squared, χ^2 /DOF, was below 3.5 for all fits where DOF is the degrees of freedom equal to the number of points minus the number of parameters fit.

4.3.5 *QCM-D Measurements*

Quartz Crystal Microbalance with Dissipation (QCM-D) measurements were conducted to study mixed surfactant adsorption on hydrophilic gold and silicon dioxide sensors. The apparatus used to collect data was a Q-Sense unit with Qsoft 401 software from Biolin Scientific (Gothenburg, Sweden). The frequency and dissipation results were fit using QTools data analysis software (Biolin Scientific). The Voigt model was used to obtain the mass and thickness of the viscoelastic surfactant adsorbed layers. All QCM-D measurements were made at room temperature, 25 °C, with a pump flow rate of 0.4 mL/min. Gold sensors were cleaned with piranha solution, and SiO_2 sensors were cleaned with sodium dodecyl sulfate solutions and a UV ozone cleaner in accord with manufacturer's instructions. Pure Isopar-L was pumped through the Q-sense device over the sensors for at least 1 hr to ensure that equilibrium was achieved before adsorption trials were conducted. Solutions of 0.05 wt% surfactant in Isopar-L were used in the QCM-D experiments.

4.4 Results and Discussion

The presence of reverse micelles was first confirmed when the critical micelle concentration (CMC) of a 50:50 SPAN 80 and OLOA 11000 surfactant mixture was determined and compared to the pure surfactant CMCs. Using the DT700 conductivity probe, the conductivity of a surfactant as a function of its wt% in Isopar-L was measured. As shown in Figure 4.4, the CMC is determined from the break in the slope, where below the CMC there is no measureable conductivity because charges aren't stable. Once concentration surpasses the CMC, conductivity increases with the increasing number of charged micelles in the bulk.

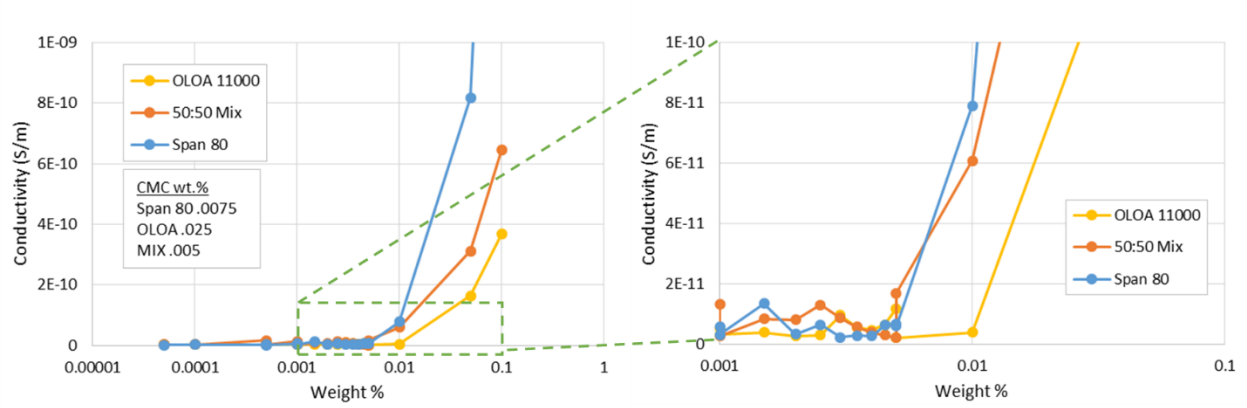

Figure 4.4. Conductometric titrations of SPAN 80, OLOA 11000, and a 50:50 mixture of the two. The graph on the right is a zoomed in graph of the left graph for CMC determination.

It appears that the CMC of the surfactant mixture was slightly lower than the CMCs of either pure SPAN 80 or OLOA 11000, suggesting that these two surfactants are forming co-micelles. This result is consistent with previous studies by Eicke and Arnold [18], who found that mixing two sulfosuccinate surfactants with different tails resulted in a lower CMC compared with their pure CMCs, and that the size of the mixed micelles was similar to that of the pure micelles.

To further confirm the presence of reverse micelles (RM) in the mixed surfactant system dynamic light scattering (DLS) was conducted on the surfactant mixture in Isopar-L to measure their size. The DLS results found that the diameter of pure SPAN 80 and pure OLOA RMs in Isopar-L were 5.53 nm and 5.81 nm, respectively. At concentrations below the CMC determined from the conductometric titration, DLS measured <1 nm size for the mixed surfactant indicating no reverse micelles below the CMC. Above the CMC, at a mixed surfactant concentration of 0.5 wt% the DLS measured size was 5.5 nm indicating the presence of reverse micelles in the mixed surfactant system.

Measuring the structures of the reverse micelles in decane was possible using small-angle neutron scattering because of the ability to create large differences in scattering length densities

(SLDs) by deuterating the decane background. In a 75% *d*-decane – 25% decane solvent the reverse micelle cores containing the surfactant head groups and trace water, the hydrophobic surfactant tails, and the bulk solvent all have different contrast and can be probed with neutrons. X-rays, on-the-other-hand, cannot detect a difference between the hydrocarbon tails and the decane solvent since the x-ray SLDs are the same. Therefore, SAXS was used in conjunction with SANS data to better fit the core radius when modeling. An example of the SANS and SAXS results for a specific surfactant mixture is shown in Figure 4.5.

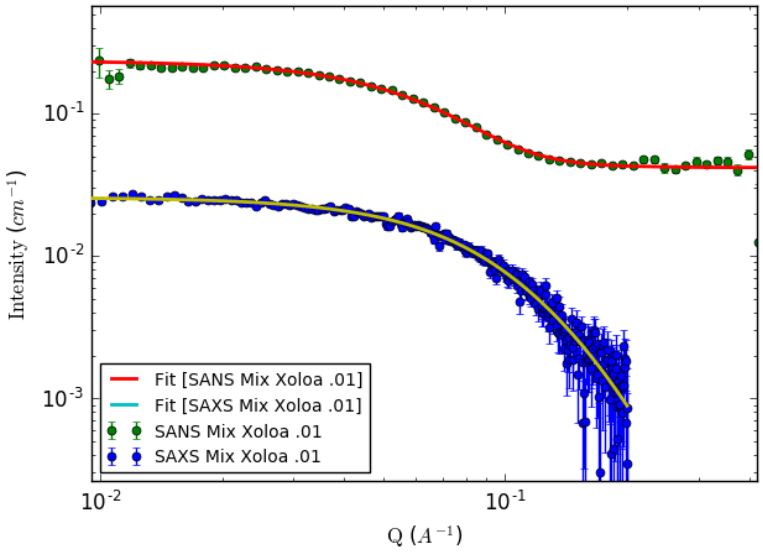

Figure 4.5. Scattering profiles (intensity (I) as a function of scattering vector (q)) for a SPAN 80 and OLOA 11000 mixture (XOLOA = 0.01). Small-angle neutron scattering data collected in a deuterated decane background (Xd-decane = 0.75) is shown above with a core shell sphere model fit. Small-angle x-ray data in decane are shown with a sphere model fit.

Both neutron and x-ray scattering curves show a distinct Guinier region between $0.02 < q < 0.1$ Å^{-1}. A simple Guinier region analysis shows that the radius as determined by SANS is larger than that from SAXS, confirming that x-rays are unable to observe the hydrophobic tails against the hydrocarbon solvent. A summary of the mixed reverse micelle dimensions determined from

modeling the small-angle scattering data is shown in Figure 4.6. Reduced chi-squared values were less than 3.5 for all fits.

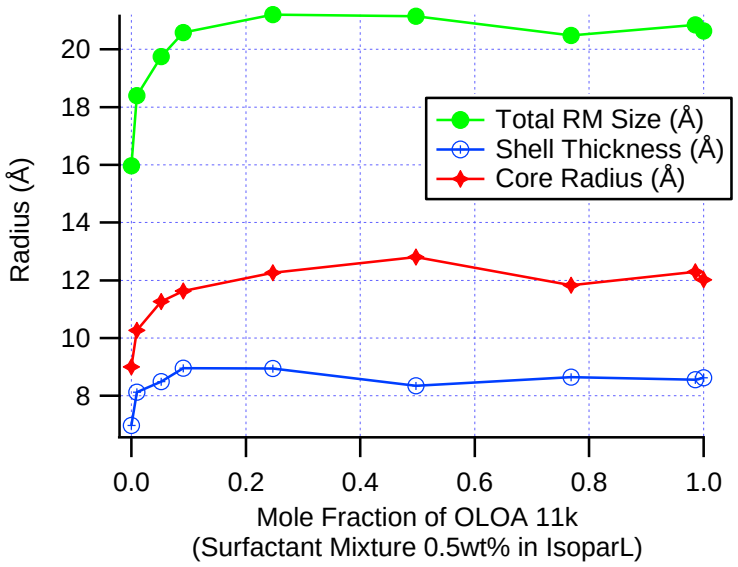

Figure 4.6. Summary of mixed reverse micelle size results from SAXS and SANS as a function of mole fraction OLOA 11000 (XOLOA).

The size results from DLS and SAXS are consistent with previous SANS results for the size of SPAN 80 reverse micelles [11] and DLS and SAXS results for the size of OLOA 11000 reverse micelles.[19] A previous SANS study from the authors' laboratory found that pure SPAN 80 ($X_{OLOA} = 0$) had a reverse micelle core radius of 8.3 Å and thickness of 7.4 Å when measured in a fully deuterated *d*-decane solvent, which matches precisely the results in Figure 4.6.[11] The sizing results in Figure 4.6 show that as OLOA is added to pure SPAN 80, the reverse micelle size increases up to a mixture ratio of about 10% OLOA ($X_{OLOA} = 0.1$). As more OLOA is added ($0.1 < X_{OLOA} < 1$) the reverse micelle size maintains a constant value equal to the size of pure OLOA reverse micelles. This supports our findings that these two surfactants do form co-micelles and that their size can be explained by the OLOA molecule being significantly larger than the SPAN molecule.

MarvinView 17.1.9.0, 2017, from ChemAxon (www.chemaxon.com) was used to determine the maximum size of the surfactant molecules by calculating the maximum extension length of the conformer perpendicular to the minimal projection area, based on their chemical structures. For SPAN 80 the maximum length was found to be 22.68 Å (9.37 Å for the head group) and for OLOA 11000 the maximum extension length was 67.21 Å (13.82 Å for the head group). It was assumed that the head group repeat unit of the OLOA structure was 1, and the tail repeat unit was 30.[3] Adding the larger surfactant, OLOA, to the mixture increased the core radius and shell thickness as expected. It appears that when OLOA is above 10% of the surfactant mixture, there is enough OLOA present in the mixed reverse micelles to define both the core and shell dimensions. A schematic of the pure and mixed reverse micelles is shown in Figure 4.7. Previous studies agree with this finding where they have found that in a mixture of adsorbed polymers of varying sizes, only a small proportion of the largest polymer is needed to significantly increase the adlayer thickness.[20] The shell thickness was measured to be much lower than expected when compared with the lengths of the surfactant structures. It is believed that the intercalation of the solvent with the surfactant tails increases the SLD in that region and results in a smaller thickness result.[11]

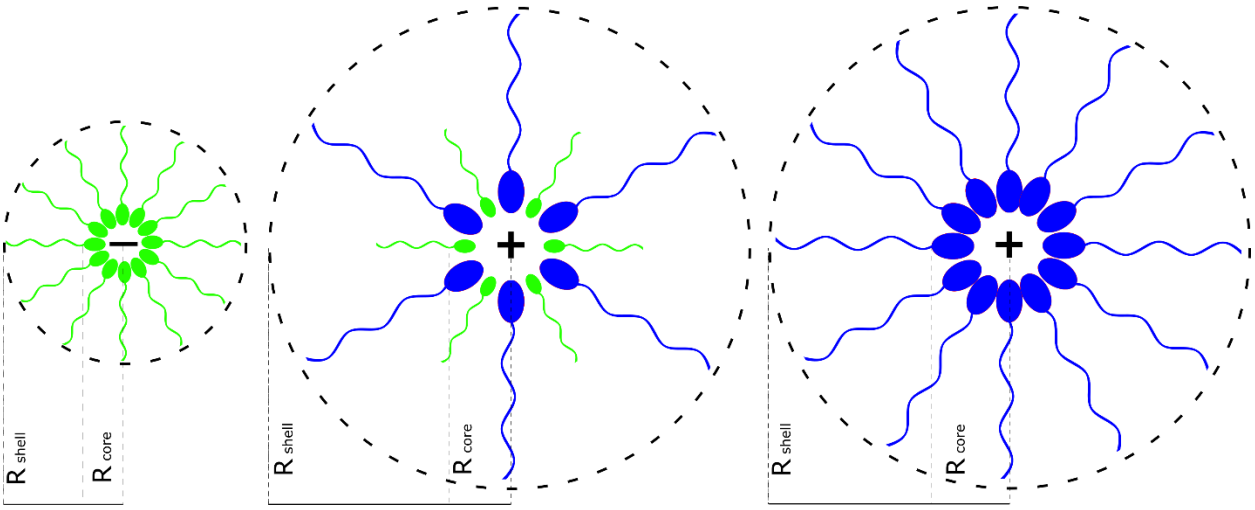

Figure 4.7. Schematic of SPAN 80 reverse micelle (Left), 50:50 SPAN OLOA mixed reverse micelle (Center), and OLOA 11000 reverse micelle (Right).

Once it was confirmed that the mixed surfactant system does form the spherical mixed reverse micelles hypothesized, a surfactant adsorption study of the mixed surfactant system was needed to determine the mechanism for the peculiar particle charging results. A QCM-D adsorption study was conducted to investigate surfactant adsorption of the mixed surfactant system on hydrophilic surfaces to mimic the metal oxide particle surfaces. Both silica and gold QCM sensors were used for this purpose and showed similar results. The rate of adsorption for both surfactants was similar, and it took only about 3 min to reach equilibrium. The adsorbed layer thickness of 0.05 wt% surfactant solutions on SiO_2 measured SPAN 80 to be 8 Å and the OLOA to be 18 Å. This trend agrees with previous size results for these two different surfactants. It was also noted that while SPAN 80 would completely desorb in a few minutes, OLOA would not desorb, and the sensors had to be cleaned every time they came into contact with OLOA during the QCM measurements. This was to be expected, as larger polymers typically bond more strongly to surfaces due to their larger number of bonding sites. Figure 4.8 shows the QCM results from

the adsorption/desorption of SPAN 80 followed by the adsorption/desorption of a 50:50 surfactant mixture on gold and SiO_2.

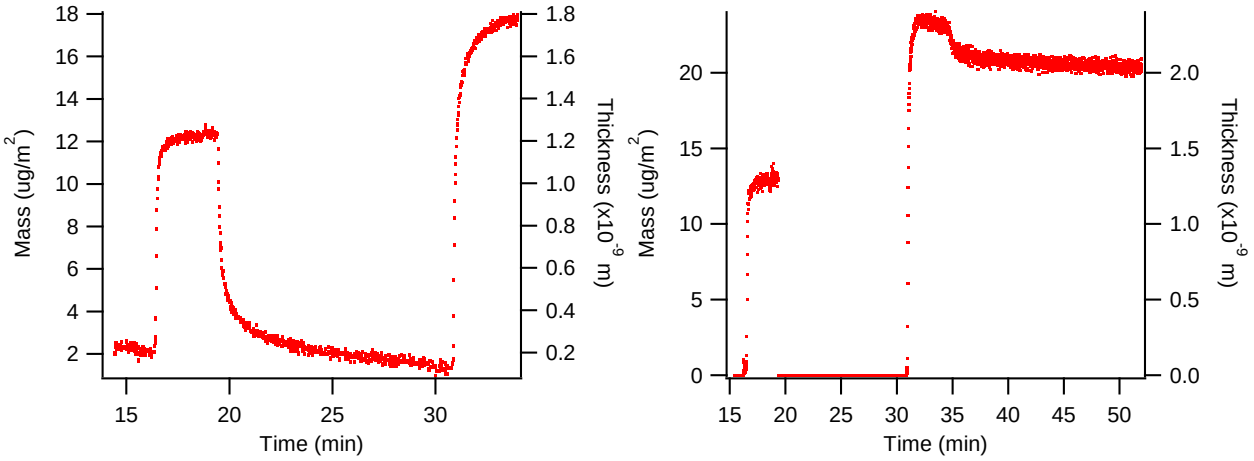

Figure 4.8. SPAN 80 (0.049wt% in Isopar-L) adsorption and desorption followed by 50:50 SPAN OLOA mix (X_{OLOA} =0.5, 0.045wt% in Isopar-L) adsorption and desorption on gold surface (left) and SiO_2 surface (right).

On both surfaces the adsorbed layer of the mixed surfactant solution was much higher than the pure SPAN 80 as expected, since OLOA is a much larger surfactant. Using the observation that only the SPAN 80 surfactant would desorb, the surfactant mixture was desorbed from the SiO_2 sensor allowing an estimate of the surface composition on the particles when exposed to a surfactant mixture. On the SiO_2 sensor the mass of pure SPAN 80 adsorbed to the surface was 13 µg/m^2, while the 50:50 mixture adsorbed a mass of 23.3 µg/m^2. As noted above, SPAN 80 readily desorbed while OLOA did not. Therefore, it was assumed that when the 50:50 mixture desorbed from the surface, nearly the entire mass change was attributed to the desorbtion of SPAN 80. When pure Isopar-L was made to flow over the mixed adsorbed layer to desorb only SPAN 80, the mass decreased by 2.7 µg/m^2, indicating that about 36% of the surfactant on the surface was SPAN 80 ($X_{OLOA}^{Surface}$= 0.64). While OLOA seems to bond more tightly to the surface, the results suggest

that with the mixed surfactant solutions, each surfactant is capable of adsorbing to the surface, and forming adducts with the surface functional groups.

A more detailed investigation of mixed surfactant reverse micelle particle charging at varying mixing ratios is shown in Figure 4.9. The acidic surfactant, SPAN 80, with an ABN of 0, charges all 3 particles positively as expected and is depicted in Figure 4.1.[1]

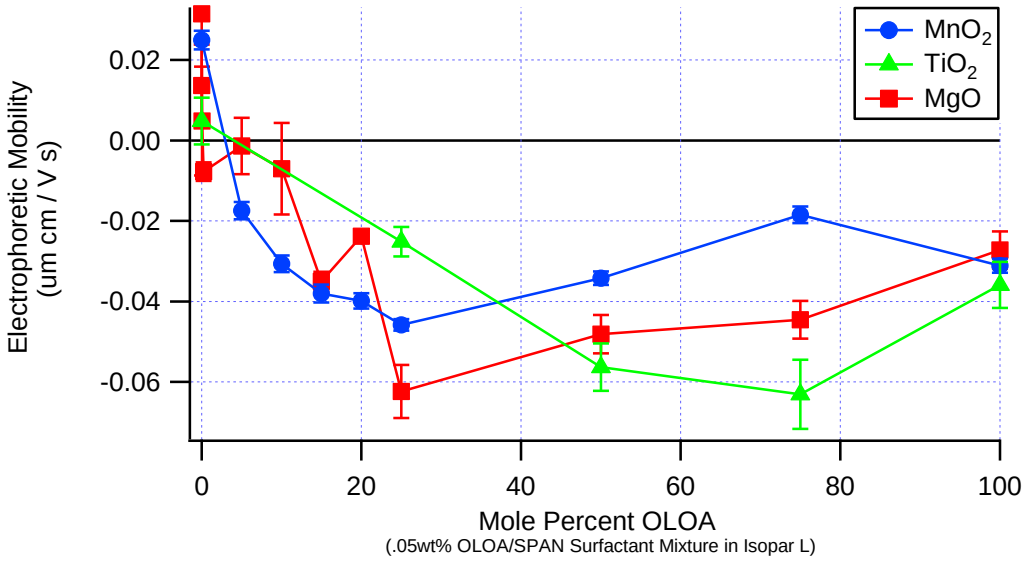

Figure 4.9. Particle electrophoretic mobilities of MnO_2, TiO_2, and MgO for different mixing ratios of SPAN 80 and OLOA 11000 (X_{OLOA}) in Isopar-L as a surfactant loading of 0.05wt%.

As the basic OLOA, with an ABN of 9, is added to the mixed surfactant systems all of the particles are charged more and more negatively, seemingly independent of particle type. In the intermediate range of the mixture, $0.2 < X_{OLOA} < 0.8$, particle charge for all three particles reaches a minimum. The results in Figure 4.9 agree with the preliminary results in Figure 4.3, where beyond a surfactant ratio of 25% to 75% all particle charge was constant and negative. Figure 4.10 shows a schematic for the proposed mixed surfactant charging mechanism.

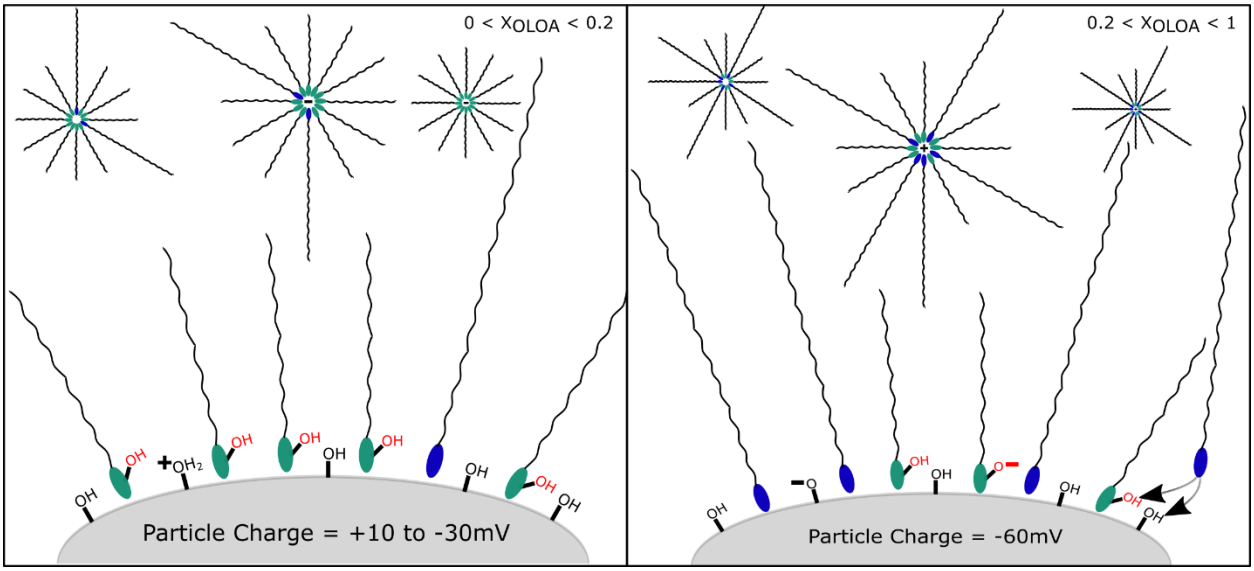

Figure 4.10. Schematic showing the mixed surfactant charging mechanism in apolar media. Basic OLOA (blue) can charge the particle's surface functional groups, or the other acidic adsorbed surfactant SPAN 80 (green).

Initially, the addition of the basic OLOA surfactant begins to decrease particle charge as the OLOA is now competing with SPAN 80 to charge different functional groups on the particle surface. The more OLOA is added, the more negative the particles charge. As addition of OLOA increases toward 20%, OLOA can now charge either functional groups on the particle surface, or adsorbed SPAN 80 head groups (Figure 4.10 right). OLOA charging the adsorbed SPAN 80 on the surface explains the particle independent charging observed over most of the mixing ratio. Finally, as the ratio of surfactant mixture moves toward pure OLOA particle charge increases as the adsorbed SPAN 80 on the surface becomes scarce, and the OLOA must resort to charging only the functional groups on the particle surface. A particle needs only approximately 15 charged surface sites to obtain the magnitude of particle charge observed here. A similar idea to adding charging sites with adsorbed SPAN 80 head groups was found in a study that treated silica particles with an alkyl-silane and observed an increase in charge.[21] It was reasoned that when the silane

attached to the surface, it brought with it up to two additional charging sites that could participate in the acid-base reverse micelle mechanism.[21]

4.5 CONCLUSIONS

The possibility of utilizing surfactant mixtures to better control particle charge in apolar media was investigated. The hope was that by mixing surfactants the practitioner could accurately tune the effective acid-base number (ABN) of a surfactant mixture to any desired value. Several metal oxides were charged using mixtures of an acidic surfactant SPAN 80 (ABN ≈0) and a basic surfactant OLOA 11000 (ABN≈9). The unexpected preliminary result that all of the particles charged equally negative independent of particle type and surfactant ratio indicated an unforeseen surfactant interaction requiring a closer investigation of the system.

Each step of the mixed reverse micelle particle charging mechanism was investigated to understand the unexpected charging behavior. The existence of mixed reverse micelles and their structure was investigated with conductometric titrations and small-angle scattering techniques. Competitive surfactant adsorption on hydrophilic surfaces was studied using a Quartz Crystal Microbalance (QCM-D). Finally, particle electrophoretic mobilities were measured to investigate particle charging for three different particles over the entire range of surfactant mixing ratios.

Conductometric titrations confirmed that the mixed surfactant system formed reverse micelles, and suggested that they were co-micelles due to a slightly lower critical micelle concentration. Small-angle neutron and x-ray scattering measurements revealed the size and spherical structure of the mixed reverse micelles. It was found that pure SPAN 80 reverse micelles were smaller than OLOA 11000 reverse micelles, which was consistent with the fact that OLOA is a significantly larger surfactant molecule. The mixed reverse micelles' core and shell

thicknesses increased with increasing OLOA concentration up to 10% OLOA (X_{OLOA} = 0.1). Beyond 10% OLOA the reverse micelle size was equal to that of pure OLOA reverse micelles.

Quartz Crystal Microbalance measurements revealed that in the mixed surfactant solution both surfactants, SPAN 80 and OLOA 11000, were able to adsorb on the particle surface. It was also found that while SPAN 80 would readily desorb, OLOA 11000 would not. The modeled surfactant monolayer thickness from the QCM-D results agreed with the surfactant sizes previously determined.

Particle charging results revealed that particle charge was negatively enhanced by using a mixture of surfactants. The three particles, MnO_2, TiO_2, and MgO, achieved a negative minimum charging value independent of particle type at an intermediate mixing ratio, $0.2 < X_{OLOA} < 0.8$. While pure SPAN 80 charged all three particles positively, the addition of OLOA 11000 initially decreased particle charge as expected since OLOA has a higher ABN. At high concentrations of OLOA 11000, particle charge began to increase to a less negative value likely due to a depletion of SPAN 80 on the particle surface. The proposed explanation for this charging behavior is that the OLOA surfactant is charging the adsorbed SPAN 80 head groups on the particle surface which is why a mixture creates a more negatively charged particle, independent of particle acid-base properties.

This study discovered that the mixed surfactant system of SPAN 80 and OLOA 11000 formed spherical reverse co-micelles and that both surfactants were able to adsorb to the particle surface when mixed. The unexpected interaction on the particle surface where OLOA would charge the adsorbed SPAN 80 head groups negatively on the particle surface explained the strange charging behavior and why charge was independent of particle type in the intermediate mixing

ratios. It turned out that tuning the surfactant charging properties is not as simple as mixing surfactants.

A portion of this research used resources at the Spallation Neutron Source, a DOE Office of Science User Facility operated by the Oak Ridge National Laboratory. An additional part of this work was conducted at the Molecular Analysis Facility, a National Nanotechnology Coordinated Infrastructure site at the University of Washington which is supported in part by the National Science Foundation (grant NNCI-1542101), the University of Washington, the Molecular Engineering & Sciences Institute, and the Clean Energy Institute. Undergraduate students Jake Fredrikson and Lane Bozman are acknowledged for their help in acquiring data for this study.

4.6 REFERENCES

(1) Gacek, M. M.; Berg, J. C. The Role of Acid–Base Effects on Particle Charging in Apolar Media. *Adv. Colloid Interface Sci.* **2015**, *220*, 108–123. https://doi.org/10.1016/j.cis.2015.03.004.
(2) Ian D. Morrison. Ions and Charged Particles in Nonpolar Media.Pdf, 2003.
(3) Smith, G. N.; Eastoe, J. Controlling Colloid Charge in Nonpolar Liquids with Surfactants. *Phys Chem Chem Phys* **2013**, *15* (2), 424–439. https://doi.org/10.1039/C2CP42625K.
(4) Pugh, R. J.; Fowkes, F. M. The Dispersibility and Stability of Coal Particles in Hydrocarbon Media with a Polyisobutene Succinamide Dispersing Agent. *Colloids Surf.* **1984**, *11* (3–4), 423–427.
(5) Ponto, B. S.; Berg, J. C. Clay Particle Charging in Apolar Media. *Appl. Clay Sci.* **2018**, *161*, 76–81. https://doi.org/10.1016/j.clay.2018.04.016.
(6) Berg, J. C. *An Introduction to Interfaces & Colloids: The Bridge to Nanoscience*; World Scientific, 2010.
(7) Gacek, M. M.; Berg, J. C. Investigation of Surfactant Mediated Acid–Base Charging of Mineral Oxide Particles Dispersed in Apolar Systems. *Langmuir* **2012**, *28* (51), 17841–17845.
(8) Gacek, M.; Brooks, G.; Berg, J. C. Characterization of Mineral Oxide Charging in Apolar Media. *Langmuir* **2012**, *28* (5), 3032–3036.
(9) Gacek, M.; Bergsman, D.; Michor, E.; Berg, J. C. Effects of Trace Water on Charging of Silica Particles Dispersed in a Nonpolar Medium. *Langmuir* **2012**, *28* (31), 11633–11638.
(10) Michor, E. L.; Berg, J. C. Temperature Effects on Micelle Formation and Particle Charging with Span Surfactants in Apolar Media. *Langmuir* **2015**, *31* (35), 9602–9607.
(11) Michor, E. L.; Ponto, B. S.; Berg, J. C. Effects of Reverse Micellar Structure on the Particle Charging Capabilities of the Span Surfactant Series. *Langmuir* **2016**, *32* (40), 10328–10333.

(12) Poovarodom, S.; Berg, J. C. Effect of Particle and Surfactant Acid–Base Properties on Charging of Colloids in Apolar Media. *J. Colloid Interface Sci.* **2010**, *346* (2), 370–377. https://doi.org/10.1016/j.jcis.2010.03.012.
(13) Kundu, K.; Das, A.; Bardhan, S.; Chakraborty, G.; Ghosh, D.; Kar, B.; Saha, S. K.; Senapati, S.; Mitra, R. K.; Paul, B. K. The Mixing Behaviour of Anionic and Nonionic Surfactant Blends in Aqueous Environment Correlates in Fatty Acid Ester Medium. *Colloids Surf. Physicochem. Eng. Asp.* **2016**, *504*, 331–342.
(14) Kundu, K.; Paul, B. K. Physicochemical Investigation of Biocompatible Mixed Surfactant Reverse Micelles: II. Dynamics of Conductance Percolation, Energetics of Droplet Clustering, Effect of Additives and Dynamic Light Scattering Studies. *J. Chem. Thermodyn.* **2013**, *63*, 148–163.
(15) Liu, D.; Ma, J.; Cheng, H.; Zhao, Z. Investigation on the Conductivity and Microstructure of AOT/Non-Ionic Surfactants/Water/n-Heptane Mixed Reverse Micelles. *Colloids Surf. Physicochem. Eng. Asp.* **1998**, *135* (1), 157–164.
(16) Kosmulski, M. *Chemical Properties of Material Surfaces*; CRC press, 2001.
(17) Espinosa, C. E.; Guo, Q.; Singh, V.; Behrens, S. H. Particle Charging and Charge Screening in Nonpolar Dispersions with Nonionic Surfactants. *Langmuir* **2010**, *26* (22), 16941–16948.
(18) Eicke, H. F.; Arnold, V. Interactions of Proton Donors with Colloidal Electrolytes in Apolar Solvents. *J. Colloid Interface Sci.* **1974**, *46* (1), 101–110.
(19) Parent, M. E.; Yang, J.; Jeon, Y.; Toney, M. F.; Zhou, Z.-L.; Henze, D. Influence of Surfactant Structure on Reverse Micelle Size and Charge for Nonpolar Electrophoretic Inks. *Langmuir* **2011**, *27* (19), 11845–11851.
(20) Stenkamp, V. S.; Berg, J. C. The Role of Long Tails in Steric Stabilization and Hydrodynamic Layer Thickness. *Langmuir* **1997**, *13* (14), 3827–3832.
(21) Poovarodom, S.; Poovarodom, S.; Berg, J. C. Effect of Alkyl Functionalization on Charging of Colloidal Silica in Apolar Media. *J. Colloid Interface Sci.* **2010**, *351* (2), 415–420.

Chapter 5. NANOPARTICLE CHARGING IN LEAKY DIELECTRICS

5.1 ABSTRACT

The use of surfactants to charge colloidal particles in solvents of intermediate dielectric constants ($5<\varepsilon<40$) is investigated. While particle charging mechanisms in aqueous ($\varepsilon=80$) and apolar ($\varepsilon<5$) media are well understood, the interplay of these different charging mechanisms, which can all occur in solvents of intermediate dielectric constants ("leaky dielectrics"), remains to be fully explored. Conductometric titrations determining the critical micelle concentration (CMC) of the surfactant (Aerosol-OT) confirm the existence of reverse micelles in leaky dielectrics and show that as the solvent dielectric constant decreases, the CMC decreases as well. Electrophoretic mobility measurements of three oxide particles (SiO_2, TiO_2, MgO) highlight the various charging mechanisms that arise from particle-solvent, particle-surfactant, and solvent-surfactant interactions in a solvent series of alcohols and ketones. The results show that a combination of donor-acceptor particle-solvent interactions, surfactant ion adsorption, and reverse micelle mediated acid-base interactions can all charge oxide particles in leaky dielectrics. Furthermore, the results show that the dielectric constant of the solvent affects the relative magnitudes of each charging mechanism.

5.2 INTRODUCTION

While particle charging has been studied in aqueous ($\varepsilon=80$) and apolar ($\varepsilon<5$) media, limited study has been conducted in solvents with intermediate dielectric constants, commonly referred to as leaky dielectrics. Exploring particle charging in leaky dielectrics is of interest because not only will surfactants play a role in the acid-base particle charging mechanisms,[1–3] but, as the polarity of the solvent increases, acid-base interactions between the solvent and the particle surface are known

to occur, as well.[4–6] Understanding colloidal particle charge in a wide range of different solvents is important because particle charge plays a vital role in its aggregation stability and it is also the basis of separation processes which utilize electrophoresis.

In aqueous media (ε=80), where particle charging is well understood, there are at least five ways particles can acquire charge.[7] First, there may be adsorption or desorption of lattice ions of sparingly soluble crystals, or with greater generality, particles that charge in accord with the Nernst equation (e.g., oxide particles, where their surface potential is dependent on the pH). Second, specific adsorption of ions onto particle surfaces can impart charge (e.g., specific adsorption of ionized surfactant molecules can confer charge to a particle).[8] Third, ionization of surface groups in latices, which depends on the pH of the surrounding medium. Fourth, isomorphic substitution can charge clay particles in water where a cation in the clay structure is exchanged for one of a different valence, creating a negative charge built into the structure of the face of the particle.[7,9,10] Finally, electron injection can generate charge, as for example between aqueous media and apolar oil droplets.[7]

It is more challenging to charge particles in apolar media (ε<5) than it is in aqueous media. The ultra-low dielectric of apolar media makes it more difficult to stabilize charge because it allows coulombic forces to be felt over much greater distances, as has been highlighted in earlier work by comparing the Bjerrum lengths.[1–3,7] The result of the instability of charges in apolar media is that particles cannot acquire charge in the absence of surfactants and the stabilizing reverse micelle structures they can form. Once a sufficient amount of surfactant is added to an apolar system to exceed its critical micelle concentration (CMC), reverse micelles spontaneously form, resulting in a measurable electrical conductivity, through the now well-accepted theory of charge disproportionation.[2,3,11] Only at surfactant concentrations above the CMC is particle charge

observed via electrophoretic mobility measurements in apolar media.[1,9] There is abundant evidence in the literature suggesting that the charging of oxides or similar colloidal particles in apolar media may ensue via a reverse micelle acid-base charging mechanism. First, the polar head group of a surfactant molecule adsorbs to the particle's surface and forms an acid-base adduct. Second, charge is transferred between the surfactant molecule and the surface functional group depending on their acid-base properties. Third, the charged surfactant molecule desorbs from the particle leaving behind a charge on the particle's surface which can be stabilized by other surfactant monomers. The charged surfactant counter-ion is then stabilized within an inverse micelle in the bulk.[1,3,12,13]

When the medium is changed from an ultra-low dielectric solvent to one with an intermediate dielectric constants ($5<\varepsilon<40$), the situation becomes more complex. In these dielectrics there are now interactions between each of the components in these systems. There exist particle-solvent interactions, particle-surfactant interactions, and solvent-surfactant interactions, all of which may lead to particle charging.

The first mechanism, the particle-solvent donor-acceptor interaction is an acid-base interaction between the particle and the medium. It was previously studied by Labib and Williams, [4,14] who used the electron donicity to relate the donor-acceptor concept to a wide range of solids in different solvents. They investigated solid particle charging in a series of organic solvents with dielectric constants ranging from 6 to 45. With no surfactant present, they found that by comparing the donicity of the solvent (D_N) to the zero charge point donicity of a solid (D_{NO}) the polarity of the solid particle charge could be determined.[4] The electron donicity is the ability of a molecule to donate electrons, and the value is defined as the enthalpy of reaction with the acid SbCl5 in 1,2-dichloroethane.[4,6,14,15] For example, if $D_N<D_{NO}$, an electron is transferred from the solid to the

liquid and therefore the solid particle will have a positive charge. There are many examples in the literature of researchers studying particle charging caused by particle-solvent interactions in such systems with these and other techniques.[4–6,8,14,16–19] In summary, as Verwey demonstrated through electroosmotic experiments, there exists a recurring acidity of solid particles (e.g., SiO_2>TiO_2>Al_2O_3>MgO) and that any oxide is more negative in water, than in acetone, and more negative in acetone than in ethanol.[5,8] While the importance of acid-base interactions between solid particles and non-aqueous liquids has been made clear, there are challenges in determining the donor numbers of solids. Literature reports D_{NO} values for TiO_2 from 1 kcal/mol[14] to 22.5 kcal/mol[20] and for Al_2O_3 from 7 kcal/mol[14] to 23 kcal/mol.[20] These discrepancies can be attributed to either the different solvents chosen or more likely the significant impact that the presence of water is known to have on particle charge.[8,16,18,21] In addition to solvent interacting with the particle's surface, studies have also shown that the solvents can affect the surfactants present in these systems.

The second mechanism stems from the possibility for an ionic surfactant like Aerosol OT (AOT) to ionize in these dielectrics. The ions AOT provides in these systems are the anionic surfactant ion and the sodium cation. This leaves the possibility for two different surfactant ion adsorptions as shown in Figure 5.1. First, the sodium ion could adsorb charging the particle positively, or second, the anionic surfactant ion could adsorb charging the particle negatively.[8,21]

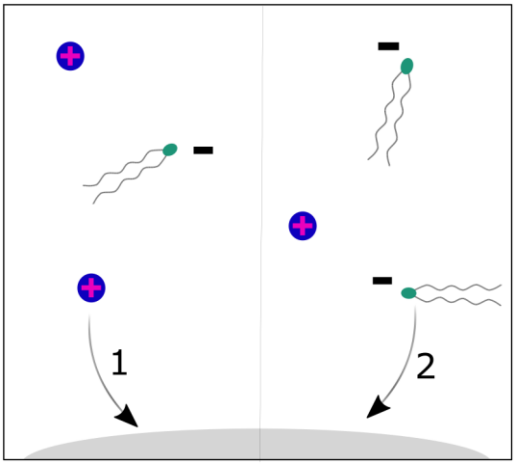

Figure 5.1. Two possibilities of ion adsorption for AOT in leaky dielectrics. (1) Sodium cation adsorption. (2) Surfactant AOT anion adsorption.

The third mechanism stems from the surfactant-solvent interactions and parallels the mechanism for apolar reverse micelle charging. A previous study investigated AOT micelle formation in an alcohol/water mixture and found that AOT would form micelles in water (ε=80), but would not form micelles in a mixture of alcohol and water with a $48<\varepsilon<80$, and would form reverse micelles in solvents with a $\varepsilon<48$.[22] Since we know that AOT reverse micelles are present in the leaky dielectric range studied here, there is potential for the acid-base reverse micelle charging mechanism to occur.

While a significant amount of research has been conducted on charging colloidal particles with surfactants in apolar media, there have been few studies investigating this charging behavior in solvents of intermediate dielectric constant. One study examined AOT charging of $YTaO_4$ particles in a solvent mixture of 58.2% butyl acetate and 41.8% propanol and found that charge increased to a maximum with the addition of AOT above its CMC and with the addition of water.[23] Another research group studied how various surfactants charged TiO_2 and Al_2O_3 particles in water, hexane, and a few small alcohols,[24,25] though, particle charging with surfactants over the broader range of leaky dielectrics remains to be explored.

The objective of the present work was to determine the effect that solvent dielectric constant has on charging particles with AOT. A series of straight chain alcohols was selected so that the dielectric constant could be changed while maintaining the same functionality on the solvent. The alcohol solvents selected are shown in Table 5.1. Additional ketones were studied to compare results to a solvent with similar dielectric constants and different functionality. To conduct this study, the AOT critical micelle concentration (CMC) was determined in each of these solvents and then particle charging trends were determined.

5.3 EXPERIMENTAL

5.3.1 *Chemicals*

Eight different straight chain alcohol solvents were examined in this study: methanol HPLC grade ≥99.9% from Sigma-Aldrich (St. Luis, MO), ethanol 200 proof from Decon Laboratories, Inc. (King of Prussia, PA), 1-propanol and 1-butanol both HPLC grade from Fisher Scientific (Pittsburgh, PA), 1-pentanol 99% pure from Acros Organics (part of Thermo Fisher Scientific), and 1-hexanol 99%, 1-heptanol 99%, and 1-octanol 99% all from Alfa Aesar (Ward Hill, MA). Table 1 lists the dielectric constant and viscosity for each of these 8 alcohol solvents. The donicity of the alcohol series (D_N) has been reported to be around 19 kcal/mol for methanol and the other shorter alcohols and as high as 30 kcal/mol for octanol.[26]

Table 5.1. Series of straight chain alcohols and their relevant properties. Dielectric constants (20°C) and Viscosities (25°C). [27]

Solvent	# of Carbons	Dielectric Constant, (ε)	Viscosity, (cP)
Methanol	1	33.0	0.6
Ethanol	2	25.3	1.1
n-Propanol	3	20.8	1.9
n-Butanol	4	17.84	2.6
n-Pentanol	5	15.13	3.5
n-Hexanol	6	13.03	4.6
n-Heptanol	7	11.75	5.8
n-Octanol	8	10.3	7.7

Three ketone solvents were also investigated as a comparison to the alcohol series with different functionality: Acetone 99.8% HPLC grade from Fisher Scientific (Pittsburgh, PA), methyl ethyl ketone 99.9% from Fisher Scientific (Pittsburgh, PA), and 3-pentanone (diethyl ketone) reagent grade ≥ 99% from Honeywell (Charlotte, NC). The reported donor numbers for these three ketones are 17.4, 17, and 15 kcal/mol respectively.[26]

There were five different mineral oxides tested during this study. Two silica particles with different crystal structures were used so that their refractive index could be altered without changing their surface functionality: a 250 nm diameter amorphous silica (SiO_2) from Fiber Optics Center, Inc. (New Bedford, MA) and a 1µm quartz silica from GetNanoMaterials (Las Cruces, NM). Both silica particles were required because some of the solvents had refractive indices that were too close to that of amorphous silica, making precise light scattering measurements difficult to obtain. Manganese dioxide (MnO_2) particles with a 50 nm diameter, 300 nm titania (TiO_2) particles, and 300 nm magnesia (MgO) particles all from US Research Nanomaterials, Inc. (Houston, TX) were also investigated in this study. The aqueous point of zero charge (PZC) for SiO_2, MnO_2, TiO_2, and MgO is approximately 2.5, 4, 6.5, and 11, respectively.[1,7,28] The particle donor numbers (D_{NO}) have been reported as < 0, 1, and 12 for SiO_2, TiO_2, and MgO respectively;

however, it can be assumed that the donor number ranking follows the PZC ranking and therefore, one would expect MnO_2 to have a donor number between that of silica and titania.[14]

The surfactant used in this experiment was solid, anhydrous sodium dioctylsulfosuccinate (Aerosol-OT or AOT) from Fisher Scientific (Pittsburgh, PA) and was used as received. AOT is an ionic surfactant with an acid-base number (ABN) of 5.[1,29] It was chosen for this experiment because of its known ability to form spherical reverse micelles over the entire range of solvent dielectric constant explored in this study.[22,30,31] Samples were prepared by first making AOT solutions in a given solvent at various concentrations ranging from 0 to 150 mM. The higher concentrations were approaching the solubility limit of AOT in these solvents. Each solution was filtered with a 20nm Whatman Anotop^{TM} 25 plus inorganic membrane filter to remove all dust and contamination from the samples. Conductivity measurements were conducted without particles. For particle charging samples, metal oxide particles were dried in an oven for 2 hr at 150^{o}C and added to the solutions at a loading of 500 ppm (~0.001g/10mL). Each solution sample was then sonicated for 3 min and allowed to equilibrate for 12 hr before measuring its electrophoretic mobility. Surfactant and particle concentrations were assumed to be low enough to have a negligible effect on the viscosity or density of the samples. Therefore, the properties of the solutions were assumed to be equal to those of the specific solvent.

Water content was monitored throughout these experiments with a C20 Coulometric Karl Fischer titration from Mettler Toledo (Columbus, OH). In addition to oven drying particles, 3 Å molecular sieves were used to dry solvents, and a desiccator was used to store both AOT and the oxide particles. Maintaining low water content was a challenge due to the hygroscopic nature of the solvents and AOT.[1,16] Water content was held below 1000 ppm (< 0.1wt%) during this study.

5.3.2 *Conductometric Titrations*

Conductivity of the AOT solutions was measured using a Mettler-Toledo (Columbus, OH) SevenCompact conductivity meter with the InLab 741 probe which has a range of 10^{-3} – 500 µS/cm. Each sample was measured 5 times at 22°C. Conductometric titrations were completed over the surfactant range of 0 to 12mM and a plot of conductivity versus AOT concentration was made. Two linear regions were established as shown in Figure 5.2 for methanol, ethanol, and hexanol. The intersection of two linear trendlines determines the critical micelle concentration (CMC) of the surfactant in a given solvent. This technique for determining CMC has been previously described.[7,22]

5.3.3 *Electrophoretic Mobility Measurments*

Phase analysis light scattering (PALS) was used to measure the electrophoretic mobility of each sample using a ZetaPals zeta potential analyzer from the Brookhaven Instruments Corporation (Holtsville, NY). Electrophoretic mobility measurements were conducted at 25°C across 0.5 cm spaced electrodes with a sinusoidal frequency of 2 Hz. Applied voltages were set between 10 V and 50 V depending on the dielectric constant of the solvent being tested. The voltage setting was often optimized by the machine. Samples were measured at two different voltages to monitor induced charging effects.[29,32] Particle charging results were presented in electrophoretic mobilities because in the range of leaky dielectrics, the determination of zeta potential requires the use of O'Brien and White computations.[7]

5.4 RESULTS AND DISCUSSION

The critical micelle concentration (CMC) of Aerosol-OT (AOT) in each solvent was determined using a conductometric titration. Figure 5.2 shows three examples of conductometric

titrations used to determine AOT's CMC in the series of straight chain alcohols. Note that the conductivity of methanol, ethanol, and hexanol decreases as the dielectric constant decrease as has been shown before.[33] The CMC was determined from the point of slope change on the plot of conductivity vs. AOT concentration. Comparing the CMC for each of the alcohols, Figure 5.2 (panel 4), it is clear that as the chain length of the alcohol increases the CMC of AOT decreases. This was expected and is consistent with previous studies.[22,34]

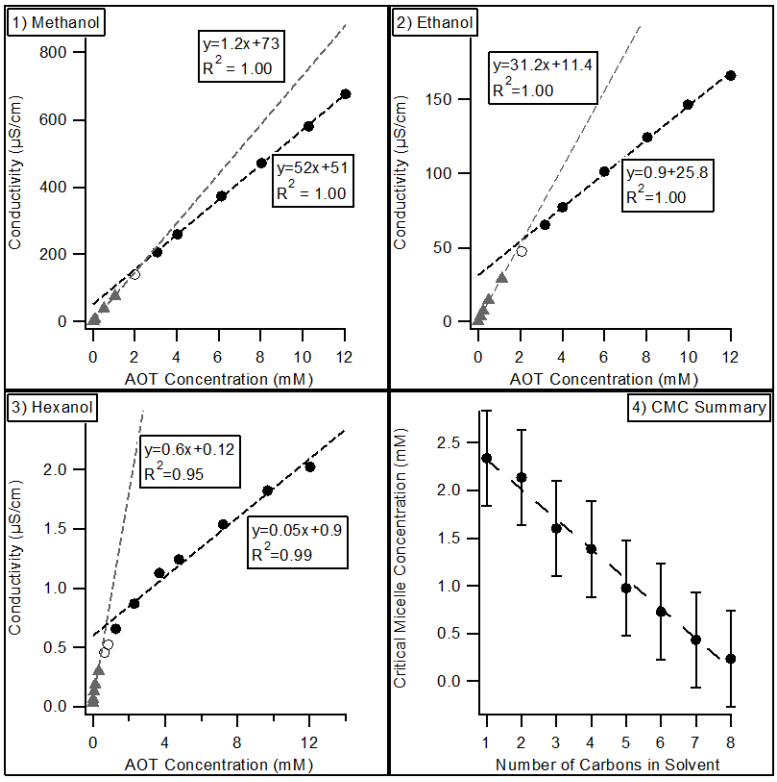

Figure 5.2. Critical micelle concentrations (CMC) determined by conductometric titration. Conductometric titration of AOT in methanol, ethanol, and hexanol (panels 1, 2, & 3). CMC results of AOT in the alcohol series (panel 4). Error bars were estimated to be 0.5 because the largest uncertainty in the conductometric CMC technique is from selecting points for each linear trendline.

The CMCs of the alcohol series determined in this study range from 2.3 mM in methanol, 2.1 mM in ethanol, 1.6 mM in propanol, down to 0.2 mM in octanol. While the CMC values for AOT in ethanol and propanol agree very well with previous results, (6.3 mM in methanol, 2.1 mM in

ethanol, and 1.3 mM in propanol)[22], methanol was quite different. As shown in Figure 5.2 methanol presented difficulties due to the small slope change in the conductometric titration. While conductivity measurements suggest the existence of AOT reverse micelles in methanol, other techniques used in previous studies have claimed that methanol would have the smallest reverse micelles compared to the other solvents, and if they exist are more likely to be sub-micellar clusters of surfactant molecules.[35] The difference in slope between the two linear trendlines increases as the alcohol chain length increases, making it easier to determine the CMC. Previous studies have found the CMC of AOT in apolar media (e.g., benzene, cyclohexane, and dodecane) to be approximately 0.1 mM, which is less than that of octanol.[36] This aligns with the trend that the CMC decreases as the solvent dielectric constant decreases.

The results for particle charging with no surfactant in these alcohols is shown in Figure 5.3 where electrophoretic mobility is plotted for each solvent. In each case MgO was the most positive, then TiO_2, and then SiO_2 was the most negative which was anticipated. This order of particle charge follows their relative aqueous PZCs or D_{NO}s where MgO was the most basic particle and SiO_2 was the most acidic. The decrease in magnitude of particle mobility as alcohol chain length increases can be attributed to the increase in viscosity as shown in Table 5.1.

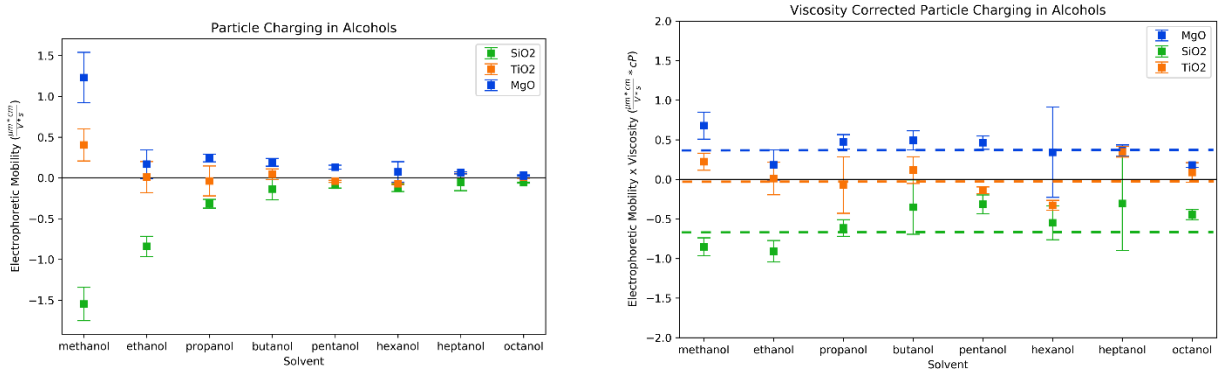

Figure 5.3. Particle charging via particle-solvent interactions without the presence of surfactant. (Left) Electrophoretic mobility of SiO2, TiO2, and MgO in each of the alcohol series. (Right) Viscosity corrected particle charge. The lines have been added to guide the eye.

When viscosity was accounted for by multiplying the viscosity and the particle's electrophoretic mobility, as shown on the right of Figure 5.3, all particles charged similarly as expected since the alcohols have the same R-OH functionality. Particle charging without the presence of surfactants was described as Mechanism 1, i.e., a miss-match between particle and solvent donicity, and contributes to charging in all of these cases of leaky dielectrics.

Methanol, having the highest dielectric constant of the alcohols studied here (ε ≈33) was the most complex and will be discussed first. The particle charging trend of AOT in methanol is shown in Figure 5.4 where the particle electrophoretic mobility is plotted against the surfactant concentration of AOT. Without surfactant present, the three particles charged from only the particle-solvent interaction as described by the particle-solvent interactions.

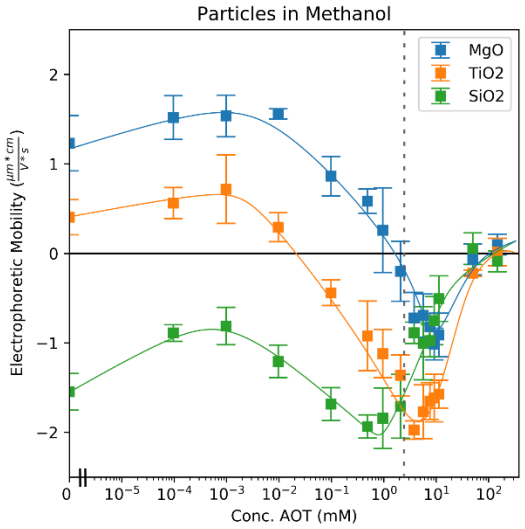

Figure 5.4. AOT particle charging in methanol as a function of surfactant (AOT) concentration. Lines have been added to help guide the eye. Dotted line marks the CMC.

When the AOT surfactant was added to the system (10^{-5} to 10^{-3} mM) ions were introduced which have the ability to adsorb onto the particle's surface, charging them. At first it appeared that the sodium cations adsorbed causing the charge to become more positive for each of the three particles.

Then, adding even more surfactant (10^{-3} to 10^{0} mM) to the system caused each of the particles to charge more negative, and in the case of SiO_2 and TiO_2, the particle charge even reversed sign. This suggests that the surfactant anions are adsorbing to the surface, driven by a solvophobic effect.

Once the surfactant concentration reached its CMC in methanol (~2.3 mM), the negative charge of the particles was reduced. There are three possible explanations for this: first, the reverse micelle charging mechanism could be charging these particles positively, second, with the presence of reverse micelles the solvophobic surfactant anions now have a new home and can be housed inside of reverse micelles instead of being adsorbed on the particle surface, and third, the increased number of ions in the bulk through reverse micelle disproportionation reactions and AOT dissociation could be electrostatically screening charge, reducing the mobility to zero.

A compilation of particle charging in methanol through octanol is shown in Figure 5.5. As the dielectric constant of the solvent was decreased by moving from methanol into the longer chained alcohols, some interesting trends arose. First, as expected from the results in Figure 5.3, the magnitude of electrophoretic mobility measurements decreased as the viscosity of the higher alcohols increased (and solvent dielectric constant decreased). Second, the sign reversal from anion adsorption below the CMC was only seen in methanol. The small size and sufficiently high dielectric constant, make methanol a good solvent for the dissociation of ions.[37] Once in ethanol, the sign reversal disappeared, and there was only limited evidence of surfactant ion adsorption. Also in ethanol, the particle charge was no longer screened to zero at the highest surfactant concentration because the number of ions was reduced due to its lower dielectric constant. In all of the alcohols, particle charging from particle-solvent interactions exists without the presence of surfactant. It appears that as the chain length of the alcohol solvent is increased (and the dielectric constant decreases), the effects from surfactant ion adsorption fade away. In octanol which was

the lowest dielectric constant alcohol tested, there appears to be only two charging mechanisms remaining: a particle-surfactant interaction below the CMC, and a reverse micelle charging mechanism trend at and above the CMC, similar to that of charging in apolar media.

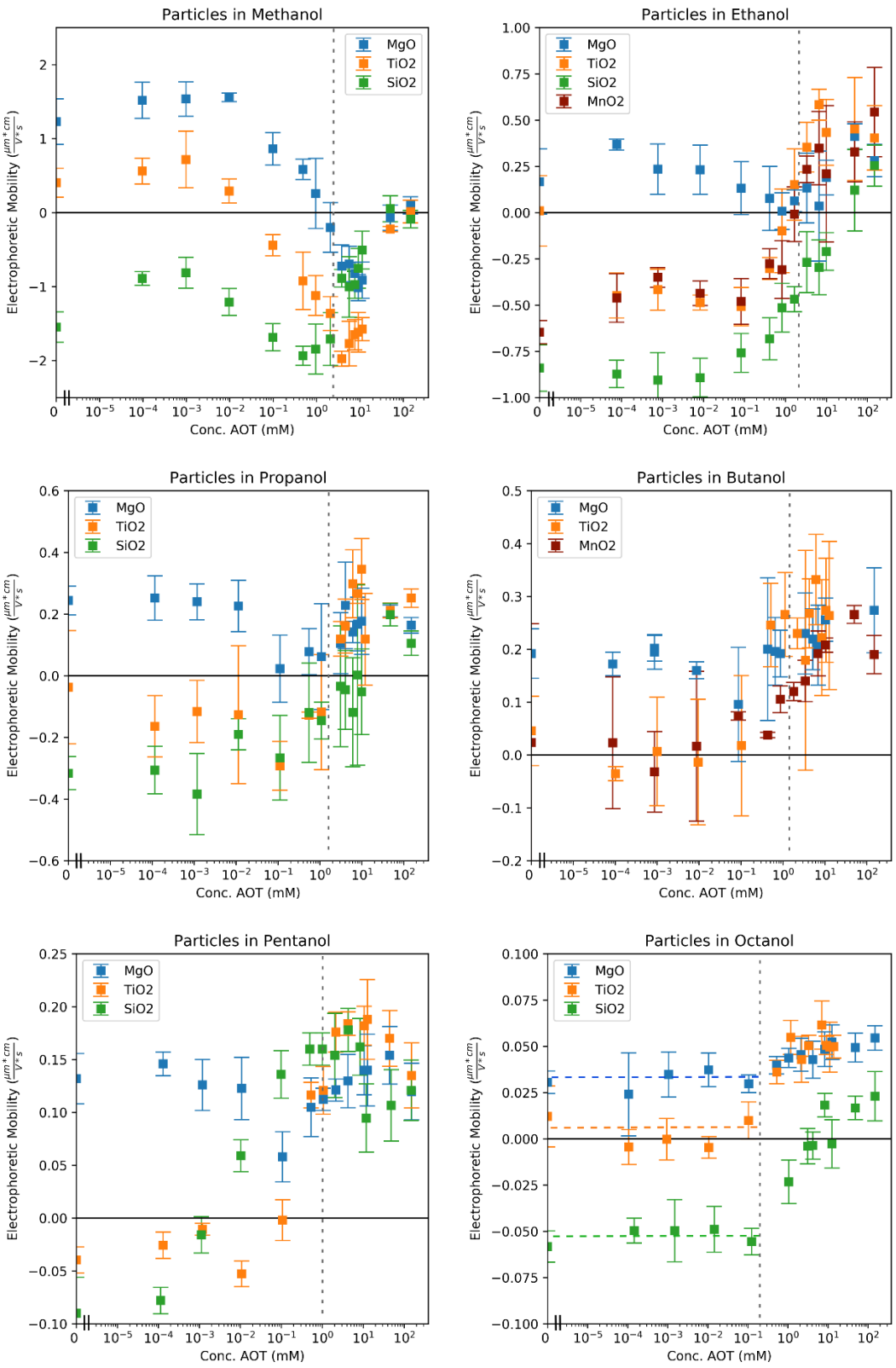

Figure 5.5. Summary of particle charging in the alcohol series. Lines added to guide the eye. Dotted line marks the CMC.

There were two key differences observed between particle charging in octanol (ε=10.3) versus apolar media (ε=2). First, in apolar media, particles do not obtain charge without the presence of reverse micelles which was shown here to be different for octanol. Second, in apolar media, silica is charged negatively by AOT in the acid-base reverse micelle particle charging mechanism due to its acidic properties (PZC = 2.5).[1] Alternatively, in octanol the more favorable stability of ions seem to loosen the sodium cations, and AOT was found to charge the surface of the silica particles positively.

To summarize particle charging in alcohol leaky dielectrics thus far, it appears that being in the intermediate range of dielectric constants allows for both apolar and aqueous charging mechanisms to occur. As dielectric constant decreases, the mechanism for ion adsorption fades away because the presence of ions themselves fades away. Even alcohols with low dielectric constant still charge by particle-solvent interactions, meaning that this charging mechanism is operational across the entire range of alcohols. A series of three ketones were chosen to investigate how these charging results from alcohols compared to other leaky dielectric solvents with different functional groups. Acetone, methyl ethyl ketone (MEK), and 3-pentanone (diethyl ketone or DEK) were chosen and have dielectric constants of 20.7, 18.5, and 17.0, respectively.[27] When comparing the relative acidity of these solvents, alcohols are more acidic than ketones according to their pKa values.

The expectation was to observe similar particle charging results with the ketone series as was observed with the alcohol series with one difference. It was hypothesized that at low surfactant concentrations, all of the particles would be charged more negatively than they were in the alcohols due to the more basic solvent. The contribution of charge from the particle-solvent

interaction will shift the charging trends to be more negative in the ketones. Conductometric titrations of AOT in the ketones resulted in the same decreasing trend of CMC as the number of carbons in the solvent increased (and dielectric constant decreased). Acetone with three carbons had an AOT CMC of 1.34 mM, MEK with four carbons had a CMC of 1.0 mM, and DEK with five carbons had a CMC of 0.81 mM. The CMC results matched closely to the alcohol CMC results.

The AOT charging results for SiO_2, TiO_2, and MgO particles in the three ketone solvents is shown in Figure 5.6.

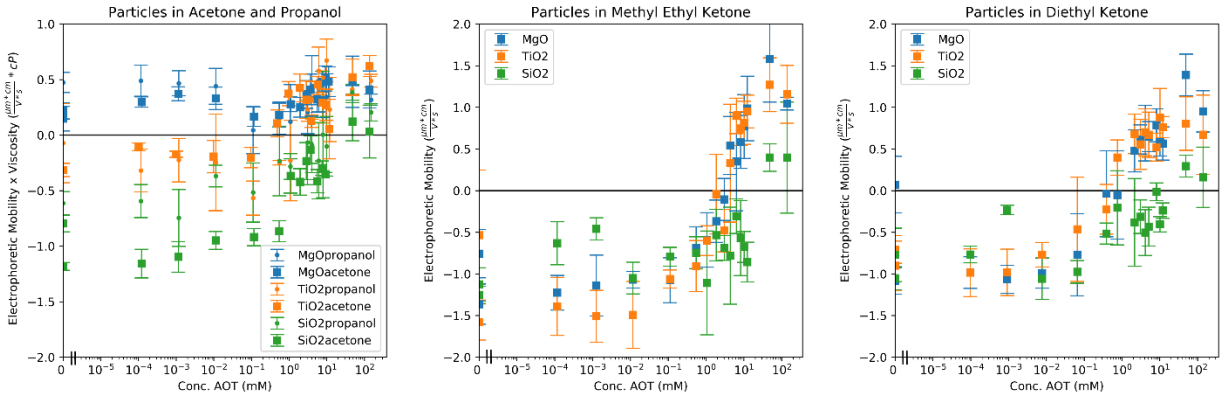

Figure 5.6. Particle charging in acetone (left), methyl ethyl ketone (middle), and 3-pentanone (right). Acetone is plotted with propanol to compare the similarity between solvents with similar dielectric constants and number of carbons.

Figure 5.6 shows that the particle charge of SiO2 and MgO in acetone is more negative than their charge in propanol, as expected. While TiO2 particle charging appears more negative with no surfactant present, the results from the charging trends are very similar between propanol and acetone. All three ketone solvents show a positive increase in particle charge above the CMC, indicating a reverse micelle charging mechanism similar to what was discovered in the other leaky and apolar solvents. However, a surprising result was that all three particles charged negatively in MEK and DEK below the CMC. It was thought that the particle-solvent interaction in the more

basic MEK and DEK solvent led to negatively charged particles. The results from the ketone solvents supported the leaky dielectric charging results from the alcohol series.

5.5 CONCLUSIONS

While particle charging with surfactants has been extensively studied in both aqueous (ε=80) and apolar (ε<5) media, the study of particle charging in solvents with intermediate dielectric constants (5<ε<40), remains to be fully explored. Particle charging in these solvents, which we refer to as "leaky dielectrics", is of interest because of the many colloidal applications where using particle charge to improve aggregation stability is important. Previous studies demonstrated that Aerosol-OT (AOT) forms reverse micelles in leaky solvents with dielectric constants ranging from 0 to 40.[22,30] Furthermore, the elevated dielectric constant of leaky dielectrics allows ions to exist in these solvents. The presence of reverse micelles and the solvent's favorability towards ionization creates the possibility for any number of aqueous and apolar particle charging mechanisms to occur in leaky dielectrics. Particle charging with AOT in a series of 8 straight-chained alcohols and a series of three ketones was examined.

Conductometric titrations determined the critical micelle concentration (CMC) of AOT in each leaky dielectric solvent. It was found that as the dielectric constant of the solvent in a series decreased, the CMC also decreased. This finding agreed with previous studies and the CMC of AOT in apolar media.[22,36]

Particle charging results revealed that particles can acquire charge via different charging mechanisms in surfactant leaky dielectric solutions. Mineral oxide particles in AOT solutions in various alcohol and ketone solvents demonstrated three different charging mechanisms. First, particle charge can occur from the particle-solvent interaction without the presence of surfactant. Second, surfactant ion adsorption can impart charge due to the dissociation and adsorption of the

ionic surfactant in leaky dielectrics. Third, a reverse micelle charging mechanism similar to that in apolar media can occur. It was found that as the dielectric constants of the solvents decreased, the effects of the surfactant ion adsorption were reduced, resulting in only charging from particle-solvent interactions and the reverse micelle charging mechanism. Overall, the mineral oxide particles were charged in the solvents in order of their acid-base properties. Silica being acidic was the most positive and magnesia being basic, was the most negative. All particles were charged positively by the addition of AOT above its CMC, indicating a reverse micelle charging mechanism with a Na+ ion being donated to the particles surface.[21]

5.6 REFERENCES

(1) Gacek, M. M.; Berg, J. C. The Role of Acid–Base Effects on Particle Charging in Apolar Media. *Adv. Colloid Interface Sci.* **2015**, *220*, 108–123. https://doi.org/10.1016/j.cis.2015.03.004.

(2) Morrison, I. D. Electrical Charges in Nonaqueous Media. *Colloids Surf. Physicochem. Eng. Asp.* **1993**, *71* (1), 1–37.

(3) Smith, G. N.; Eastoe, J. Controlling Colloid Charge in Nonpolar Liquids with Surfactants. *Phys Chem Chem Phys* **2013**, *15* (2), 424–439. https://doi.org/10.1039/C2CP42625K.

(4) Labib, M. E.; Williams, R. The Use of Zeta-Potential Measurements in Organic Solvents to Determine the Donor—Acceptor Properties of Solid Surfaces. *J. Colloid Interface Sci.* **1984**, *97* (2), 356–366.

(5) Verwey, E. J. W. Properties of Suspensions, Especially in Non-Aqueous Media. *Recl. Trav. Chim. Pays-Bas* **1941**, *60* (8), 618–624.

(6) Gutmann, V. *The Donor-Acceptor Approach to Molecular Interactions*; Plenum Press: New York, 1978.

(7) Berg, J. C. *An Introduction to Interfaces & Colloids: The Bridge to Nanoscience*; World Scientific, 2010.

(8) Lyklema, J. Principles of the Stability of Lyophobic Colloidal Dispersions in Non-Aqueous Media. *Adv. Colloid Interface Sci.* **1968**, *2* (2), 67–114.

(9) Ponto, B. S.; Berg, J. C. Clay Particle Charging in Apolar Media. *Appl. Clay Sci.* **2018**, *161*, 76–81. https://doi.org/10.1016/j.clay.2018.04.016.

(10) Yariv, S.; Cross, H. *Organo-Clay Complexes and Interactions*; CRC Press, 2001.

(11) Guo, Q.; Singh, V.; Behrens, S. H. Electric Charging in Nonpolar Liquids Because of Nonionizable Surfactants. *Langmuir* **2010**, *26* (5), 3203–3207. https://doi.org/10.1021/la903182e.

(12) Pugh, R. J.; Matsunaga, T.; Fowkes, F. M. The Dispersibility and Stability of Carbon Black in Media of Low Dielectric Constant. 1. Electrostatic and Steric Contributions to Colloidal Stability. *Colloids Surf.* **1983**, *7* (3), 183–207.

(13) Pugh, R. J.; Fowkes, F. M. The Dispersibility and Stability of Coal Particles in Hydrocarbon Media with a Polyisobutene Succinamide Dispersing Agent. *Colloids Surf.* **1984**, *11* (3–4), 423–427.
(14) Labib, M. E.; Williams, R. An Experimental Comparison between the Aqueous PH Scale and the Electron Donicity Scale. *Colloid Polym. Sci.* **1986**, *264* (6), 533–541.
(15) Wingrave, J. A. *Oxide Surfaces*; CRC Press, 2001.
(16) Romo, L. A. Effect of C 3, C 4 and C 5 Alcohols and Water on the Stability of Dispersions with Alumina and Aluminum Hydroxide. *Discuss. Faraday Soc.* **1966**, *42*, 232–237.
(17) Romo, L. A. Stability of Non-Aqueous Dispersions. *J. Phys. Chem.* **1963**, *67* (2), 386–389.
(18) McGown, D. N. L.; Parfitt, G. D. Stability of Non-Aqueous Dispersions. Part 4.—Rate of Coagulation of Rutile in Aerosol OT + p-Xylene Solutions. *Discuss. Faraday Soc.* **1966**, *42* (0), 225–231. https://doi.org/10.1039/DF9664200225.
(19) Kolling, O. W. Comparison of Donor-Acceptor Parameters in Nonaqueous Solvents. *Anal. Chem.* **1982**, *54* (2), 260–264.
(20) Siffert, B.; Eleli-Letsango, J.; Jada, A.; Papirer, E. Experimental Determination of the Electron Donor and Acceptor Numbers of Oxides by Zetametry in Organic Media. *Colloids Surf. Physicochem. Eng. Asp.* **1994**, *92* (1), 107–111. https://doi.org/10.1016/0927-7757(94)02788-9.
(21) Lyklema, J. Principles of Interactions in Non-Aqueous Electrolyte Solutions. *Curr. Opin. Colloid Interface Sci.* **2013**, *18* (2), 116–128.
(22) Michor, E. L.; Berg, J. C. Micellization Behavior of Aerosol OT in Alcohol/Water Systems. *Langmuir* **2014**, *30* (42), 12520–12524.
(23) Mysko, D. D.; Berg, J. C. Mechanisms Influencing the Stability of a Nonaqueous Phosphor Dispersion. *Ind. Eng. Chem. Res.* **1993**, *32* (5), 854–858.
(24) Kosmulski, M.; Próchniak, P.; Rosenholm, J. B. Solvents, in Which Ionic Surfactants Do Not Affect the Zeta Potential. *J. Colloid Interface Sci.* **2010**, *342* (1), 110–113.
(25) Kosmulski, M.; Próchniak, P.; Rosenholm, J. B. Electrokinetic Study of Adsorption of Ionic Surfactants on Titania from Organic Solvents. *Colloids Surf. Physicochem. Eng. Asp.* **2009**, *348* (1), 298–300.
(26) Cataldo, F. A Revision of the Gutmann Donor Numbers of a Series of Phosphoramides Including TEPA. *Eur. Chem. Bull.* **2015**, *4* (1–3), 92–97.
(27) Handbook of Chemistry and Physics 100th Edition http://hbcponline.com/faces/contents/InteractiveTable.xhtml?search=true&tableId=48 (accessed Aug 21, 2019).
(28) Kosmulski, M. *Chemical Properties of Material Surfaces*; CRC press, 2001.
(29) Gacek, M. M.; Berg, J. C. Investigation of Surfactant Mediated Acid–Base Charging of Mineral Oxide Particles Dispersed in Apolar Systems. *Langmuir* **2012**, *28* (51), 17841–17845.
(30) Hollamby, M. J.; Tabor, R.; Mutch, K. J.; Trickett, K.; Eastoe, J.; Heenan, R. K.; Grillo, I. Effect of Solvent Quality on Aggregate Structures of Common Surfactants. *Langmuir* **2008**, *24* (21), 12235–12240.
(31) Kotlarchyk, M.; Huang, J. S.; Chen, S. H. Structure of AOT Reversed Micelles Determined by Small-Angle Neutron Scattering. *J. Phys. Chem.* **1985**, *89* (20), 4382–4386.

(32) Espinosa, C. E.; Guo, Q.; Singh, V.; Behrens, S. H. Particle Charging and Charge Screening in Nonpolar Dispersions with Nonionic Surfactants. *Langmuir* **2010**, *26* (22), 16941–16948.
(33) Prego, M.; Cabeza, O.; Carballo, E.; Franjo, C. F.; Jime, E. Measurement and Interpretation of the Electrical Conductivity of 1-Alcohols from 273 K to 333 K. *J. Mol. Liq.* **2000**, *89* (1–3), 233–238.
(34) Santhanalakshmi, J.; Maya, S. I. Solvent Effects on Reverse Micellisation of Tween 80 and Span 80 in Pure and Mixed Organic Solvents. In *Proceedings of the Indian Academy of Sciences-Chemical Sciences*; Springer, 1997; Vol. 109, pp 27–38.
(35) Peri, J. B. The State of Solution of Aerosol OT in Nonaqueous Solvents. *J. Colloid Interface Sci.* **1969**, *29* (1), 6–15.
(36) Smith, G. N.; Brown, P.; James, C.; Rogers, S. E.; Eastoe, J. The Effect of Solvent and Counterion Variation on Inverse Micelle CMCs in Hydrocarbon Solvents. *Colloids Surf. Physicochem. Eng. Asp.* **2016**, *494*, 194–200.
(37) Mazzini, V.; Craig, V. S. Specific-Ion Effects in Non-Aqueous Systems. *Curr. Opin. Colloid Interface Sci.* **2016**, *23*, 82–93.

Chapter 6. FUTURE WORK

Significant progress has been made in understanding surfactant mediated particle charging in nonaqueous media. This final chapter discusses two potential projects for continuing the research presented in this dissertation. It is anticipated that the majority of continued work in this field will be focused on specific applications tied to industrial problems. Using the foundation from decades of past research in this field, new problems may be efficiently solved.

The first project proposed here continues the investigation of reverse micelle charging in leaky dielectrics by exploring the effect of Aerosol-OT (AOT) reverse micelle structure on particle charging in different solvents. The second proposed project explores the use of AOT microemulsions (formed by adding excess water to an apolar-surfactant system) to charge particles in apolar media.

6.1 PROJECT 1: THE EFFECT OF AOT STRUCTURE ON PARTICLE CHARGING IN LEAKY DIELECTRICS

6.1.1 *Introduction*

The reverse micelle charging behavior of Aerosol-OT (AOT) reverse micelles in leaky dielectrics (Ch. 5) may also correlate to the surfactant structures AOT forms in these solvents. As has previously been shown in Figure 3.3, the micelle structure of the Span surfactant series correlated with the charging results of oxide particles in apolar media.[1] A similar correlation may also exist in leaky dielectrics where the structure of the AOT reverse micelles (RM) may impact the contribution of particle charging via the reverse micelle charging mechanism. To investigate the structure of AOT micelles in leaky dielectrics, small-angle scattering techniques are required.

Preliminary measurements of AOT reverse micelle structures were conducted in three fully

deuterated solvents (methanol, butanol, and hexanol) with small-angle neutron scattering. The scattering intensity (*I*) vs. scattering vector (*q*) results are shown in Figure 6.1.

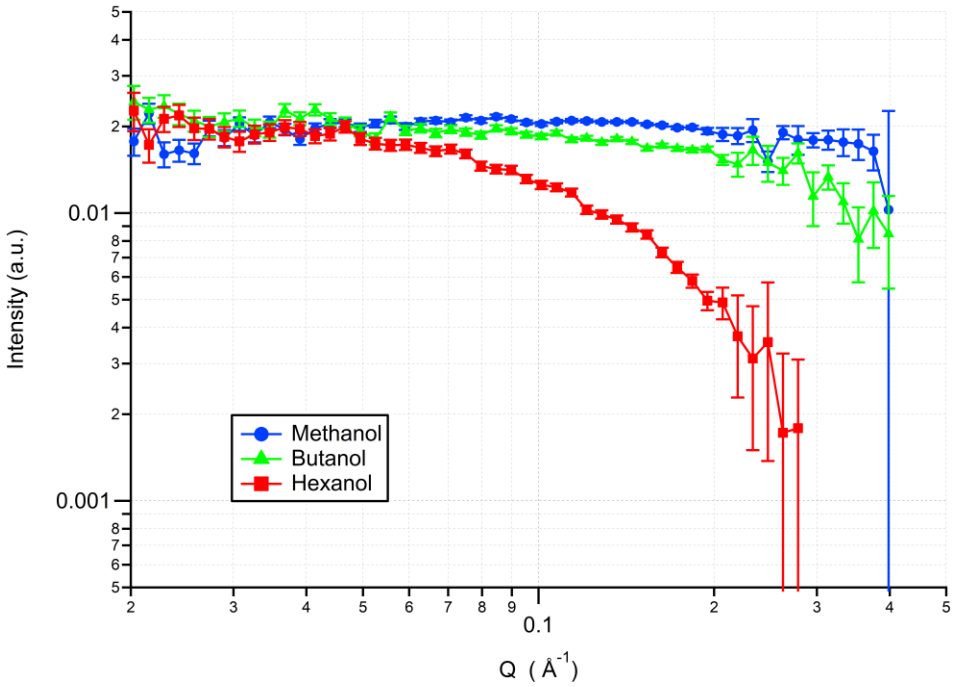

Figure 6.1. Intensity (*I*) vs. scattering vector (*q*) plots for Aerosol-OT in methanol, butanol, and hexanol.

While the low signal-to-noise ratio made fitting the data challenging, comparing the decrease in intensity of each solvent suggests that the reverse micelle size decreases as the dielectric constant decreases as shown in Table 5.1. Analyzing the reverse micelle sizes from low *q* values using Guinier plots resulted in the calculated sizes shown in Table 6.1 below.[2]

Table 6.1. Guinier analysis sizing results of AOT in methanol, butanol, and hexanol.

Solvent	**Radius (Å)**
Methanol	3.5
Butanol	7.4
Hexanol	9.8

This limited trend of decreasing RM radius is consistent with previous studies by Peri[3] who concluded that the reverse micelle size was related to the molar volume of the solvent. It was

found that as the molar volume of the solvent increased the size of the AOT reverse micelle also increased. Additionally, this study was skeptical of the existence of reverse micelles in methanol and concluded that if they exist, they would more likely be a small cluster of surfactant molecules.[3] This skepticism agrees with the fairly constant scattering intensity in methanol over the whole range of *Q*. Other SANS studies of AOT reverse micelles in decane demonstrated that AOT forms spherical reverse micelles with a total size around 17.4 Å and a core radius of 9.4 Å.[4] This aligns with the preliminary trend found here where RM size increases as the solvent dielectric constant decreases (or the molar volume of the solvent increases).

While the scattering trends suggest the presence of reverse micelles and the trend shows a decrease in size as the solvent dielectric constant decreases, further investigation is needed to accurately and precisely determine AOT reverse micelle structures in leaky dielectrics. Pursuing contrast matching techniques with SANS measurements would provide a better method of conducting these measurements generating adequate data for fitting.

The objective of this future study would be to accurately determine the size and aggregation numbers of AOT in the series of straight chained alcohols. Next, using the obtained results, determine the impact that the reverse micelle structure has on the reverse micelle charging mechanism's contribution to particle charging in leaky dielectrics. Correcting for the relevant solvent properties, e.g., viscosity, dielectric constant, etc., a comparison between the charging contributions in different solvents may be made.

6.1.2 *Materials and Methods*

The preliminary three alcohols measured were deuterated n-hexanol (D13, 98%), n-butanol (D9, 98%), and n-methanol (D4, 99.8%) purchased from Cambridge Isotope Laboratories (Andover, MA). It is suggested that future measurements using contrast matching should be

conducted with the four alcohols: ethanol; butanol; hexanol; and octanol; in their deuterated and hydrogenated forms.

Preliminary small-angle neutron scattering (SANS) measurements were conducted using the Extended Q-Range Small-Angle Neutron Scattering Diffractometer (EQ-SANS) on beam line six at the Spallation Neutron Source at Oak Ridge National Lab (Oak Ridge, TN). Samples were loaded into 0.3 mL Banjo cells with a 1 mm path length and measured for 1 hrs. A 2.5 Å neutron wavelength with the detector at the 4 m position was used to obtain scattering data at a *q* range of .01 – 1 $Å^{-1}$. It is recommended that future measurements are conducted at a facility with similar capabilities in order to use contrast matching techniques with longer measurement durations to increase neutron counts.

6.1.3 *Hypothesis*

The expectation is that the AOT reverse micelle structures of the four alcohols will agree with the preliminary data and results from previous studies. The size of the reverse micelles should increase as the solvent becomes less polar and the dielectric constant decreases. This would be consistent with the enthalpic driving force of reverse micellization where the interactions between the head groups is stronger as the solvent becomes less polar. Comparing the RM structures to their contributions of particle charging in apolar media will be interesting and it is expected to observe the contribution increase as the RM size increases because the probability of reverse micelle charging events increases with size.

6.2 Project 2: The Effect of Excess Water Content on the AOT Reverse Micelle Charging Mechanism in Apolar Media

6.2.1 *Background*

One area that remains to be completely explored in the quest to fully understand surfactant mediated particle charging in nonaqueous media is the effect of water. Previous studies have shown that the presence of water can have a major effect on particle charge in solvents without surfactants and can even cause the sign of particle charge to change.[5–8] With surfactant present, it has been suggested that the presence of water is a prerequisite for surfactants to be able to form reverse micelles (RM) and that the critical micelle concentration (CMC) can change based on water content.[8,9] Furthermore, in apolar media ($\varepsilon<5$) it has been shown that as the water content increases, the size of the Aerosol OT (AOT) reverse micelles will also increase even into the size range of microemulsions as shown in Figure 6.2 below.[10–12] This relationship between the RM size and water content was found to be linear in a recent molecular dynamic study.[10]

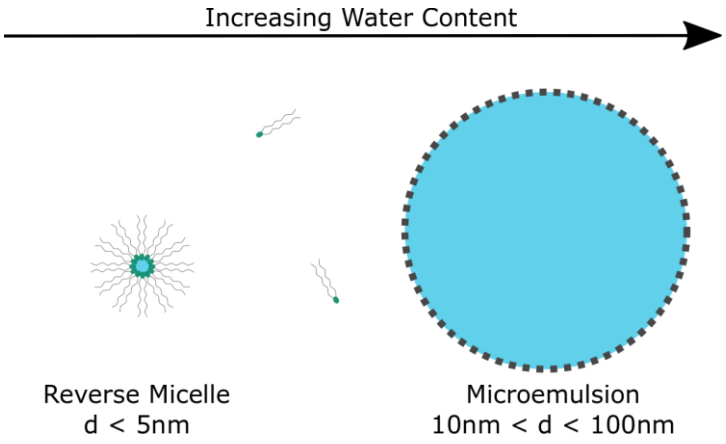

Figure 6.2. Reverse micelles turn into water-in-oil microemulsion droplets as water content increases.

When it comes to selecting a surfactant for these systems, Aerosol OT (AOT) is a common choice because it can form thermodynamically stable microemulsions without the requirement of short chain alcohol additives (cosurfactants).[7,13] Additionally, AOT has the capability of forming reverse micelles and water-in-oil (w/o) microemulsions in a wide variety of different nonaqueous solvents.[3,14–16]

While many studies have been conducted investigating the various effects that water content has on the conductivity and the stability of particles in AOT solutions of various solvents, the complete picture investigating the effect of water on AOT charging particles in apolar media over a broad range of water content has not yet been attained. Up to this point, the experimental work has strived to maintain an ultra-low water content (< 50 ppm) in apolar systems by using molecular sieves and desiccators. With recent challenges maintaining low water content in leaky dielectrics, there is interest in fully investigating the impact water content has on AOT particle charging in nonaqueous media. This investigation should begin in apolar media where a better understanding and control of the system exists.

There are a few examples of studies in the literature which begin to investigate the effect of water on surfactant mediated particle charging in different nonaqueous systems; however, in each case their solvent, particles, surfactant, or range of water content were different from the goal here. Mysko and Berg[17] studied AOT charging of $YTaO_4$ particles in a solvent mixture of 58.2% butyl acetate and 41.8% propanol and found that charged increased with added water over a range of AOT concentrations. They also found that charge decreased toward zero as the water content reached extremely high values (10^5 ppm).[17] A second study looked at the effect of water on AOT charging of S-copper phthalocyanine and monochloro substituted a-copper phthalocyanine dispersed in heptane and benzene and found that added water at 100 ppm increased charge but

above 300 ppm decreased charge.[18] A third study found a similar result for rutile TiO_2 in xylene.[19,20] Another previous study looked at water effects on SiO_2 charging with a different surfactant, OLOA 11000, but again only went up to 600 ppm.[21]

The closest a previous study has come to investigating the effect that water has on charging particles with AOT in apolar media was found in Kitahara's work in 1967.[22] The graph is recreated below in Figure 6.3 where the zeta potential of carbon black particles in a heptane-AOT solution was plotted as a function of water content.

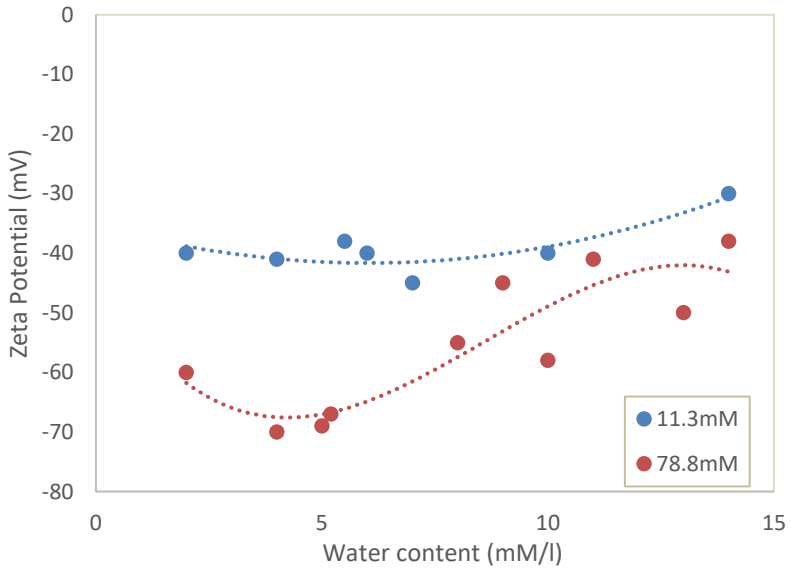

Figure 6.3. Reproduced graph from Kitahara 1967. The zeta potential of carbon black particles in n-Heptane with AOT concentrations of 11.3mM and 78.8mM plotted as a function of water content.[22] (Reproduced from reference 22)

The explanation of this trend was that a lower water content RMs could house a sodium cation in their core while an AOT anion would adsorb to the surface. As water content increased more water would be adsorbed to the particle surface allowing sodium cations to adsorb to the surface and decrease the surface charge. A closer look at the data, however, suggests that the results were inconclusive, and did not address water contents higher than 400 ppm.

While some progress has been made looking at the effect water content has on particle charge in different solvents, a single study investigating how water content affects AOT particle charging in apolar media over the entire range of water content from "dry" to the solubility limit of water, has yet to be conducted. By increasing the water content to higher levels, it is expected that the RMs will transition to microemulsions. Reverse micelles can only house a monovalent charge within their core while microemulsion droplets have the ability to carry more.[16,23] An interesting thought is that since microemulsions may have the ability to hold more than a single charge, leading to a divalent ion in apolar media, they might also enhance particle surface charging. The mechanism for charging droplets through a disproportionation reaction in apolar media has been previously worked out.[24,25] Equation (6.11) below describes the fraction of RMs or microemulsion droplets that will have a charge with valence Z.

$$\frac{C_Z}{C_o} = \exp\left(-\frac{Z^2e^2}{8\pi\varepsilon\varepsilon_o k_b T r}\right), \tag{6.11}$$

where $\frac{C_Z}{C_o}$ is the probability of a droplet having a charge of valence Z, ε is the dielectric constant of the medium, ε_o is the permittivity of free space, k_b is the Boltzmann constant, T is the temperature, r is the radius, and e is the protonic charge. A plot of the probability as a function of droplet radius for three different valences is shown below in Figure 6.4.

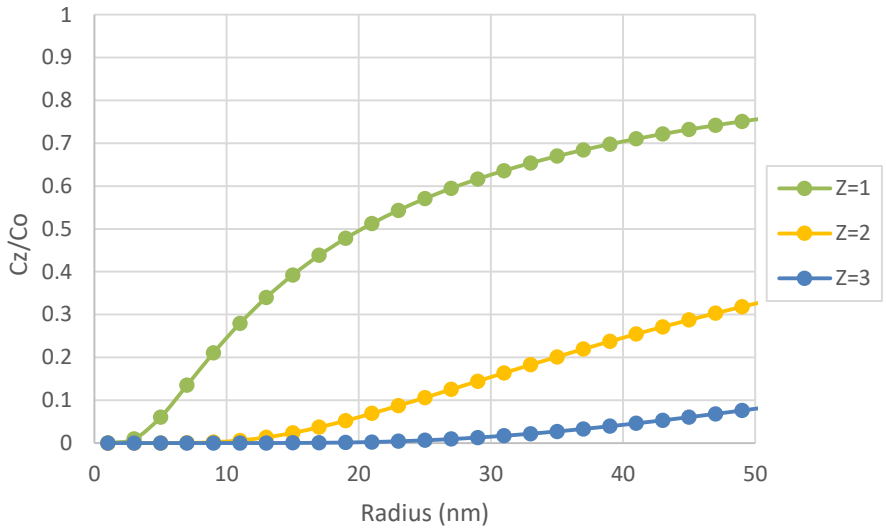

Figure 6.4. The fraction of RM or microemulsion droplets that can carry a charge with valence (Z) as a function of droplet radius.

In Figure 6.4, it is clear that small reverse micelles can only house a single charge but as the RM size increases into the range of microemulsion droplets by adding more water, the probability of charging increases and the possibility for a single droplet to house two charges becomes possible.

The objective of this study would be to investigate colloidal particle charging in apolar media with AOT over the entire range of water content (<50 ppm to ~10^5 ppm). By starting with AOT reverse micelles in relatively dry apolar media and increasing water content as high as possible, forming AOT microemulsions, the hope is to find out how important the role of water is in charging particles in apolar media and if increasing water content could be a method for increasing colloidal particle charge.

6.2.2 *Experimental*

As done previously, three different metal oxide particles will be tested in this study: silica (SiO_2) from Fiber Optics Center Inc. (New Bedford, MA), titania (TiO_2) from Rutile US Research Nanomaterials, Inc. (Houston, TX), and magnesia (MgO) from US Research Nanomaterials Inc. (Houston, TX). The aqueous isoelectric points (IEP) of SiO_2, TiO_2, and MgO are 2, 4, and 8.5 respectively.[26] The apolar solvent selected for this experiment is Isopar-L supplied by ExxonMobil Chemical (Houston, TX). Sodium dioctylsulfosuccinate (Aerosol-OT or AOT) from Fisher Scientific (Pittsburgh, PA) will be the surfactant used in this experiment. AOT is an ionic surfactant with an ABN of 5.[26,27] The critical micelle concentration (CMC) of AOT is approximately 0.001wt%.[26,28,29] It is recommended that AOT is chosen for this experiment because of its ability to swell in size allowing for a full range of water contents to be explored. Dispersions in Isopar-L with a particle loading of 500 ppm at AOT concentrations ranging from 10^{-5} to 5 wt% will be made.

Water content will be measured for the driest samples with a C20 coulometric Karl Fischer titration from Mettler Toledo (Columbus, OH). To increase the water content of samples deionized (DI) water will be pipetted into the samples increasing water content up to 10 wt%. Each solution sample will then be sonicated for 1 min and allowed to equilibrate for 12 hours before measuring its electrophoretic mobility. Surfactant and particle concentrations will be low enough to have a negligible effect on the viscosity or density of the samples and will be assumed to be equal to that of Isopar-L. Water, however, will be increased to levels where it will impact the density, viscosity, and dielectric constant of the solvent and will therefore have to be dealt with accordingly.

Phase analysis light scattering (PALS) will be used to measure the electrophoretic mobility of each sample using the ZetaPals zeta potential analyzer from the Brookhaven Instruments

Corporation (Holtsville, NY) across 0.5 cm spaced electrodes with a sinusoidal frequency of 2 Hz. Electric field induced charging will be monitored accordingly by measuring mobilities at different applied voltages.[21,27,30]

Conductivity will be measured using a DT-700 Nonaqueous Conductivity Probe from Dispersion Technologies (Bedford Hills, NY). The conductivity of each sample will be measured 20 times with a sinusoidal frequency of 1 Hz, and averaged.

Particles will be removed from the samples by centrifuging them in a Marathon 22K from Fisher Scientific (Hampton, NH). Once the particles have settled the supernatant will be taken and measured with Dynamic light scattering (DLS) to determine the size distribution of the AOT aggregates. DLS will be performed on the same ZetaPals device from the Brookhaven Instruments Corporation (Holtsville, NY). If needed to confirm DLS results, small-angle x-ray scattering (SAXS) will be conducted on the supernatant with an Anton Paar SAXSess instrument (Graz, Austria) which has a Cu K_α source and a 1.54Å wavelength.

6.2.3 *Hypothesis*

It is hypothesized that the added presence of water will affect particle charging with AOT at concentrations below and above the CMC. At pre-micelle concentrations of AOT, it is anticipated that the added water will enhance the ionizability of the surfactant, which should increase the conductivity and perhaps increase particle charge. At post-micelle concentrations the increased amount of water will increase the size of the reverse micelles (or microemulsions) which could have two effects. First, the added size of the AOT microemulsion droplets might increase their ability to charge via disproportionation reactions which would increase the total number of charges in the bulk and could screen out particle charge. The second possibility is that the larger microemulsion droplets will be able to carry more charges which might in turn allow a single

droplet to impart more charge on the dispersed particles. Investigating AOT reverse micelle (or microemulsion) particle charging in apolar media over the entire range of water content is important to determine the impact water has on these systems and to find the optimal water content to maximize particle charge in nonaqueous media. Depending on the effect water content has on charging particles in apolar media with AOT, an additional study exploring its effect in leaky dielectrics may be required.

6.3 REFERENCES

(1) Michor, E. L.; Ponto, B. S.; Berg, J. C. Effects of Reverse Micellar Structure on the Particle Charging Capabilities of the Span Surfactant Series. *Langmuir* **2016**, *32* (40), 10328–10333.

(2) Berg, J. C. *An Introduction to Interfaces & Colloids: The Bridge to Nanoscience*; World Scientific, 2010.

(3) Peri, J. B. The State of Solution of Aerosol OT in Nonaqueous Solvents. *J. Colloid Interface Sci.* **1969**, *29* (1), 6–15.

(4) Kotlarchyk, M.; Huang, J. S.; Chen, S. H. Structure of AOT Reversed Micelles Determined by Small-Angle Neutron Scattering. *J. Phys. Chem.* **1985**, *89* (20), 4382–4386.

(5) Labib, M. E.; Williams, R. An Experimental Comparison between the Aqueous PH Scale and the Electron Donicity Scale. *Colloid Polym. Sci.* **1986**, *264* (6), 533–541.

(6) Romo, L. A. Effect of C 3, C 4 and C 5 Alcohols and Water on the Stability of Dispersions with Alumina and Aluminum Hydroxide. *Discuss. Faraday Soc.* **1966**, *42*, 232–237.

(7) Morrison, I. D. Electrical Charges in Nonaqueous Media. *Colloids Surf. Physicochem. Eng. Asp.* **1993**, *71* (1), 1–37.

(8) Smith, G. N.; Eastoe, J. Controlling Colloid Charge in Nonpolar Liquids with Surfactants. *Phys Chem Chem Phys* **2013**, *15* (2), 424–439. https://doi.org/10.1039/C2CP42625K.

(9) Eicke, H.-F.; Christen, H. Is Water Critical to the Formation of Micelles in Apolar Media?? *Helv. Chim. Acta* **1978**, *61* (6), 2258–2263.

(10) Eskici, G.; Axelsen, P. H. The Size of AOT Reverse Micelles. *J. Phys. Chem. B* **2016**, *120* (44), 11337–11347.

(11) Eicke, H.-F.; Rehak, J. On the Formation of Water/Oil-Microemulsions. *Helv. Chim. Acta* **1976**, *59* (8), 2883–2891.

(12) Mathews, M. B.; Hirschhorn, E. Solubilization and Micelle Formation in a Hydrocarbon Medium. *J. Colloid Sci.* **1953**, *8* (1), 86–96.

(13) Hou, M. J.; Kim, M.; Shah, D. O. A Light Scattering Study on the Droplet Size and Interdroplet Interaction in Microemulsions of AOT? Oil? Water System. *J. Colloid Interface Sci.* **1988**, *123* (2), 398–412.

(14) Michor, E. L.; Berg, J. C. Micellization Behavior of Aerosol OT in Alcohol/Water Systems. *Langmuir* **2014**, *30* (42), 12520–12524.
(15) Hollamby, M. J.; Tabor, R.; Mutch, K. J.; Trickett, K.; Eastoe, J.; Heenan, R. K.; Grillo, I. Effect of Solvent Quality on Aggregate Structures of Common Surfactants. *Langmuir* **2008**, *24* (21), 12235–12240.
(16) Salabat, A.; Eastoe, J.; Mutch, K. J.; Tabor, R. F. Tuning Aggregation of Microemulsion Droplets and Silica Nanoparticles Using Solvent Mixtures. *J. Colloid Interface Sci.* **2008**, *318* (2), 244–251.
(17) Mysko, D. D.; Berg, J. C. Mechanisms Influencing the Stability of a Nonaqueous Phosphor Dispersion. *Ind. Eng. Chem. Res.* **1993**, *32* (5), 854–858.
(18) Cooper, W. D.; Wright, P. Electrophoresis of Colloidal Copper Phthalocyanines in Low Permittivity Liquids. *J. Chem. Soc. Faraday Trans. 1 Phys. Chem. Condens. Phases* **1974**, *70*, 858–867.
(19) Kitahara, A. Zeta Potential in Nonaqueous Media and Its Effect on Dispersion Stability. *Prog. Org. Coat.* **1973**, *2* (2), 81–98.
(20) McGown, D. N. L.; Parfitt, G. D.; Willis, E. Stability of Non-Aqueous Dispersions. I. The Relationship between Surface Potential and Stability in Hydrocarbon Media. *J. Colloid Sci.* **1965**, *20* (7), 650–664.
(21) Gacek, M.; Bergsman, D.; Michor, E.; Berg, J. C. Effects of Trace Water on Charging of Silica Particles Dispersed in a Nonpolar Medium. *Langmuir* **2012**, *28* (31), 11633–11638.
(22) Kitahara, A.; Karasawa, S.; Yamada, H. The Effect of Water on Electrokinetic Potential and Stability of Suspensions in Nonpolar Media. *J. Colloid Interface Sci.* **1967**, *25* (4), 490–495.
(23) Eicke, H. F.; Borkovec, M.; Das-Gupta, B. Conductivity of Water-in-Oil Microemulsions: A Quantitative Charge Fluctuation Model. *J. Phys. Chem.* **1989**, *93* (1), 314–317.
(24) Guo, Q.; Singh, V.; Behrens, S. H. Electric Charging in Nonpolar Liquids Because of Nonionizable Surfactants. *Langmuir* **2010**, *26* (5), 3203–3207. https://doi.org/10.1021/la903182e.
(25) Hall, D. G. Conductivity of Microemulsions: An Improved Charge Fluctuation Model. *J. Phys. Chem.* **1990**, *94* (1), 429–430.
(26) Gacek, M. M.; Berg, J. C. The Role of Acid–Base Effects on Particle Charging in Apolar Media. *Adv. Colloid Interface Sci.* **2015**, *220*, 108–123. https://doi.org/10.1016/j.cis.2015.03.004.
(27) Gacek, M. M.; Berg, J. C. Investigation of Surfactant Mediated Acid–Base Charging of Mineral Oxide Particles Dispersed in Apolar Systems. *Langmuir* **2012**, *28* (51), 17841–17845.
(28) Gacek, M.; Brooks, G.; Berg, J. C. Characterization of Mineral Oxide Charging in Apolar Media. *Langmuir* **2012**, *28* (5), 3032–3036.
(29) Gacek, M. M.; Berg, J. C. Effect of Surfactant Hydrophile-Lipophile Balance (HLB) Value on Mineral Oxide Charging in Apolar Media. *J. Colloid Interface Sci.* **2015**, *449*, 192–197.
(30) Espinosa, C. E.; Guo, Q.; Singh, V.; Behrens, S. H. Particle Charging and Charge Screening in Nonpolar Dispersions with Nonionic Surfactants. *Langmuir* **2010**, *26* (22), 16941–16948.

BIBLIOGRAPHY

Berg, J. C. *An Introduction to Interfaces & Colloids: The Bridge to Nanoscience*; World Scientific, 2010.

Cataldo, F. A Revision of the Gutmann Donor Numbers of a Series of Phosphoramides Including TEPA. *Eur. Chem. Bull.* **2015**, *4* (1–3), 92–97.

Cooper, W. D.; Wright, P. Electrophoresis of Colloidal Copper Phthalocyanines in Low Permittivity Liquids. *J. Chem. Soc. Faraday Trans. 1 Phys. Chem. Condens. Phases* **1974**, *70*, 858–867.

Duc, M.; Gaboriaud, F.; Thomas, F. Sensitivity of the Acid–Base Properties of Clays to the Methods of Preparation and Measurement: 1. Literature Review. *J. Colloid Interface Sci.* **2005**, *289* (1), 139–147.

Eicke, H. F.; Arnold, V. Interactions of Proton Donors with Colloidal Electrolytes in Apolar Solvents. *J. Colloid Interface Sci.* **1974**, *46* (1), 101–110.

Eicke, H. F.; Borkovec, M.; Das-Gupta, B. Conductivity of Water-in-Oil Microemulsions: A Quantitative Charge Fluctuation Model. *J. Phys. Chem.* **1989**, *93* (1), 314–317.

Eicke, H.-F.; Christen, H. Is Water Critical to the Formation of Micelles in Apolar Media?? *Helv. Chim. Acta* **1978**, *61* (6), 2258–2263.

Eicke, H.-F.; Rehak, J. On the Formation of Water/Oil-Microemulsions. *Helv. Chim. Acta* **1976**, *59* (8), 2883–2891.

Esfandiari, A.; Nazokdast, H.; Rashidi, A.-S.; Yazdanshenas, M.-E. Review of Polymer-Organoclay Nanocomposites. *J. Appl. Sci.* **2008**, *8* (3), 545–561.

Eskici, G.; Axelsen, P. H. The Size of AOT Reverse Micelles. *J. Phys. Chem. B* **2016**, *120* (44), 11337–11347.

Espinosa, C. E.; Guo, Q.; Singh, V.; Behrens, S. H. Particle Charging and Charge Screening in Nonpolar Dispersions with Nonionic Surfactants. *Langmuir* **2010**, *26* (22), 16941–16948.

Espinosa, C. E.; Guo, Q.; Singh, V.; Behrens, S. H. Particle Charging and Charge Screening in Nonpolar Dispersions with Nonionic Surfactants. *Langmuir* **2010**, *26* (22), 16941–16948. https://doi.org/10.1021/la1033965.

Gacek, M. M.; Berg, J. C. Effect of Surfactant Hydrophile-Lipophile Balance (HLB) Value on Mineral Oxide Charging in Apolar Media. *J. Colloid Interface Sci.* **2015**, *449*, 192–197.

Gacek, M. M.; Berg, J. C. Effect of Surfactant Hydrophile-Lipophile Balance (HLB) Value on Mineral Oxide Charging in Apolar Media. *J. Colloids Interface Sci.* **2015**.

Gacek, M. M.; Berg, J. C. Effect of Synergists on Organic Pigment Particle Charging in Apolar Media. *Electrophoresis* **2014**, *35* (12–13), 1766–1772.

Gacek, M. M.; Berg, J. C. Investigation of Surfactant Mediated Acid–Base Charging of Mineral Oxide Particles Dispersed in Apolar Systems. *Langmuir* **2012**, *28* (51), 17841–17845.

Gacek, M. M.; Berg, J. C. Investigation of Surfactant Mediated Acid–Base Charging of Mineral Oxide Particles Dispersed in Apolar Systems. *Langmuir* **2012**, *28* (51), 17841–17845. https://doi.org/10.1021/la303943k.

Gacek, M. M.; Berg, J. C. The Role of Acid–Base Effects on Particle Charging in Apolar Media. *Adv. Colloid Interface Sci.* **2015**, *220*, 108–123. https://doi.org/10.1016/j.cis.2015.03.004.

Gacek, M.; Bergsman, D.; Michor, E.; Berg, J. C. Effects of Trace Water on Charging of Silica Particles Dispersed in a Nonpolar Medium. *Langmuir* **2012**, *28* (31), 11633–11638.

Gacek, M.; Brooks, G.; Berg, J. C. Characterization of Mineral Oxide Charging in Apolar Media. *Langmuir* **2012**, *28* (5), 3032–3036.

Guo, Q.; Lee, J.; Singh, V.; Behrens, S. H. Surfactant Mediated Charging of Polymer Particles in a Nonpolar Liquid. *J. Colloid Interface Sci.* **2013**, *392*, 83–89. https://doi.org/10.1016/j.jcis.2012.09.070.

Guo, Q.; Singh, V.; Behrens, S. H. Electric Charging in Nonpolar Liquids Because of Nonionizable Surfactants. *Langmuir* **2009**, *26* (5), 3203–3207. https://doi.org/10.1021/la903182e.

Guo, Q.; Singh, V.; Behrens, S. H. Electric Charging in Nonpolar Liquids Because of Nonionizable Surfactants. *Langmuir* **2010**, *26* (5), 3203–3207. https://doi.org/10.1021/la903182e.

Gutmann, V. *The Donor-Acceptor Approach to Molecular Interactions*; Plenum Press: New York, 1978.

Hall, D. G. Conductivity of Microemulsions: An Improved Charge Fluctuation Model. *J. Phys. Chem.* **1990**, *94* (1), 429–430.

Hammouda, B. Probing Nanoscale Structures-the sans Toolbox. *Natl. Inst. Stand. Technol.* **2008**, 1–717.

Handbook of Chemistry and Physics 100th Edition http://hbcponline.com/faces/contents/InteractiveTable.xhtml?search=true&tableId=48 (accessed Aug 21, 2019).

Hollamby, M. J.; Tabor, R.; Mutch, K. J.; Trickett, K.; Eastoe, J.; Heenan, R. K.; Grillo, I. Effect of Solvent Quality on Aggregate Structures of Common Surfactants. *Langmuir* **2008**, *24* (21), 12235–12240.

Hou, M. J.; Kim, M.; Shah, D. O. A Light Scattering Study on the Droplet Size and Interdroplet Interaction in Microemulsions of AOT? Oil? Water System. *J. Colloid Interface Sci.* **1988**, *123* (2), 398–412.

HP ElectroInk FAQ Document. Hewlett-Packard Development Co. 2012.

Hsu, M. F.; Dufresne, E. R.; Weitz, D. A. Charge Stabilization in Nonpolar Solvents. *Langmuir* **2005**, *21* (11), 4881–4887.

Ian D. Morrison. Ions and Charged Particles in Nonpolar Media.Pdf, 2003.

Israelachvili, J. N. *Intermolecular and Surface Forces: Revised Third Edition*; Academic press, 2011.

Jackson, A. J. Introduction to Small-Angle Neutron Scattering and Neutron Reflectometry. *NIST Cent. Neutron Res.* **2008**, 1–24.

Jones, T. R. The Properties and Uses of Clays Which Swell in Organic Solvents. *Clay Miner.* **1983**, *18* (4), 399–401.

Kitahara, A. Zeta Potential in Nonaqueous Media and Its Effect on Dispersion Stability. *Prog. Org. Coat.* **1973**, *2* (2), 81–98.

Kitahara, A.; Karasawa, S.; Yamada, H. The Effect of Water on Electrokinetic Potential and Stability of Suspensions in Nonpolar Media. *J. Colloid Interface Sci.* **1967**, *25* (4), 490–495.

Klinkenberg, A.; van der Minne, J. L. *Electrostatics in the Petroleum Industry: The Prevention of Explosion Hazards*; Elsevier, 1958.

Kolling, O. W. Comparison of Donor-Acceptor Parameters in Nonaqueous Solvents. *Anal. Chem.* **1982**, *54* (2), 260–264.

Kosmulski, M. *Chemical Properties of Material Surfaces*; CRC press, 2001.

Kosmulski, M.; Próchniak, P.; Rosenholm, J. B. Electrokinetic Study of Adsorption of Ionic Surfactants on Titania from Organic Solvents. *Colloids Surf. Physicochem. Eng. Asp.* **2009**, *348* (1), 298–300.

Kosmulski, M.; Próchniak, P.; Rosenholm, J. B. Solvents, in Which Ionic Surfactants Do Not Affect the Zeta Potential. *J. Colloid Interface Sci.* **2010**, *342* (1), 110–113.

Kotlarchyk, M.; Huang, J. S.; Chen, S. H. Structure of AOT Reversed Micelles Determined by Small-Angle Neutron Scattering. *J. Phys. Chem.* **1985**, *89* (20), 4382–4386.

Kundu, K.; Das, A.; Bardhan, S.; Chakraborty, G.; Ghosh, D.; Kar, B.; Saha, S. K.; Senapati, S.; Mitra, R. K.; Paul, B. K. The Mixing Behaviour of Anionic and Nonionic Surfactant Blends in Aqueous Environment Correlates in Fatty Acid Ester Medium. *Colloids Surf. Physicochem. Eng. Asp.* **2016**, *504*, 331–342.

Kundu, K.; Paul, B. K. Physicochemical Investigation of Biocompatible Mixed Surfactant Reverse Micelles: II. Dynamics of Conductance Percolation, Energetics of Droplet Clustering, Effect of Additives and Dynamic Light Scattering Studies. *J. Chem. Thermodyn.* **2013**, *63*, 148–163.

Labib, M. E.; Williams, R. An Experimental Comparison between the Aqueous PH Scale and the Electron Donicity Scale. *Colloid Polym. Sci.* **1986**, *264* (6), 533–541.

Labib, M. E.; Williams, R. The Use of Zeta-Potential Measurements in Organic Solvents to Determine the Donor—Acceptor Properties of Solid Surfaces. *J. Colloid Interface Sci.* **1984**, *97* (2), 356–366.

Lee, J.; Zhou, Z.-L.; Alas, G.; Behrens, S. H. Mechanisms of Particle Charging by Surfactants in Nonpolar Dispersions. *Langmuir* **2015**, *31* (44), 11989–11999.

Lee, J.; Zhou, Z.-L.; Behrens, S. H. Charging Mechanism for Polymer Particles in Nonpolar Surfactant Solutions: Influence of Polymer Type and Surface Functionality. *Langmuir* **2016**, *32* (19), 4827–4836.

Liu, D.; Ma, J.; Cheng, H.; Zhao, Z. Investigation on the Conductivity and Microstructure of AOT/Non-Ionic Surfactants/Water/n-Heptane Mixed Reverse Micelles. *Colloids Surf. Physicochem. Eng. Asp.* **1998**, *135* (1), 157–164.

Liu, J.; Gaikwad, R.; Hande, A.; Das, S.; Thundat, T. Mapping and Quantifying Surface Charges on Clay Nanoparticles. *Langmuir* **2015**, *31* (38), 10469–10476.

Lyklema, J. Principles of Interactions in Non-Aqueous Electrolyte Solutions. *Curr. Opin. Colloid Interface Sci.* **2013**, *18* (2), 116–128.

Lyklema, J. Principles of the Stability of Lyophobic Colloidal Dispersions in Non-Aqueous Media. *Adv. Colloid Interface Sci.* **1968**, *2* (2), 67–114.

Masliyah, J.; Czarnecki, J.; Xu, Z. Handbook on Theory and Practice of Bitumen Recovery from Athabasca Oil Sands. *Theor. Basis* **2011**, *1*.

Mathews, M. B.; Hirschhorn, E. Solubilization and Micelle Formation in a Hydrocarbon Medium. *J. Colloid Sci.* **1953**, *8* (1), 86–96.

Mazzini, V.; Craig, V. S. Specific-Ion Effects in Non-Aqueous Systems. *Curr. Opin. Colloid Interface Sci.* **2016**, *23*, 82–93.

McGown, D. N. L.; Parfitt, G. D. Stability of Non-Aqueous Dispersions. Part 4.—Rate of Coagulation of Rutile in Aerosol OT + p-Xylene Solutions. *Discuss. Faraday Soc.* **1966**, *42* (0), 225–231. https://doi.org/10.1039/DF9664200225.

McGown, D. N. L.; Parfitt, G. D.; Willis, E. Stability of Non-Aqueous Dispersions. I. The Relationship between Surface Potential and Stability in Hydrocarbon Media. *J. Colloid Sci.* **1965**, *20* (7), 650–664.

Michor, E. L.; Berg, J. C. Micellization Behavior of Aerosol OT in Alcohol/Water Systems. *Langmuir* **2014**, *30* (42), 12520–12524.

Michor, E. L.; Berg, J. C. Temperature Effects on Micelle Formation and Particle Charging with Span Surfactants in Apolar Media. *Langmuir* **2015**, *31* (35), 9602–9607.

Michor, E. L.; Berg, J. C. The Particle Charging Behavior of Ion-Exchanged Surfactants in Apolar Media. *Colloids Surf. Physicochem. Eng. Asp.* **2017**, *512*, 1–6.

Michor, E. L.; Berg, J. C. The Temperature Effects on Micelle Formation and Particle Charging with Span Surfactants in Apolar Media. *Langmuir* **2015**, *31* (35), 9602–9607.

Michor, E. L.; Ponto, B. S.; Berg, J. C. Effects of Reverse Micellar Structure on the Particle Charging Capabilities of the Span Surfactant Series. *Langmuir* **2016**, *32* (40), 10328–10333.

Michor, E. L.; Ponto, B. S.; Berg, J. C. Effects of Reverse Micellar Structure on the Particle Charging Capabilities of the Span Surfactant Series. *Langmuir* **2016**, *32* (40), 10328–10333.

Moraru, V. N. Structure Formation of Alkylammonium Montmorillonites in Organic Media. *Appl. Clay Sci.* **2001**, *19* (1–6), 11–26. https://doi.org/10.1016/S0169-1317(01)00053-9.

Morrison, I. D. Electrical Charges in Nonaqueous Media. *Colloids Surf. Physicochem. Eng. Asp.* **1993**, *71* (1), 1–37.

Muhr, H. J.; Rohner, R. Good Titration Practice TM in Karl Fischer Titration. *Mettler Toledo* **2011**, *98*.

Murray, H. H. Current Industrial Applications of Clays. *Clay Sci.* **2006**, *12* (Supplement2), 106–112.

Mysko, D. D.; Berg, J. C. Mechanisms Influencing the Stability of a Nonaqueous Phosphor Dispersion. *Ind. Eng. Chem. Res.* **1993**, *32* (5), 854–858.

Nelson, S.; Pink, R. Solutions of Metal Soaps in Organic Solvents .14. Direct-Current Conductivity in Solutions of Some Metal Oleates in Toluene. *J. Chem. Soc.* **1954**, No. DEC, 4412–4417. https://doi.org/10.1039/jr9540004412.

Nelson, S.; Pink, R. Solutions of Metal Soaps in Organic Solvents .3. the Aggregation of Metal Soaps in Toluene, Isobutyl Alcohol, and Pyridine. *J. Chem. Soc.* **1952**, No. MAY, 1744–1750. https://doi.org/10.1039/jr9520001744.

Parent, M. E.; Yang, J.; Jeon, Y.; Toney, M. F.; Zhou, Z.-L.; Henze, D. Influence of Surfactant Structure on Reverse Micelle Size and Charge for Nonpolar Electrophoretic Inks. *Langmuir* **2011**, *27* (19), 11845–11851.

Peri, J. B. The State of Solution of Aerosol OT in Nonaqueous Solvents. *J. Colloid Interface Sci.* **1969**, *29* (1), 6–15.

Ponto, B. S.; Berg, J. C. Clay Particle Charging in Apolar Media. *Appl. Clay Sci.* **2018**, *161*, 76–81. https://doi.org/10.1016/j.clay.2018.04.016.

Poovarodom, S.; Berg, J. C. Effect of Particle and Surfactant Acid–Base Properties on Charging of Colloids in Apolar Media. *J. Colloid Interface Sci.* **2010**, *346* (2), 370–377. https://doi.org/10.1016/j.jcis.2010.03.012.

Poovarodom, S.; Poovarodom, S.; Berg, J. C. Effect of Alkyl Functionalization on Charging of Colloidal Silica in Apolar Media. *J. Colloid Interface Sci.* **2010**, *351* (2), 415–420.

Prego, M.; Cabeza, O.; Carballo, E.; Franjo, C. F.; Jime, E. Measurement and Interpretation of the Electrical Conductivity of 1-Alcohols from 273 K to 333 K. *J. Mol. Liq.* **2000**, *89* (1–3), 233–238.

Pugh, R. J.; Fowkes, F. M. The Dispersibility and Stability of Coal Particles in Hydrocarbon Media with a Polyisobutene Succinamide Dispersing Agent. *Colloids Surf.* **1984**, *11* (3–4), 423–427.

Pugh, R. J.; Matsunaga, T.; Fowkes, F. M. The Dispersibility and Stability of Carbon Black in Media of Low Dielectric Constant. 1. Electrostatic and Steric Contributions to Colloidal Stability. *Colloids Surf.* **1983**, *7* (3), 183–207.

Romo, L. A. Effect of C 3, C 4 and C 5 Alcohols and Water on the Stability of Dispersions with Alumina and Aluminum Hydroxide. *Discuss. Faraday Soc.* **1966**, *42*, 232–237.

Romo, L. A. Stability of Non-Aqueous Dispersions. *J. Phys. Chem.* **1963**, *67* (2), 386–389.

Salabat, A.; Eastoe, J.; Mutch, K. J.; Tabor, R. F. Tuning Aggregation of Microemulsion Droplets and Silica Nanoparticles Using Solvent Mixtures. *J. Colloid Interface Sci.* **2008**, *318* (2), 244–251.

Santhanalakshmi, J.; Maya, S. I. Solvent Effects on Reverse Micellisation of Tween 80 and Span 80 in Pure and Mixed Organic Solvents. In *Proceedings of the Indian Academy of Sciences-Chemical Sciences*; Springer, 1997; Vol. 109, pp 27–38.

Schoonheydt, R. A.; Johnston, C. T. The Surface Properties of Clay Minerals. *Layer. Struct. Their Appl. Adv. Technol.* **2011**, *11*, 337–373.

Schroth, B. K.; Sposito, G. Surface Charge Properties of Kaolinite. In *MRS Proceedings*; Cambridge Univ Press, 1996; Vol. 432, p 87.

Siffert, B.; Eleli-Letsango, J.; Jada, A.; Papirer, E. Experimental Determination of the Electron Donor and Acceptor Numbers of Oxides by Zetametry in Organic Media. *Colloids Surf. Physicochem. Eng. Asp.* **1994**, *92* (1), 107–111. https://doi.org/10.1016/0927-7757(94)02788-9.

Sivia, D. S. *Elementary Scattering Theory: For X-Ray and Neutron Users*; Oxford University Press, 2011.

Smith, G. N.; Brown, P.; James, C.; Rogers, S. E.; Eastoe, J. The Effect of Solvent and Counterion Variation on Inverse Micelle CMCs in Hydrocarbon Solvents. *Colloids Surf. Physicochem. Eng. Asp.* **2016**, *494*, 194–200.

Smith, G. N.; Eastoe, J. Controlling Colloid Charge in Nonpolar Liquids with Surfactants. *Phys Chem Chem Phys* **2013**, *15* (2), 424–439. https://doi.org/10.1039/C2CP42625K.

Smith, P. G.; Patel, M. N.; Kim, J.; Milner, T. E.; Johnston, K. P. Effect of Surface Hydrophilicity on Charging Mechanism of Colloids in Low-Permittivity Solvents. *J. Phys. Chem. C* **2007**, *111* (2), 840–848.

Stenkamp, V. S.; Berg, J. C. The Role of Long Tails in Steric Stabilization and Hydrodynamic Layer Thickness. *Langmuir* **1997**, *13* (14), 3827–3832.

Tombácz, E.; Szekeres, M. Colloidal Behavior of Aqueous Montmorillonite Suspensions: The Specific Role of PH in the Presence of Indifferent Electrolytes. *Appl. Clay Sci.* **2004**, *27* (1–2), 75–94. https://doi.org/10.1016/j.clay.2004.01.001.

Tombácz, E.; Szekeres, M. Surface Charge Heterogeneity of Kaolinite in Aqueous Suspension in Comparison with Montmorillonite. *Appl. Clay Sci.* **2006**, *34* (1–4), 105–124. https://doi.org/10.1016/j.clay.2006.05.009.

Van Olphen, H. H. *An Introduction to Clay Colloid Chemistry: For Clay Technologists, Geologists, and Soil Scientists*; 1977.

Verwey, E. J. W. Properties of Suspensions, Especially in Non-Aqueous Media. *Recl. Trav. Chim. Pays-Bas* **1941**, *60* (8), 618–624.

Wingrave, J. A. *Oxide Surfaces*; CRC Press, 2001.

Yariv, S.; Cross, H. *Organo-Clay Complexes and Interactions*; CRC Press, 2001.

BENJAMIN S. PONTO

EDUCATION

University of Washington, Seattle, WA

Doctor of Philosophy in Chemical Engineering **October 2019**
- Current GPA: 3.89

Master of Science in Chemical Engineering **March 2018**
- Current GPA: 3.89

Bachelor of Science in Chemical Engineering & **June 2013**
Bachelor of Science in Bioresource Science and Engineering
- Graduated Cum Laude with 3.81 GPA
- Chemical Engineering Departmental Honors

EXPERIENCE

Graduate Research: Particle Charging in Apolar Media **2015-2019**
Prof. John C. Berg, Colloids and Interface Science Group, University of Washington
- Studied colloidal particle charging in apolar media using surfactant reverse micelles
- Experience with small-angle neutron scattering, dynamic light scattering, phase analysis light scattering, scanning electron microscopy, surfactants, zeta potential, conductivity, atomic force microscopy, colloids

Washington Pulp and Paper Foundation Board of Directors **2015-2019**
University of Washington, Seattle, WA

Process Engineer **2013-2015**
Sonoco, Sumner, WA & Newport, TN
- Implemented lean six-sigma methodologies into a paper manufacturing plant as an active member of the mill leadership team
- Led improvement teams to reduce both steam and chemical costs
- Managed Focused Improvement Pillar as member of mill leadership team
- Facilitated safety meetings and sponsored crew-led hazcom safety team
- Improved efficiency in Quality Pillar
- Completed environmental reporting, permitting, and audits

Undergraduate Research Mentoring **2015-2019**
Prof. John C. Berg, Colloids and Interface Science Group, University of Washington
- Helped 16 undergraduate chemical engineering students complete independent research projects
- Taught/graded surface and colloid science laboratory experiments (Chem E 455 TA)

Chemistry Tutor and Exam Review Instructor **2009-2013**
The Center for Learning and Undergraduate Enrichment (CLUE), University of Washington
- Tutored university students in undergraduate chemistry
- Taught exam reviews for chemistry classes (100+ students attending)

Laboratory Technician **June-Sept, 2012**

G.R. Silicate Nano-Fibers and Carbonates, Tacoma, WA

- Conducted high pressure reactions to produce silicate nano-fibers
- Designed and conducted experiments investigating the effectiveness of replacing TiO_2 with silicate nano-fibers in paper products
- Collected, analyzed, and presented experimental data to potential customers and investors

Process Engineer CO-OP **Mar-Sept, 2011**

Kimberly-Clark, Everett, WA

- Planned and coordinated a group of engineers, lab technicians, and operators to successfully acid cure a pulp digester
- Conducted lab fermentation and distillation of spent sulfite liquor for fuel grade ethanol production and testing
- Optimized the daily product quality report to increase usability and clarity
- Collected and analyzed daily production data to aid in problem solving

PUBLICATIONS

- B. S. Ponto and J.C. Berg, "Exploring new avenues of particle charging in apolar media," COLL 559. Paper number 2990244. Presented at the 256th ACS National Meeting, Boston, MA, Aug. 2018.
- B. S. Ponto and J. C. Berg, "Clay particle charging in apolar media," Appl. Clay Sci., vol. 161, pp. 76–81, Sep. 2018.
- E. L. Michor, B. S. Ponto, and J. C. Berg, "Effects of Reverse Micellar Structure on the Particle Charging Capabilities of the Span Surfactant Series," Langmuir, vol. 32, no. 40, pp. 10328– 10333, 2016.
- B. S. Ponto, and J. C. Berg, "Nanoparticle Charging with Mixed Reverse Micelles in Apolar Media," (Submitted for publication Sept. 2019)
- B. S. Ponto, and J. C. Berg, "Nanoparticle Charging in Leaky Dielectrics," (Submitted for publication Sept. 2019)

COMPUTER SKILLS

Aspen, Python, Jupyter Notebooks, GitHub, WinGEMS, MATLAB, Mathematica, Minitab, Excel, Parcview, PI ProcessBook, Microsoft Office, LabView

CERTIFICATIONS

- 19th National School on Neutron and X-Ray Scattering **2017**
- ASQ-Certified Six Sigma Black Belt **2015**